STRATEGIES FOR IMPROVING THERMAL AND MECHANICAL PROPERTIES OF WOOD-STRAND COMPOSITES

By

NATHAN BRYCE WHITE

A thesis submitted in partial fulfillment of
the requirements for the degree of

MASTER OF SCIENCE IN CIVIL ENGINEERING

WASHINGTON STATE UNIVERSITY
Department of Civil and Environmental Engineering

DECEMBER 2011

To the Faculty of Washington State University:

The members of the committee appointed to examine the thesis of NATHAN BRYCE WHITE find it satisfactory and recommend that it be accepted.

_____
Vikram Yadama, Ph.D., Chair

_____
Donald Bender, Ph.D.

_____
William Cofer, Ph.D.

ACKNOWLEDGMENTS

I'd like to thank my committee members Dr. Vikram Yadama, Dr. Donald Bender, and Dr. William Cofer for help and support during this project. I'd also like to acknowledge the CSREES/USDA PL 89-106, Inland Northwest Forest Products Research Consortium for funding this research. I'd like to thank the faculty, staff, and lab mates at the Washington State University Composite Material & Engineering Center (CMEC) for help during work in the lab. Lastly, I'd like to thank my parents, Rick and Judi White, my brothers and sister-in-law, and my friends for endless support and encouragement in everything that I do.

STRATEGIES FOR IMPROVING THERMAL AND MECHANICAL PROPERTIES OF WOOD-STRAND COMPOSITES

Abstract

by Nathan Bryce White, MS
Washington State University
December 2011

Chair: Vikram Yadama

Wood-strand sandwich panel development over recent years found a sustainable means to use undervalued small-diameter timber to create a building envelope material with similar bending stiffness as typical sheathing [oriented strand board (OSB) and plywood]. Changing resources and demand for reduced energy dependency have led to consideration of combining energy and structural performance codes for construction of sustainable buildings and reduced operational energy (residential and commercial buildings account for 39% of total U.S. energy consumption and 38% of U.S. carbon dioxide emissions). This research is aimed toward replacing OSB sheathing with this energy efficient sandwich panel for “green” building construction.

Thermal properties of sandwich panels were evaluated to determine effectiveness of their use in reducing operational energy. By replacing 12.7 mm OSB with 32 mm sandwich panels (half the density yet stiffer panels compared to OSB), thermal resistance (R-value) of a wall cross-section increased by 6%. Incorporation of

insulating type materials (foam or radiant barrier) within the sandwich panel cavities improved thermal performance more significantly, creating a more desirable building envelope material. Rigid foam insulation within panel cavities increased wall cross-section R-value by 20% while incorporation of radiant barrier increased R-value by 10% compared to 12.7 mm OSB. Improvements in energy efficiency by addition of materials may affect structural integrity of a material, thus mechanical properties were also analyzed. Sandwich panels with foam yielded bending stiffness 41% greater than OSB of similar thickness and 16% stiffer than sandwich panels without foam. Similar to wood-strand sandwich panels, the more energy efficient sandwich panel with foam still utilized 40% less strand and resin material than OSB of equal thickness while only increasing density of the sandwich panels about 10%.

A finite element model was developed to predict standard beam flexure tests of sandwich panels. This aids in understanding material behavior and allows for future alterations to panel geometry without a need to fabricate a costly mold to produce the corrugated core. Analysis discovered that Young's modulus in the strong direction for thin ply material, along with experimental deformation occurring at support bars, drastically affect accuracy of the model compared to experimental results.

TABLE OF CONTENTS

PAGE

ACKNOWLEDGEMENTS iii

ABSTRACT iv

LIST OF TABLES x

LIST OF FIGURES xi

CHAPTER

1. INTRODUCTION TO CREATING A MORE SUSTAINABLE WOOD-STRAND SANDWICH PANEL WITH 3-D CORE 1

1.1. Introduction 1

1.2. Objectives 3

1.3. Motivation 4

1.4. Background 6

1.4.1. Core Design for Sandwich Panel 6

1.4.2. Manufacturing of Wood-Strand Sandwich Panels 7

1.5. Scope of the Thesis 11

1.6. References 11

2. EXPERIMENTAL AND ANALYTICAL EVALUATION OF WOOD-STRAND SANDWICH PANELS 13

2.1. Introduction 13

2.2. Objectives 17

2.3. Background 18

2.3.1. Heat Transfer 18

2.3.2. Thermal Properties 19
2.3.3. Previous Thermal Testing 20
2.3.4. Previous Finite Element Analysis 22
2.4. Materials and Methods 24
2.4.1. Sandwich Panel Material 24
2.4.2. Empirical Determination of Thermal Conductivity 24
2.4.3. Specimen Tests 25
2.4.3.1. Thermal Tests 25
2.4.3.2. Mechanical Tests 27
2.4.3.3. Tensile Testing of Thin Plies 33
2.4.4. Finite Element Model and Analysis 36
2.4.4.1. Geometry and Boundary Conditions 36
2.4.4.2. Element Selection 37
2.4.4.3. Material Properties 38
2.4.4.4. Mesh and Load 40
2.4.4.5. Core/Ply Interface 41
2.4.4.6. Analysis Options 43
2.5. Results and Discussion 43
2.5.1. Thermal Properties Determined by Heat Flow Meter 43
2.5.2. Empirical Thermal Conductivity 47
2.5.3. Results of Mechanical Testing 47
2.5.3.1. Flexure Tests 47
2.5.3.2. Core Shear Flexure Tests 49

2.5.3.3. Flatwise Compression Tests 50
2.5.4. Tensile Testing of Thin Plies 53
2.5.5. Finite Element Model 55
2.6. Summary and Conclusions 61
2.7. References 63
3. STRATEGIES FOR IMPROVING THERMAL AND MECHANICAL PROPERTIES OF WOOD-STRAND SANDWICH PANELS 65
3.1. Introduction 65
3.2. Objectives 69
3.3. Methods 70
3.3.1. Incorporated Materials 70
3.3.1.1. Rigid Foam 70
3.3.1.2. Radiant Barrier 71
3.3.2. Material Installation 73
3.3.2.1. Rigid Foam 73
3.3.2.2. Radiant Barrier 76
3.3.3. Specimen Tests 78
3.3.3.1. Thermal Tests 78
3.3.3.2. Mechanical Tests 79
3.4. Results and Discussion 81
3.4.1. Thermal Properties Determined by Heat Flow Meter 81
3.4.2. Mechanical Tests 84
3.4.2.1. Flexure Tests 84
3.4.2.2. Core Shear Flexure Tests 88

3.4.2.3. Flatwise Compression Tests 90
3.5. Building Envelope Thermal Resistance 96
3.6. Summary and Conclusions 98
3.7. References 99
4. PROJECT SUMMARY AND CONCLUSIONS 101
APPENDIX
A. Strand and Resin Amount Calculations 105
B. Empirical Thermal Conductivity Calculations 108
C. R-Value Estimation Calculations 110
D. Wall R-Value Calculations 112

LIST OF TABLES

2.3.1 PSW panel thermal properties found by Kawasaki and Kawai..... 22

2.4.1 Material properties defined in FE model..... 39

2.5.1 Summary of wood-strand sandwich panel and OSB panel thermal properties..... 44

2.5.2 Summary of wood-strand sandwich panel mechanical properties compared to results from Voth 53

2.5.3 Summary of wood-strand ply properties from various studies..... 55

2.5.4 FE model results compared to experimental results 58

2.5.5 Material properties representing flexure testing 59

3.1.1 Current R-value requirements compared to future code requirements by zone 66

3.3.1 Emittance values of surfaces and effective emittances of air spaces 72

3.3.2 Thermal resistance, R-value, of plane air spaces 73

3.4.1 Summary of thermal properties for wood-strand sandwich panels and OSB 82

3.4.2 Summary of wood-strand sandwich panel properties..... 95

LIST OF FIGURES

1.4.1 Wood-strands drying in box dryer 7

1.4.2 Resin applied to wood-strands in rotating mixing drum and strands after resin has been applied 8

1.4.3 Wood-strand mat on shake table and forming box 9

1.4.4 Hot press with 3-D mold installed 9

1.4.5 Clamping of wood-strand sandwich panels 10

2.1.1 Comparison of bending stiffness of selected panels versus their weight of materials 16

2.1.2 Normalized bending stiffness comparison between plywood, OSB, and wood-strand sandwich panels 17

2.3.1 Simple corrugated core shape used in Hunt's FE model 23

2.4.1 Fox 304™ heat flow meter with 305 mm x 305 mm specimen 26

2.4.2 Beam flexure test apparatus 29

2.4.3 Core shear flexure test apparatus 31

2.4.4 215 mm x 215 mm and 108 mm x 108 mm flatwise compression test apparatus 33

2.4.5 Typical tensile test apparatus with 25.4 mm and 12.7 mm extensometer 36

2.4.6 FE model in ADINA 37

2.4.7 FE model showing displacement controlled loading 41

2.4.8 Typical rigid link connection from node to node 42

2.4.9 Rigid links defined in FE model 42

2.5.1 R-values of wood-strand panels, both experimental and calculated, compared to Kawasaki's PSW, OSB, plywood, and commercial insulators (EPS, XPS, Fiberglass 45

2.5.2 R-values normalized by thickness and given in U.S. units 46

2.5.3 Thicker sandwich panel construction 46

2.5.4 Failure of longitudinal specimen 48

2.5.5 Typical local ply failure for transverse specimens. Flexural failure in transverse specimen 49

2.5.6 Delamination and crushing at support in longitudinal specimens. Top ply failure and bottom ply failure in transverse specimens 50

2.5.7 Delamination, core failure, and ply failure of 215 mm x 215 mm compression specimens. Delamination and core failure in 108 mm x 108 mm specimens 52

2.5.8 Failure of thin ply tensile specimens perpendicular (90°) to load and 45° to load 54

2.5.9 Comparison of FE model and experimental results found by Voth 56

2.5.10 FE model range compared to experimental results 61

3.1.1 Zoned U.S. map with regard to thermal performance requirements 66

3.3.1 Foam it Green® incorporated within air voids created by the 3-D core for a typical shear specimen 71

3.3.2 Ply removed showing even foam expansion. End and longitudinal cuts showing consistent foam distribution 74

3.3.3 Tubing attached to end of nozzle. Typical foaming result of longer specimens prior to trimming 74

3.3.4 Voids discovered in test specimens and additional foam placed due to voids discovered 75

3.3.5 Typical radiant barrier installation at roof framing 76

3.3.6 Radiant barrier installation within wood-strand sandwich panels .. 77

3.3.7 Typical installation of radiant barrier 78

3.3.8 Foam incorporated wood-strand sandwich panel and radiant barrier incorporated sandwich panel 79

3.3.9 Longitudinal flexure test and transverse core shear flexure test showing foam 80

3.4.1 R-values for commercial products and wood-strand sandwich panels 83

3.4.2 R-values normalized by thickness for commercial products and wood-strand sandwich panels 84

3.4.3 Longitudinal flexural specimen failure between core and bottom ply and top ply buckling. Transverse flexural specimen failing in bottom ply tension and top ply buckling 85

3.4.4 Load versus displacement of sandwich panels with and without foam 86

3.4.5 Bending stiffness for wood-strand sandwich panels with and without foam, OSB, and plywood 87

3.4.6 Normalized bending stiffness for wood-strand sandwich panels with and without foam, OSB, and plywood 88

3.4.7 Delamination and flexure failure in longitudinal core shear specimen. Bottom ply tension and delamination failure in transverse core shear specimen 89

3.4.8 Core shear modulus comparison 90

3.4.9 Load versus displacement showing specimen stiffening 91

3.4.10 Load versus displacement zooming in at wood-strand failure 92

3.4.11 Delamination failure in 215 mm x 215 mm specimen at wood-strand failure prior to stiffening caused by foam. Delamination failure in 108 mm x 108 mm specimen at wood-strand failure 92

3.4.12 Compressive strength of wood-strand sandwich panels with and without foam 93

3.4.13 Compression modulus of sandwich panels with and without foam 94

3.5.1 Parallel thermal resistance through wall 96

3.5.2 R-values for typical wall construction 97

3.6.1 Possible panelized wall system utilizing wood-strand sandwich panel research 99

Chapter 1

Introduction to Creating a More Sustainable Wood-Strand Sandwich Panel With 3-D Core

1.1. Introduction:

With the advent of green building design and emphasis on reduction of greenhouse gas (GHG) emissions and carbon footprint, there is a demand for sustainably produced building materials with improved energy performance in addition to structural performance. Typical building design and construction practices must follow sustainable development. The definition of sustainable development is accepted around the world as “development that meets the needs of the present without compromising the ability of future generations to meet their own need” (Brundtland Commission 1987). In the United States, designers and contractors are focusing on sustainable construction. This is defined as any construction that focuses more on minimizing environmental impact than typical construction during the construction phase and the operational life cycle of the facility. Green building is another main focus that is a subcomponent of sustainable construction and focuses on vertical construction (buildings). Sustainable construction is an international concern and energy efficiency is a high priority in many countries (Haselbach 2008). This research is aimed toward development of a more energy efficient building envelope component than oriented strand board (OSB) for “green” building construction.

A majority of GHG emissions from residential and commercial buildings can be attributed to operational energy. These buildings account for almost 39% of the total U.S. energy consumption and 38% of U.S. carbon dioxide emissions. Carbon dioxide is considered to be a main reason for changes in the atmosphere, and the U.S. Green Building Council (USGBC) has been looking at methods to lower the emission of carbon dioxide by setting goals for reducing carbon emissions by at least 50% in all newly registered projects. Improving operational energy performance not only decreases carbon emissions but also increases our energy security by reducing our dependence on fossil fuels (Haselbach 2008).

Chris Voth (2009) has developed a prototype of lightweight wood-strand sandwich panels from underutilized small-diameter trees to reduce environmental impact. It is considered sustainable because the panel uses less wood-strands and adhesive and provides a functional cavity, which can be used for a variety of purposes [chases for insulation, ventilation, and inserting utilities such as electrical wiring and plumbing (Winandy, Hunt, Turk, Anderson 2006)] to reduce operational energy consumption of a building. Voth used a beam theory approach to design a mold to manufacture the corrugated core of the panel and established that panels can be used as a structural sheathing element in a typical building envelope. The goal of this study was to employ strategies to improve the thermal properties of wood-strand sandwich panels while meeting or exceeding the structural performance requirements.

1.2. Objectives:

The goal of this study was to develop a more sustainable building envelope material that meets the requirements of both structural and energy performance for use in residential construction. Research was continued from past work on wood-strand sandwich panels by Voth (2009). Methods to improve thermal performance of a building envelope material are vital as energy and building codes begin to mesh. However, improvements in energy efficiency may affect structural integrity of a material, thus mechanical properties were also analyzed.

More efficient design and analysis of the corrugated core of the sandwich panel will also be required for future improvements and development of panelized systems. Finite element modeling is a common means to analyze structural products with complex geometries once material properties and boundary conditions are known. Objectives to reach this goal are to:

- Construct sandwich panels based on previous research and revaluate their mechanical properties to ensure they can be replicated.
- Develop a finite element model to predict the behavior of a flexure specimen from sandwich panel and validate the model.
- Evaluate thermal properties of sandwich panels for comparison against similar sheathing materials in the building construction market.
- Explore strategies for improvement of sandwich panel thermal properties using commercially available materials within panel cavities.
- Determine the effects of incorporated materials on the structural integrity of the wood-strand sandwich panels.

1.3. Motivation:

The federal government has been involved in sustainable development with the creation of the U.S. Department of Energy's (DOE) Building America program along with Federal Executive Orders (U.S. Department of Energy 2010). Building America focuses on research and development of next generation energy efficient components and materials with a goal of producing new residential buildings that use 30% to 50% less energy on average by 2011 to 2016 compared to 2009 energy codes. Goals to achieve are based on climate zones such that housing in cold climates have until 2016 to achieve the 50% mark, while housing in marine climates have until 2014 to reach the same mark. The program also strives for reduced time of construction and on-site wastage aside from increased energy efficiency of existing homes. In addition to the creation of DOE's Building America program, former President George W. Bush signed Executive Order 13423 in 2007, stating that Federal agencies shall improve energy efficiency and reduce GHG emissions through reduction of energy consumption by 3% annually through the end of 2015, or 30% by the end of 2015 based on the agency's energy use in 2003 (Strengthening Federal Environmental, Energy, and Transportation Management 2007). In 2009, President Barack Obama signed Executive Order 13514, expanding on energy reduction requirements of Executive Order 13423 by stipulating that all new Federal buildings entering the design phase in 2020 or later are required to achieve net zero energy by 2030 (Federal Leadership in Environmental, Energy, and Economic Performance 2009).

Declining forest health of our national forests is also motivation for more sustainable practices. Overgrowth and dense national forests due to non-removal of

small-diameter timber is one of the leading causes for forest fires in the United States. According to USDA Forest Service Forest Inventory Analysis data (U.S. Department of Agriculture 2002), in the combined forested areas of Colorado, Idaho, Montana, and Wyoming, there are more than 29.7 x 10^6 metric tons (32.8 x 10^6 tons) (oven-dry basis) of unmerchantable timber less than 100 mm (4 in) in diameter (Hunt and Supan 2005). Without an economically viable solution to recover fuel treatment costs, small-diameter timber are left standing or felled and left on the ground thus becoming a fire hazard as it dries (Hunt 2004). Additionally, as communities grow closer to forested areas, risk of property loss and even life increase (Hunt and Winandy 2003). Finding high-value markets for this low-value and underutilized woody biomass is a potential solution to cost-effective removal of hazardous fuel from our forests to mitigate forest fires and improve forest health. Wood-strand sandwich panels offer a value-added opportunity to convert underutilized small-diameter timber into high performance building envelope components.

With structural and energy performances combined in building codes, the wood and wood-based composite products industry should consider new strategies to produce premium wall, flooring, and roofing materials for green building construction. If these panels can be constructed off-site to specifications, it will shorten the time of construction as well as reduce on-site wastage, leading to sustainable materials and construction practices. Developing composites with improved thermal efficiencies while meeting structural requirements will revitalize our forest products industry by providing new markets.

1.4. Background:

1.4.1. Core Design for Sandwich Panel:

Recent development of lightweight sandwich panels at Washington State University by Yadama and his team (Voth 2009) was the basis for this study. A mold was developed and both wood-strand and old newsprint (ONP) 3-D core sandwich panels were constructed and tested at the Composite Materials and Engineering Center (CMEC). In designing the 3-D core, beam theory was applied to determine required shear bonding area at the interface of the 3-D core and outer plies and adequacy of 3-D core wall thickness to carry compression loads without crushing or buckling. Wood-strand sandwich panel specimens were tested for beam flexure, core shear flexure, and flatwise compression.

Compared to OSB and plywood, sandwich panels were stiffer, and their normalized performance (to density) is superior to currently used panels. However, potential improvement in mechanical properties may come from changes in shear area width in future studies. Assumed shear stress for the wood-strand material during mold design resulted in a shear area calculation that was not adequate to withstand stresses at the interface of the core and outer plies. It is estimated that shear area width has to increase from 19.05 mm (0.75 in) to 31.5 mm (1.24 in). Further analysis done by Voth determined that with the current core geometry, required rib width would need to be 40.6 mm (1.6 in). Manufacturing a new mold with the revised rib width is extremely costly and development of a computer model may be a more feasible means of initial analysis. Development of a finite element model representing tests done at WSU is

discussed in Chapter 2. Future studies may use the model as a basis for improved core geometry and subsequent mold design.

1.4.2. Manufacturing of Wood-Strand Sandwich Panels:

Wood-strand sandwich panels were manufactured by bonding thin plies of wood strands (Weight 2007) on either side of a core that was thermoformed using the mold designed by Voth (2009). This study employed similar methods as Weight and Voth to fabricate sandwich panel layers and laminate them to produce a lightweight panel. Ponderosa pine logs were used to produce wood-strands for the composite panels. Strands were sorted and dried in a box dryer (Figure 1.4.1) as it significantly minimizes the amount of fines produced compared to using a drum dryer.

Figure 1.4.1: *Wood strands drying in box dryer.*

Resin used and its application method (Figure 1.4.2) were similar to that discussed by Voth (2009). Waste factor was changed from 20% to 10% due to material availability. General calculations for strand and resin amounts can be found in Appendix A.

(a) *(b)*

Figure 1.4.2: *(a) Resin applied to wood-strands in a rotating mixing drum. (b) Strands after resin has been applied.*

A wood-strand mat was formed using a forming box on a shake table (Figure 1.4.3) for better distribution of density throughout the length and width of the mat by eliminating tapered depth of wood strands at mat boundaries. The mat was placed

between oil-heated platens (Figure 1.4.4) set at a temperature of 160°C (320°F) and hot-pressed using pressing schedules developed by Voth.

(a) *(b)*

Figure 1.4.3: *(a) Wood strand mat on shake table. (b) Form box utilized during mat formation.*

Figure 1.4.4: *Hot press with 3-D mold installed.*

The outer 3.18 mm (1/8 in) thick plies were bonded to the 3-D core with a modified polyisocyanate (MDI) adhesive. The MDI adhesive reacts with moisture,

therefore, plies and core were conditioned to 20°C (68°F) and 65% relative humidity (12% MC), then sanded and misted with water. Approximately 80 grams of adhesive was applied per panel and plies were clamped, as shown in Figure 1.4.5. During the initial 3-hour cure time, bar clamps were periodically tightened to minimize poor bonding due to wood relaxation. Specimens remained clamped for 24 hours to allow for full curing. Test specimens were then cut to dimensions for testing and placed back in the conditioning room until testing.

Figure 1.4.5: *Clamping of wood-strand sandwich panels. Three panels were clamped at a time.*

Rigid foam insulation and radiant barrier were incorporated within the sandwich panel core to determine the effects of the materials on thermal and mechanical properties. Incorporation of these materials within the sandwich panels is discussed further in Chapter 3.

1.5. Scope of the Thesis:

The thesis is written as compilation of two papers (Chapters 2 and 3) with an introductory chapter (Chapter 1) and summary and conclusion chapter (Chapter 4). Chapter 2 presents thermal and mechanical properties of the wood-strand sandwich panels and finite element (FE) analysis of sandwich panel beam flexure. Voth's research already determined mechanical properties; however, larger specimens will be analyzed. Chapter 3 entails strategies to improve thermal efficiencies of sandwich panels and reevaluation of structural performance of the panel to evaluate influence of insulation.

1.6. References:

Brundtland Commission (1987). *Our Common Future*, Report by the Brundtland Commission [formally the World Commission of Environment and Development (WCED)], Oxford University Press.

Federal Leadership in Environmental, Energy, and Economic Performance, 74 Fed. Reg. 52117 (2009)

Haselbach, L. (2008). *The Engineering Guide to LEED-New Construction: Sustainable Construction for Engineers*. New York, NY: McGraw-Hill Companies.

Hunt, J. F. (2004). 3D Engineered Fiberboard: Finite Element Analysis of a New Building Product. *2004 International ANSYS Conference. Pittsburgh, PA, May 24-26, 2004.* USDA Forest Service, Forest Products Laboratory.

Hunt, J.F., Supan, K. (2005). Mechanical Properties For a Wet-Processed Fiberboard Made From Small-Diameter Lodgepole Pine Treetop Material. *Forest Products Journal, 55* (5), 82-87.

Hunt, J.F., Winandy, J.E. (2003). *Lam I-Joists: A New Structural Building Product From Small Diameter, Fire Prone Timber. Res. Note FPL-RN-0291.* Madison, WI: U.S. Department of Agriculture, Forest Service, Forest Products Laboratory

Strengthening Federal Environmental, Energy, and Transportation Management, 72 Fed. Reg. 3919 (2007)

U.S. Department of Agriculture. (2002). *Draft RPA 2002 forest resource tables. North Central Res. Sta., St. Paul, MN.* Retrieved January 5, 2011 from Mechanical Properties For a Wet-Processed Fiberboard Made From Small-Diameter Lodgepole Pine Treetop Material: http://www.ncrs.fs.fed.us/4801/fiadb/rpa_tabler/2002_rpa_draft_tables.htm.

U.S. Department of Energy. (2010). *Building America. Building Technologies Program.* Retrieved November 28, 2010 from U.S. Department of Energy: http://www1.eere.energy.gov/buildings/building_america/about.html

Voth, C. R. (2009). Lightweight Sandwich Panels Using Small-Diameter Timber Wood-Strand and Recycled Newsprint Cores. *Washington State University, Department of Civil and Environmental Engineering*.

Weight, S. W. (2007). A Novel Wood-Strand Composite Laminate Using Small-Diameter Timber. *Washington State University, Department of Civil and Environmental Engineering*.

Winandy, J.E., Hunt, J.F., Turk, C., Anderson, J.R. (2006). *Emergency Housing Systems From Three-Dimensional Engineered Fiberboard.* Madison, WI: U.S. Department of Agriculture, Forest Service.

Chapter 2

Experimental and Analytical Evaluation of Wood-Strand Sandwich Panels

2.1. Introduction:

Wood-based panels are extensively used as wall, roof, and floor sheathing in residential applications. Building envelopes play a large role in achieving net zero energy buildings, thus it would be beneficial to develop a sheathing material that satisfies building code requirements of not just structural but also energy performance. Accurate prediction of thermal performance is important in net zero energy design, but there is a need for a reliable database of thermal properties of building envelope components. The ASHRAE Fundamentals Handbook (American Society of Heating, Refrigerating and Air-Conditioning Engineers 2009) lists a large portion of building materials, however wood composite panels were not included until as recently as 2009 because of a limited amount of published data. Densification of wood material during manufacturing alters wood structure, thus changing physical properties of wood based panels from those of the solid wood from which they are made (Kamke and Zylkowski 1989). Corrugated strand core of the sandwich panel developed at WSU further obscures panel properties compared to typical OSB and plywood panels. One of the goals of this study involves thermal testing to obtain more accurate properties for

corrugated core wood-strand sandwich panels than what is currently in the ASHRAE Handbook.

Lightweight panels, where a corrugated core (3-D layer) is sandwiched between stress skin panels, have potential for developing panelized construction meeting both structural and energy performance requirements for residential buildings. Recent work at Washington State University (Voth 2009) has shown that 25.4 mm (1 in) deep wood-strand 3-D cores with thin walls [6.34 mm (1/4 in)] can be placed between thin wood-strand plies to form a sandwich panel. Thin wood-strand plies were also developed at WSU (Weight 2007, Weight and Yadama 2008). Development and fabrication of these panels were briefly summarized in Chapter 1 of this thesis.

Design and evaluation of structural behavior of a new material is commonly conducted using finite element (FE) modeling. A computer model allows for manipulations in panel design without designing a mold for the complex 3-D core and constructing a full size specimen for testing. FE modeling is more economical and efficient in appropriately designing ideal sandwich panel geometry and features. A model can provide insight into areas of stress concentrations and weaknesses in material in terms of resisting external forces, such as interfacial shear stress between core and outer plies. Potential failures within the panel can be evaluated and corrected. However, accurate modeling of complex geometries and anisotropic materials is a difficult task and could require modeling that considers not only material but even geometric nonlinearities.

Viability of the wood-strand sandwich panel as a building material depends on comparison to readily available commercial products such as OSB and plywood that

dominate the residential sheathing market. After testing the wood-strand sandwich panels, Voth (2009) showed that the longitudinal (strong axis) bending stiffness of the wood-strand sandwich panel was 17% greater than OSB's bending stiffness and 7% greater than 5-ply plywood panel of equal thickness (corrections from Voth's thesis. Updated results use data from linear region). However, sandwich panels utilize 60% less wood strands and resin by weight compared to OSB of equivalent thickness (i.e., a 32 mm (1-1/4 in) thick wood-strand sandwich panel uses the same amount of material as a 14 mm (9/16 in) thick panel of OSB). Longitudinal, transverse, and furnish weight comparisons are shown in Figure 2.1.1. When normalized based on specific gravity (SG), sandwich panels' specific bending stiffness was 140% and 119% stiffer than OSB and 5-ply plywood panels (Figure 2.1.2). This assumed a density of 641 kg/m^3 (40 pcf) for plywood and OSB and 312 kg/m^3 (19.5 pcf) for the wood-strand sandwich panel. This indicates that a thicker sandwich panel of similar mechanical properties can be substituted for currently used OSB panels while lowering material usage (Voth 2009). Voth also determined that the wood-strand sandwich panel could potentially support 1915 Pa (40 psf) live load and 958 Pa (20 psf) dead load without exceeding IBC (2006) deflection limits.

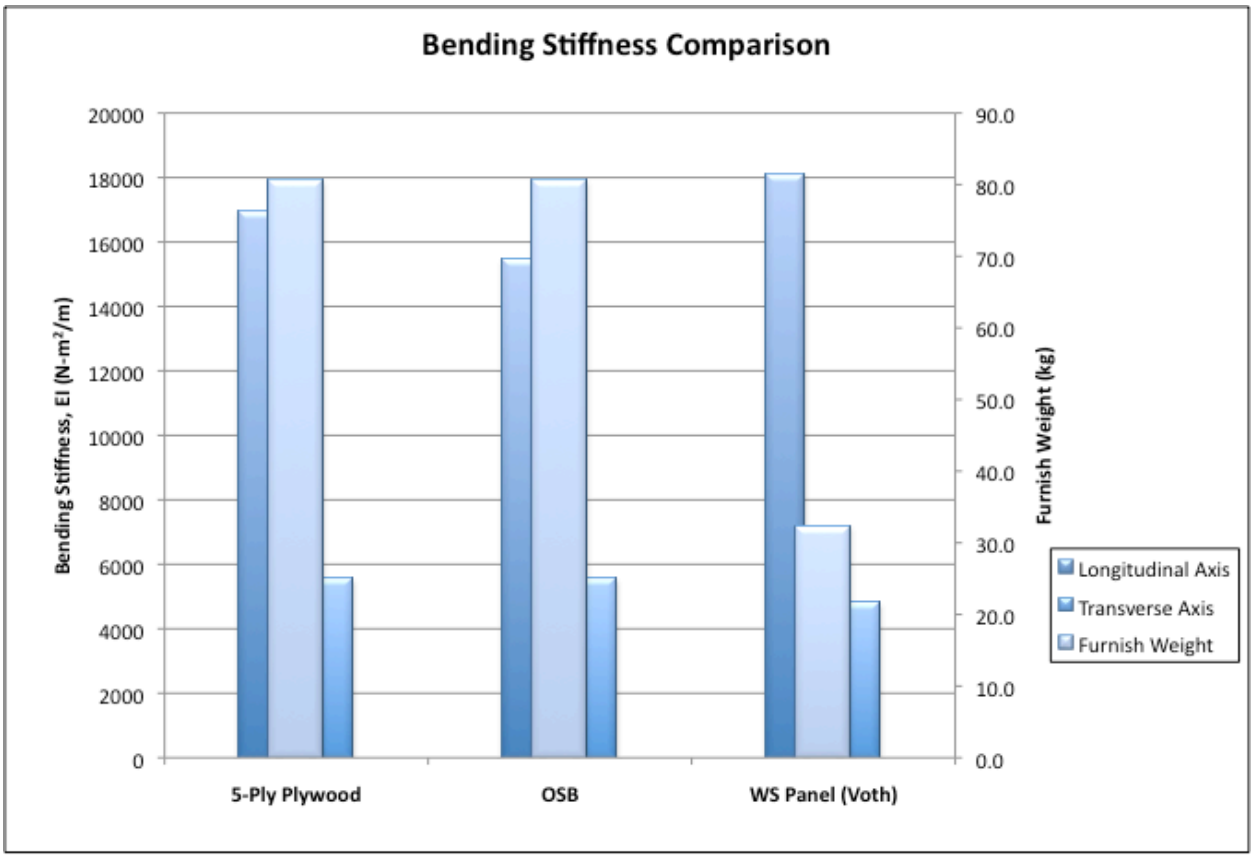

Figure 2.1.1: *Comparison of bending stiffness of selected panels versus their weight of materials. Bending stiffness values determined for 32mm (1-1/4 in) panels of 5-ply plywood and OSB (Voth 2009).*

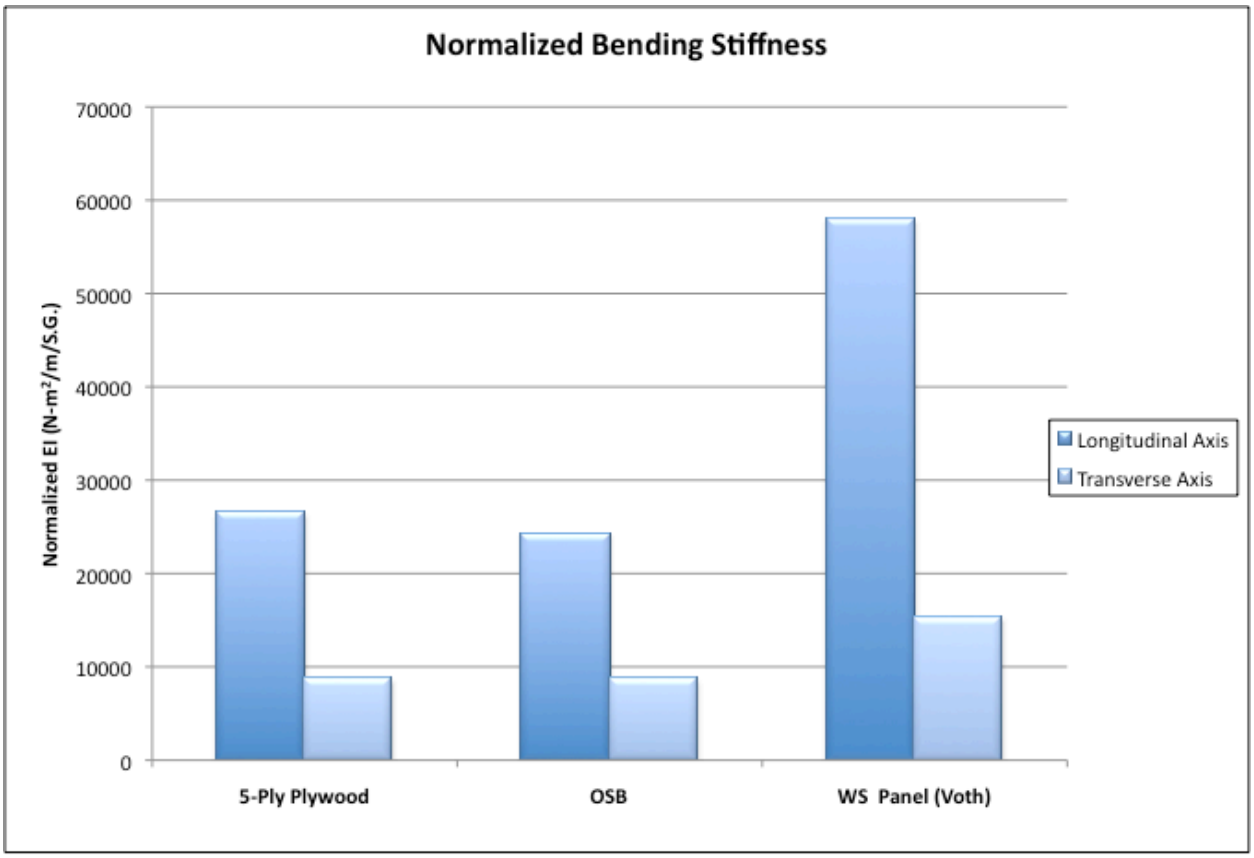

Figure 2.1.2: *Normalized bending stiffness comparison between plywood, OSB, and wood-strand sandwich panels (Voth 2009).*

Voth's thesis provided a basis for additional evaluation of sandwich panels in this study. Additional evaluation was done to determine if the properties can be replicated, and wider specimens were used to determine potential effects due to an additional longitudinal rib.

2.2. Objectives:

The primary goal of this study was to evaluate thermal properties of wood-strand sandwich panels with corrugated core and develop and validate an FE model of the

sandwich panel in flexure. An understanding of the thermal properties of panels is critical in evaluating their use as building envelope components for reducing operational energy consumption. An analytical FE model will assist in understanding panel behavior in flexure and provide insight into how to modify the core design and improve panel performance. To achieve these goals, the following objectives were undertaken:

- Estimate wood-strand sandwich panel thermal conductivity from an empirically derived equation.
- Characterize thermal behavior of wood-strand sandwich panels with a heat flow meter and compare their behavior with those of commercially available products (OSB and plywood).
- Evaluate material properties of stress skin outer plies and sandwich panels, specifically bending stiffness, core shear modulus, and flatwise compression modulus.
- Model the sandwich specimen to evaluate its behavior in flexure and compare with experimental results [results from both Voth (2009) and this study].

2.3. Background:

2.3.1. Heat Transfer:

Three modes of heat transfer exist: conduction, convection, and radiation. It is common that all three modes occur simultaneously and all modes are important with regard to building heat gain and loss. All three modes of heat transfer are a cause for concern while trying to reduce building loads on mechanical systems. In the summer, the sun's heat radiates to the building envelope, where the walls and roof conduct the

heat to the interior surface, thus heating up the interior space. In the winter, the warmer interior heat radiates and convects to the exterior surfaces and conducts heat through the building envelope to the colder exterior. To help control and reduce the heat and energy transfer that occurs during the year, insulation is placed in wall, roof, and floor cavities between framing. To further decrease the heat transfer, radiant barriers and commercial do-it-yourself (DIY) spray foam insulations may also be utilized.

2.3.2. Thermal Properties:

Thermal conductivity, λ, which is measured by the amount of heat passing through a material one meter thick with a surface area of 1 m^2 during one hour when the temperature difference across the material is one Kelvin (Davies 2001). Thermal conductivity is also temperature dependent; therefore, the average temperature when measured should be recorded. When a material continues to be in use, common factors such as temperature, ageing, and moisture affect thermal conductivity. Thermal conductivity typically decreases numerically as temperature decreases, therefore making the material a better insulator. Therefore, temperature should be considered when using sandwich panels in cold rooms or drying ovens. In the scope of this research, sandwich panels are only to be considered for wall, roof, and floor sheathing where under normal construction, λ_{10} (corresponds to an average temperature of 10°C (50°F) in a wall with an internal temperature of 20°C (68°F) and an external temperature of 0°C (32°F)) is used for the building envelope. Common insulating materials contain a gas with a lower thermal conductivity than air; therefore, as the material ages, the gas may diffuse out and be replaced by air causing the thermal conductivity to increase.

Lastly, since water is a great conductor, increasing MC in the material increases the thermal conductivity. This shows undesired effects to thermal conductivity caused by temperature, ageing, and moisture (Davies 2001).

Thermal resistance, R, is the common property used to determine how well a material insulates. Typical insulation is commonly classified based upon its R-value where the higher the R-value, the better the insulator. Once thermal conductivity of a material is known, R can be calculated using Equation 2.3.1. By knowing R-values for all building materials used in construction, an easy calculation can be done to determine the R-value of the overall building envelope.

$$R = \frac{t}{\lambda} \qquad \text{(Equation 2.3.1)}$$

R = thermal resistance, m^2-K / W (hr-ft^2-°F / Btu)

t = material thickness, m (in)

λ = material thermal conductivity, W / m-K (Btu-in / hr-ft^2-°F)

2.3.3. Previous Thermal Testing:

New federal and code requirements have created a need for more effective materials or methods to sustain comfortable temperatures in living environments while reducing energy consumption. Development of materials that have superior thermal insulation abilities and warmth keeping properties is a must for the wood based panel industry, thus resulting in testing of thermal properties. Thermal conductivity, λ, thermal resistance, R (insulation ability), and thermal diffusivity, D (warmth keeping property) of

a wood based sandwich panel were recorded in a study by Kawasaki and Kawai (2006) and compared to commercial wood based panels, solid wood, and commercial insulators.

Kawasaki's and Kawai's plywood-faced sandwich (PSW) panel consisted of plywood faces with a fiberboard core made from lauan (*Shorea Negrosensis*) with a total thickness of approximately 96 mm (3-3/4 in) and a density of approximately 680 kg/m^3 (42.5 pcf). Thermal conductivity was determined by a heat flow meter following guidelines provided in ASTM C 518 (American Society of Testing Materials 1981) where the upper cold plate and lower hot plate were set to 7°C (45°F) and 35°C (95°F) respectively. Thermal conductivity was first measured for PSW panels, and then broken down into face and core components to determine thermal conductivity of individual pieces. Using composite theory (Kawasaki and Kawai 2006), the thermal conductivity of the panel as a whole was calculated and found to be appropriate as the calculated results were approximately within 10% of the measured PSW panel results. Thermal conductivity, R-values, and other results for components and composite can be seen in Table 2.3.1.

Table 2.3.1: *PSW panel thermal properties found by Kawasaki and Kawai (2006)* [1,2,3]

Sample	Specimen	Thickness (mm)	Density (kg/m^3)	Thermal Conductivity, λ, (W/m-K)	Thermal Resistance, R, (m^2-K/W)	Thermal Diffusivity, D, (m^2/h)
PSW350	Upper face	9	670 (41.8)	0.14 (0.972)	0.063 (0.358)	0.00053
	Lower face	9	690 (43.1)	0.14 (0.972)	0.064 (0.364)	0.00050
	Core	78 (3.07)	270 (16.9)	0.062 (0.430)	1.3 (7.38)	0.00057
	Composite	96 (3.78)	340 (21.2)	0.070 (0.486)	1.4 (7.95)	0.00050
PSW400	Upper face	9	660 (41.2)	0.13 (0.902)	0.068 (0.386)	0.00049
	Lower face	9	690 (43.1)	0.14 (0.972)	0.065 (0.369)	0.00049
	Core	78 (3.07)	350 (21.8)	0.069 (0.479)	1.1 (6.25)	0.00049
	Composite	96 (3.78)	410 (25.6)	0.077 (0.534)	1.2 (6.82)	0.00046

[1] PSW350 and PSW400 represent different density specimens defined in Kawasaki's and Kawai's study

[2] Mean temperature was approximately 21°C

[3] U.S. units (inch, pcf, Btu-in / ft^2-hr-°F, and ft^2-hr-°F / Btu respectively) shown in parentheses

Kawasaki and Kawai (2006) found that these well-balanced thermal insulation and thermal diffusivity properties of the PSW panels could improve comfort and energy efficiency of indoor environments by maintaining temperatures and minimize severe temperature fluctuations in residences exposed to diurnal and seasonal temperature changes. It is the intention of this study to accomplish similar thermal performances as Kawasaki's and Kawai's material, thus making an efficient panelized system for residential construction.

2.3.4. Previous Finite Element Analysis:

Recent work with FE modeling of wood-composite sandwich panels has been done at the Forest Products Laboratory by Hunt (2004). Hunt used FE modeling to simulate ASTM C 393 (core shear of sandwich constructions) for 3-D engineered fiberboard and evaluated the influence of core rib angle, core rib thickness, rib spacing, and pattern width. Modeling was based on simple corrugated geometry, as shown in Figure 2.3.1, and he modeled both 2-D and 3-D representations of the panel for

compression and bending behavior, respectively. To represent the panel as a whole, Hunt took advantage of symmetry within the panel geometry and defined symmetry boundary conditions (BC) at the beam's mid-point cross-sectional area and along each side of the model.

Figure 2.3.1: *Simple corrugated core shape used in Hunt's FE model (Hunt 2004).*

Hunt also considered large displacement for the FE analysis, where displacement "may be 'large' if it is as little as half the plate thickness" (Cook, Malkus, Plesha, Witt 2002). Corrugation of the wood-strand panels causes significant membrane stress to occur within the material. These membrane stresses make lateral deflection smaller than it would be if load was supported by only bending moments. Because membrane stresses have an appreciable effect, it is important to include their variation with large displacement.

Small-diameter timber material was utilized in Hunt's study where material properties were determined from previous work done by Hunt and Winandy (2002). However, the material properties were assumed isotropic and linearly elastic with an

estimated Poisson's ratio of 0.3 (Hunt 2004). The wood-strand composite in this study should be considered transversely isotropic rather than assuming panel construction to be isotropic. Hunt noted that until material properties of fiberboard are more accurately represented, it is possible that failure may occur significantly before the FE model would predict it. This is especially true for wood-strand sandwich panels with a complex 3-D core.

2.4. Materials and Methods:

2.4.1. Sandwich Panel Material:

Wood-strands utilized in fabrication of sandwich panels (corrugated core and stress skin plies) were taken from Ponderosa Pine logs per Voth (2009) and Weight (2007) and were described in Chapter 1 (White 2011). Panel manufacturing and fabrication were also discussed in Chapter 1.

2.4.2. Empirical Determination of Thermal Conductivity:

A study by Kamke and Zylkowski (1989) found that thermal conductivity of wood based composites is strongly dependent on specific gravity (SG) with little evidence of species influence. Specimens in their study with the lowest SG had the lowest thermal conductivity while the highest SG had the highest thermal conductivity. In this study, determination of specimen specific gravity (SG) and knowledge of specimen conditioning (specimen MC) allowed thermal conductivity to be estimated by using Equation 2.4.1 developed by MacLean (1941). MacLean developed the equation for wood based composites with MCs less than 40% by measuring thermal conductivity of

multiple wood specimens over a large range of SGs and MCs (Siau 1995). Kamke and Zylkowski also determined that variation in thickness for OSB and hardboard fiberboard showed little or no effect on measured thermal conductivity, thus stressing the influence of only SG and MC variables in MacLean's equation.

$$\lambda_T = G \times (0.200 + 0.0038M) + 0.024 \qquad \text{(Equation 2.4.1)}$$

λ_T = transverse thermal conductivity, W/m-K

G = specific gravity

M = moisture content (as a percentage)

2.4.3. Specimen Tests:

2.4.3.1. Thermal Tests:

A Fox 304™ heat flow meter based on Fourier Law (Laser Comp 1999-2011) was used to determine thermal conductivity, λ, of wood-strand sandwich panels and commercial OSB. Three wood-strand sandwich panel specimens were tested and compared to three OSB specimens to evaluate any advantages over a commonly used sheathing material in residential construction. Specimen density was determined after being cut to 305 mm by 305 mm (12 in x 12 in) and conditioned to 20°C (70°F) and 50% RH. Wood-strand sandwich panels were placed in the heat flow meter such that three longitudinal ribs could be seen pointing upright and on the left wall of the heat flow meter chamber as shown in Figure 2.4.1. This oriented longitudinal axis of wood strands parallel to the front and back walls of the chamber. OSB specimens were also aligned

such that the length of the strands were parallel to the front and back walls, keeping consistent with sandwich panel specimens.

(a) (b)

Figure 2.4.1: *(a) Fox 304™ heat flow meter with 305 mm x 305 mm (12 in x 12 in) specimen. Note two of the three ribs being shown along the left wall of the chamber. (b) Chamber of Fox 304™ heat flow meter.*

The heat flow meter consisted of a cold plate on the top and a hot plate on the bottom of the chamber. Temperatures for each plate could be set to obtain a mean temperature for the specimen being tested. As stated earlier, λ_{10} is commonly used for normal construction. To achieve sandwich panel and OSB specimen mean temperatures comparable to in use conditions, the cold and hot plate were set to 0°C (32°F) and 25°C (77°F) respectively [mean temperature of 12.5°C (54.5°F)]. However, a mean temperature of 24°C (75°F) is defined for thermal properties of building materials tabulated in the ASHRAE Fundamentals Handbook (2009). For comparison to these tabulated values, a second test was conducted on all sandwich panel and OSB specimens at a mean temperature of 22.5°C (72.5°F). This defined cold and hot plate temperatures to be 10°C (50°F) and 35°C (95°F) respectively. Establishment of thermal

conductivity for sandwich panels and OSB allowed for thermal resistance, R, of the specimens to be calculated using Equation 2.3.1.

2.4.3.2. Mechanical Tests:

Beam flexure (ASTM D 7249 2006), core-shear flexure (ASTM C393 2006), and flatwise compression tests (ASTM C 365 2005) were conducted on sandwich specimens. To determine sandwich panel and its components' (3-D core and plies) densities, length, width, thickness, and weight were recorded prior to panel fabrication and panel testing. Voth's (2009) study also included these three tests; however, beam flexure and flatwise compression specimen width was changed from 108 mm (4-1/4 in) to 215 mm (8-1/2 in). The reason for increasing specimen width was to determine effects of an additional longitudinal rib. Core shear flexure specimen width remained at 108 mm (4-1/4 in) because of the short span length of 203 mm (8 in).

Beam flexure specimens measured 215 mm by 610 mm (8-1/2 in x 24 in) and were tested on an Instron™ 4400R test frame following guidelines set by ASTM D 7249. Five specimens were tested in the strong (longitudinal) direction and five were tested in the weak (transverse) direction (longitudinal correlating with supports being perpendicular to panel ribs while transverse correlates with supports being parallel to ribs). The standard sets a maximum width of 190 mm (7-1/2 in); however, the additional 25.4 mm (1 in) was allowed in this study to include the additional rib (rib geometry repeats every 108 mm). Wider specimens (215 mm) allowed for two longitudinal ribs to be aligned facing upward when testing longitudinal specimens. Alignment of load bars and support bars with the ribs for transverse specimens was difficult because of the

geometry of the 3-D core, consequently leading to a greater chance of ply failure. As a result of preparing wider specimens from the small panels that were fabricated, geometry between specimens did not match, which could lead to irregularities in the results.

Specimens spanned 560 mm (22 in) and were placed under a 4-point loading configuration with load bars at third points (Figure 2.4.2). To determine load rate for flexure specimens, a trial test followed the suggested standard load rate of 6 mm/min (0.25 in/min). The standard states that specimen failure shall occur within three to six minutes, however, the suggested load rate did not meet this criteria. Therefore, load rate was changed to 2 mm/min (0.075 in/min). Deflection was measured in the center of the specimen on the top ply surface using a linear variable differential transformer (LVDT). Bending stiffness, D, was calculated for the longitudinal and transverse specimens using results within the linear elastic region and Equation 2.4.2.

(a) *(b)*

Figure 2.4.2: *Beam flexure test apparatus. (a) Longitudinal specimen. Note two longitudinal ribs facing upward. (b) Transverse specimen with LVDT in place at mid-span.*

$$D = \frac{Pl^3}{28\Delta} \qquad \text{(Equation 2.4.2)}$$

D = bending stiffness, EI, N-m^2 (lb-in^2)

P = flexural load, N (lb)

l = span length, m (in)

Δ = deflection at mid-span at P, mm (in)

Ten core shear flexure specimens (five longitudinal and five transverse) were tested on an Instron™ 4400R test frame and measured 108 mm by 254 mm (4-1/4 in x 10 in).

Longitudinal specimens were tested such that the longitudinal rib was upward, similar to beam flexure specimens. Transverse specimen geometry did not allow for 3-D core ribs to be aligned with both the loading bar and the support bars, resulting in a greater chance for ply failure. To ensure failure within the three to six minute standard to minimize viscoelastic effects of the material, load was applied at a rate of 2 mm/min (0.085 in/min). A 3-point loading configuration with a specimen span length of 203 mm (8 in) was used per ASTM C 393 (test apparatus is shown in Figure 2.4.3). An LVDT was placed at the center of the specimen on the bottom surface to measure deflection. Once specimens were no longer within the linear elastic region, the LVDT was removed to prevent damage to the instrument. Results from the linear region and Equation 2.4.3 were used to determine the core shear rigidity, U. After obtaining core shear rigidity of the specimens, core shear modulus, G, was calculated using Equation 2.4.4.

$$U = \frac{Pl}{4\left[\Delta - \frac{Pl^3}{48D}\right]} \qquad \text{(Equation 2.4.3)}$$

$$G = \frac{4cU}{(d+c)^2 b} \qquad \text{(Equation 2.4.4)}$$

U = core shear rigidity, N (lb)

G = core shear modulus, MPa (psi)

P = flexural load, N (lb)

l = span length, mm (in)

Δ = deflection at mid-span, mm (in)

D = bending stiffness, EI, N-m^2 (lb-in^2)

d = total specimen depth, mm (in)

c = core depth, mm (in)

b = specimen width, mm (in)

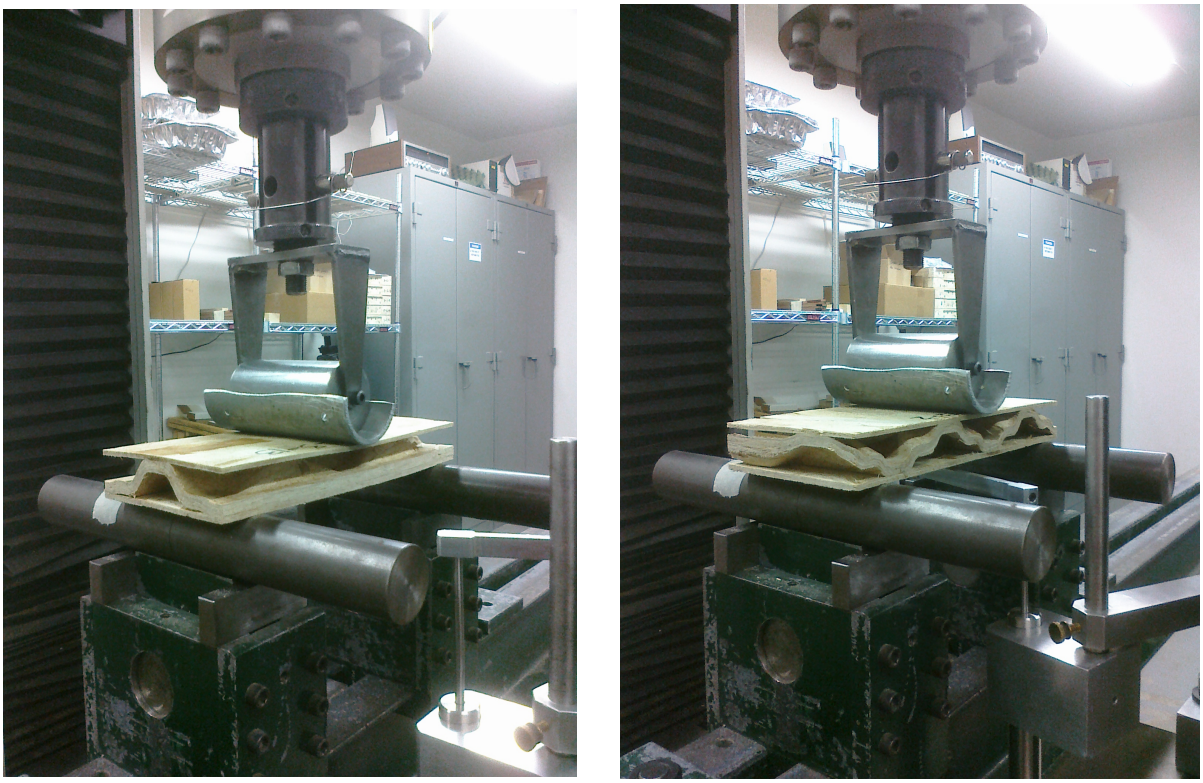

(a) *(b)*

Figure 2.4.3: *Core shear flexure test apparatus. (a) Longitudinal specimen. Note rib aligned upward in specimen. (b) Transverse specimen with LVDT placed on bottom ply.*

Compression tests were conducted on an Instron™ 4400R with a fixed bottom load platen and top load platen free to rotate [both platens measured 152 mm (6 in) in

diameter]. Five 108 mm by 108 mm (4-1/4 in x 4-1/4 in) and five 215 mm by 215 mm (8-1/2 in x 8-1/2 in) specimens were tested. The larger specimens had a specimen area [46,200 mm^2 (72.25 in^2)] greater than the standard maximum of 10,000 mm^2 (16 in^2) to analyze the effects of the additional bonding between ply and core. Additional bonding surfaces may prevent delamination on the edges or core crushing failure that occur commonly in smaller specimens. The middle rib of test specimens was aligned facing up as seen in Figure 2.4.4 to remain constant with Voth's (2009) test methods for a fair comparison of results. Following guidelines set by the ASTM standard; specimens were preloaded to an initial load of 45 N (10 lb), and then zeroed. Load rate was changed from the standard 0.50 mm/min (0.02 in/min) to 1.2 mm/min (0.045 in/min) to cause failure within three to six minute criteria. Ultimate flatwise compression strength and modulus were calculated using Equation 2.4.5 and Equation 2.4.6, respectively.

$$\sigma = \frac{P_{\max}}{A} \qquad \text{(Equation 2.4.5)}$$

$$E_c = \frac{St}{A} \qquad \text{(Equation 2.4.6)}$$

σ = flatwise compressive strength, MPa (psi)

E_c = compression modulus, MPa (psi)

P_{max} = ultimate force prior to failure, N (lb)

A = surface area of small specimen or platen for large specimen, mm^2 (in^2)

t = thickness of specimen, mm (in)

S = slope of linear region for load vs. displacement, N/mm (lb/in)

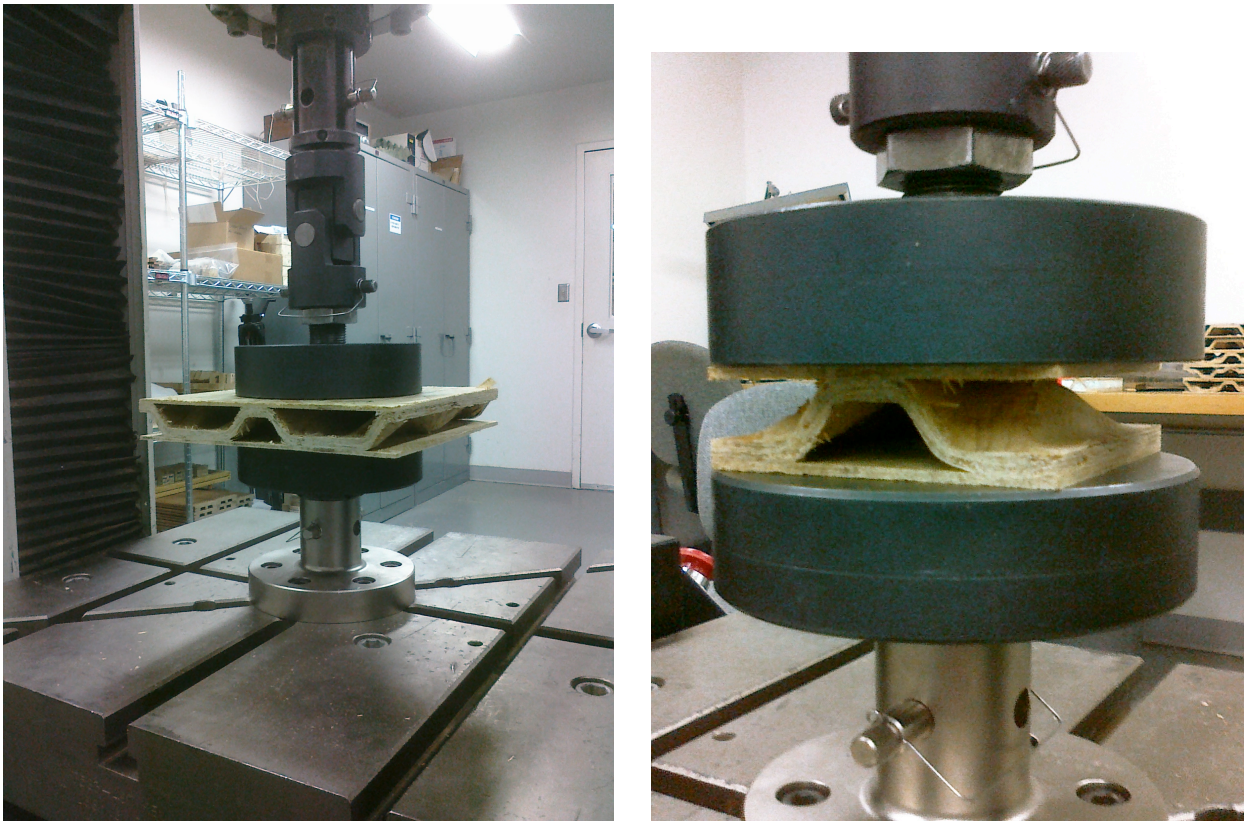

(a) (b)

Figure 2.4.4: *(a) 215 mm x 215 mm flatwise compression test apparatus. (b) 108 mm x 108 mm flatwise compression test. Note that both have rib aligned facing upward at center of load platen.*

2.4.3.3. Tensile Testing of Thin Plies:

For accurate representation of layers in the sandwich panel in an FE model, tensile specimens from thin wood-strand plies were tested. Material properties such as MOE, Poisson's ratio, ν, and shear modulus, G, of individual components of the sandwich panel must be known. Tensile testing of thin ply material with different strand orientations enables use of transformation equations to determine required material properties for modeling [wood-strands were aligned such that strands within the

specimen were parallel (0°), perpendicular (90°), and 45° to the direction of loading]. A total of 18 dog-boned thin ply tensile specimens (six of each orientation) were tested on an Instron™ 4466 test frame (Figure 2.4.5). Center of specimens measured 32 mm (1-1/4 in) wide rather than the ASTM D 1037 standard of 38 mm (1-1/2 in) because of the mold used to cut specimens. The specimen was loaded at a rate of 4 mm/min (0.15 in/min) following ASTM D1037, while a 25.4 mm (1 in) extensometer was used to measure strain in the direction parallel to the load. To determine Poisson's ratio, parallel (0°) specimens were loaded to approximately 30% of maximum capacity while using a 12.7 mm (1/2 in) extensometer to measure strain perpendicular to the load (transverse strain) (Figure 2.4.5 b). This allowed for strain data to be recorded while specimens stayed within the elastic region. Specimens were unloaded and then loaded again until failure, while recording strain parallel to the load. Strain and load data were used to calculate E_a, E_b, E_θ, ν_{ab}, and G_{ab} where a, b, and θ represent parallel/longitudinal, perpendicular/transverse, and 45° directions with respect to strand orientation, respectively (subscripts of "a" and "b" were used to correspond with the FE program, whereas subscripts of 1 and 2 are commonly used). Shear modulus, G_{ab}, is often difficult to obtain experimentally for new wood panel products. However, from tensile results in the longitudinal, transverse, and 45° directions and a rearranged transformation equation (Weight 2007), G_{ab} can be calculated per Equation 2.4.7.

$$G_{ab} = \left[\frac{2\nu_{ab}}{E_a} + \frac{\frac{1}{E_\theta} - \frac{\cos^4\theta}{E_a} - \frac{\sin^4\theta}{E_b}}{(\sin^2\theta)(\cos^2\theta)} \right]^{-1}$$ (Equation 2.4.7)

G_{ab} = shear modulus, MPa (psi)

E_a = longitudinal modulus of elasticity, MPa (psi)

E_b = transverse modulus of elasticity, MPa (psi)

E_θ = modulus of elasticity at θ, MPa (psi)

θ = angle of strands with respect to load, degrees

ν_{ab} = Poisson's ratio

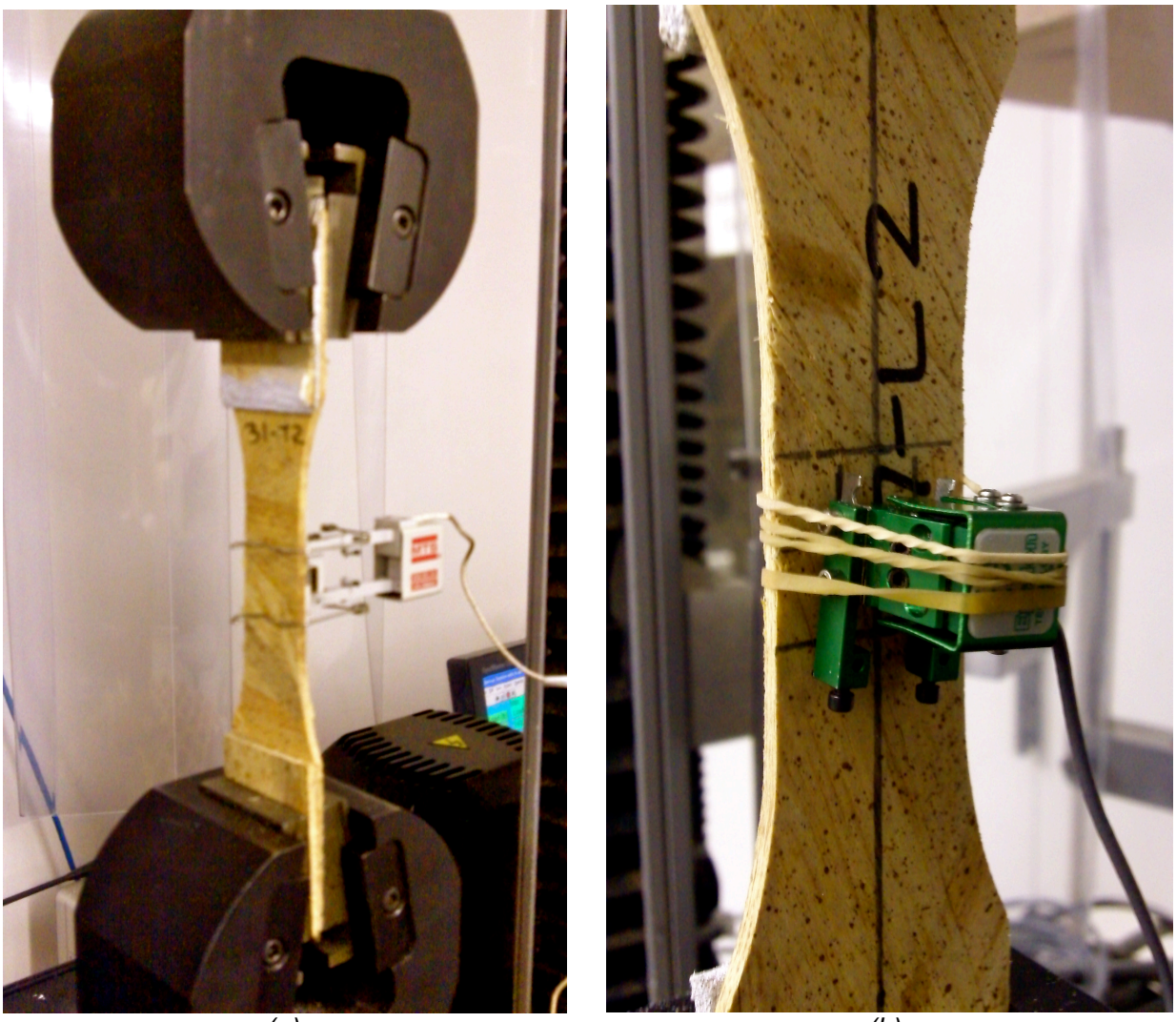

(a) (b)

Figure 2.4.5: *(a) Typical tensile test apparatus. (b) 12.7mm extensometer measuring strain perpendicular to load.*

2.4.4. Finite Element Model and Analysis:

2.4.4.1. Geometry and Boundary Conditions:

The initial FE model was developed within the software, ADINA™ (2008), and it represented the 108 mm by 610 mm (4-1/4 inch x 24 in) specimen spanning 520 mm (20-1/2 in) used by Voth (2009) in flexure tests following ASTM D 7249. A 4-point loading configuration with load applied at third points was used. Symmetrical sandwich

panel geometry allowed the FE model to have symmetry boundary conditions (BC), similar to Hunt's (2004) study, defined at the mid-span of the beam and at the peak of the rib. This configuration produced a model with overall dimensions of 54 mm by 305 mm (2-1/8 in x 12 in) with the support being 44.5 mm (1-3/4 in) from the end of the specimen (Figure 2.4.6). Appropriate symmetry BCs were input and the support was assumed to act as a roller, allowing rotation about the y- and z-axes and translation along the x- and y-axes per Figure 2.4.6.

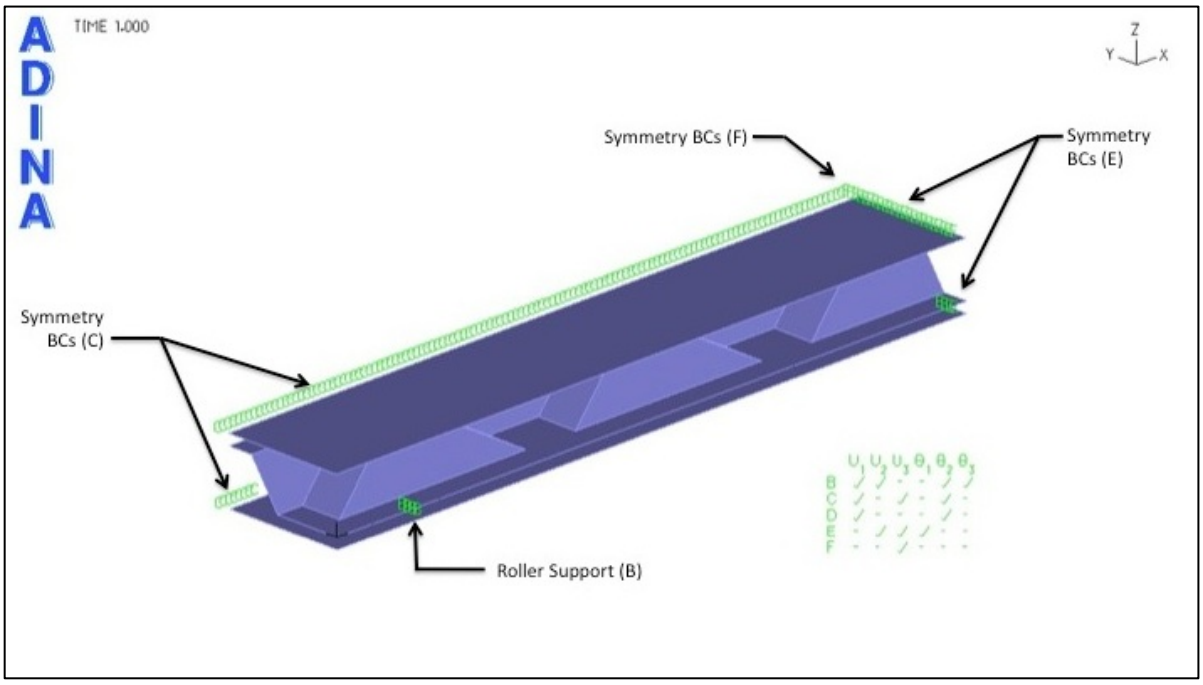

Figure 2.4.6: *FE model in ADINA. Coordinate system as shown in corner.*

2.4.4.2. Element Selection:

Three dimensional 9-node shell elements were utilized in the model rather than solid elements because of concerns with using 3-D solids to model relatively thin panels. When the structure/material modeled has a dimension that is extremely small

compared to the others, the use of 3-D solid elements is impractical due to the need for several elements through the thickness. To have reasonable element aspect ratios, an impractically large number of elements would be required. Shell elements are defined at the mid-surface of the thin material with a director vector prescribed in the direction perpendicular to the shell from each node location, thereby defining top and bottom surfaces. A 3x3x2 Gauss quadrature was used to integrate through the shell element thickness.

2.4.4.3. Material Properties:

Material properties were assumed to be linearly elastic and transversely isotropic. Ply and 3-D core materials were defined to have the same properties, as they were manufactured with the same wood-strands and resin, having similar resin content and density, but varying only in thickness. Values were obtained from Voth's (2009) study, as the objective was to create an FE representation of his experimental results. However, only modulus of elasticity, E, could be obtained from Voth. Shear modulus, G, and Poisson's ratio, ν, were obtained from Weight (2007). Voth followed Weight's study to manufacture thin wood-strand plies, therefore making it ideal to accurately obtain properties that were not recorded in Voth's study. Material properties can be seen in Table 2.4.1 where the local coordinate system a-b-c was defined as longitudinal, transverse, and through the panel thickness, respectively.

Table 2.4.1: *Material properties defined in FE model [1].*

E_a[2] (MPa)	E_b[2] (MPa)	E_c (MPa)	ν_{ab}[3]	ν_{ac}	ν_{bc}	G_{ab}[3] (MPa)	G_{ac} (MPa)	G_{bc} (MPa)
6370 (924000)	5840 (847600)	5840 (847600)	0.358	0.358	0.1	1364 (197800)	1364 (197800)	2660 (385273)

[1] a-axis aligned along longitudinal direction, b-axis aligned along transverse direction, c-axis aligned through material thickness.
[2] Denotes properties obtained from Voth (2009).
[3] Denotes properties obtained from Weight (2007).

Transversely isotropic material assumptions, such as the requirement that E_b is equal to E_c and Equation 2.4.8, were utilized to determine other required properties.

$$G_{bc} = \frac{E_b}{2(1+\nu_{bc})} \qquad \text{(Equation 2.4.8)}$$

Since shell elements were used and stress through the thickness is not considered, modulus through the panel thickness, E_c, has no effect. However, ADINA requires a value to be input, thus, values shown were defined.

The value of Poisson's ratio obtained from Weight is comparable to the assumed value of 0.3 used in Hunt's (2004) analysis. During the literature review of this study, recommendations for material properties were explored from previous FE modeling research for OSB material (Grandmont, Cloutier, Gendron, Desjardins 2010 and Zhu, Guan, Rodd, Pope 2005). The material properties generally were similar to values defined in this study. However, there were some discrepancies dealing with principles of a transversely isotropic material such as E_b not equal to E_c [E_b ranging from 2600 MPa (377000 psi) to 2760 MPa (401000 psi) versus E_c equal to 130 MPa (18850 psi)]. The

reason for these discrepancies is unknown; therefore this study continued using values and assumptions discussed earlier.

2.4.4.4. Mesh and Load:

FE analysis yields greatest accuracy when a fine mesh is defined. Mesh density was defined by an element length of 5 mm (0.2 in), which is relatively fine compared to the 3-D core thickness of 6.4 mm (0.25 in) and ply thickness of 3.2 mm (0.125 in). This mesh density, incorporated with 9-node elements, provided an average spacing of 2.5 mm (0.1 in) for the nodes.

Force controlled loading based on the mean maximum flexural load of 2710 N (609 lbs) found by Voth (2009) was originally modeled. Since there were two loading heads, point loads were defined at each node by linearly distributing 1355 N (304.5 lbs) over all nodes below the loading head. Results were compared to the mean maximum flexural deflection of 12.8 mm (0.503 in) found by Voth. However, force-controlled loading resulted in heavy local buckling in the top ply. Therefore displacement controlled loading was considered.

Displacement controlled loading is a better representation of the test, as load heads apply load by head displacements defined in mm/min (in/min). A displacement of 19 mm (0.75 in) was defined as shown in Figure 2.4.7 to ensure Voth's recorded deflection of 12.8 mm (0.503 in) was achieved at the mid-span of the specimen. With the mean maximum deflection of 12.8 mm (0.503 in) compared to the overall sandwich panel thickness of 31.8 mm (1-1/4 in), large displacement was used in the analysis similar to Hunt's (2004) study. The FE analysis was assumed nonlinear and a time

function with 10 time steps was defined, thus representing experimental loading as the model gradually loaded the specimen to the defined deflection.

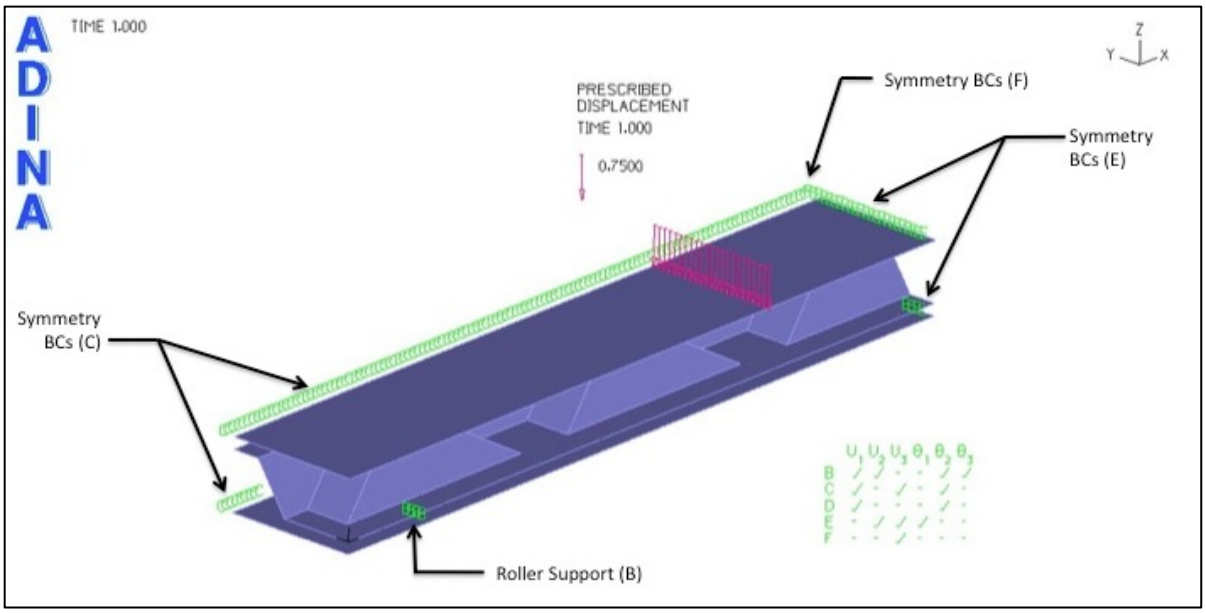

Figure 2.4.7: *FE model showing displacement controlled loading.*

2.4.4.5. Core/Ply Interface:

To account for bonding between the plies and the 3-D core, rigid links were modeled between nodes of the two components (Figure 2.4.8 and Figure 2.4.9). Surfaces were defined as master and slave such that slave surface nodes were constrained to have the same translation and rotation as master surface nodes. This caused the distance and rotation between master and slave nodes to remain constant (ADINA 2008). Slave nodes did not have any fixed degrees of freedom (DOF). Therefore, BCs were only defined at master surfaces. When a rigid link is attached to a node of a shell element, 6 DOFs must be used for the node. In this study, the default

number of DOFs associated with shell nodes were defined as “automatic”, allowing the program to define 5 or 6 DOFs based on the geometry of the model.

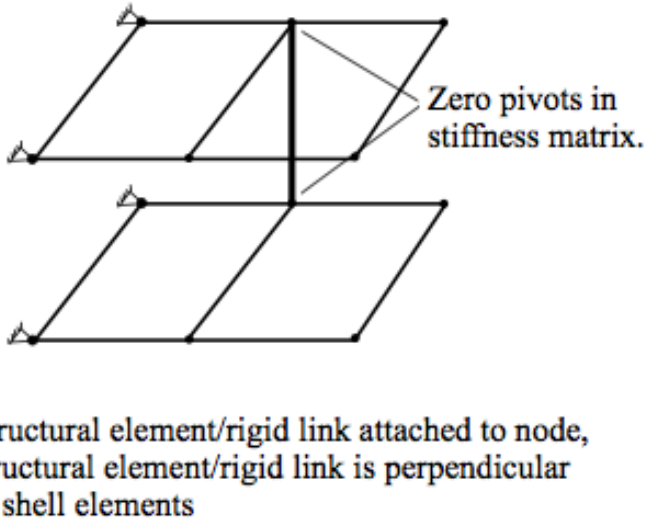

Figure 2.4.8: *Typical rigid link connection from node to node (ADINA 2008).*

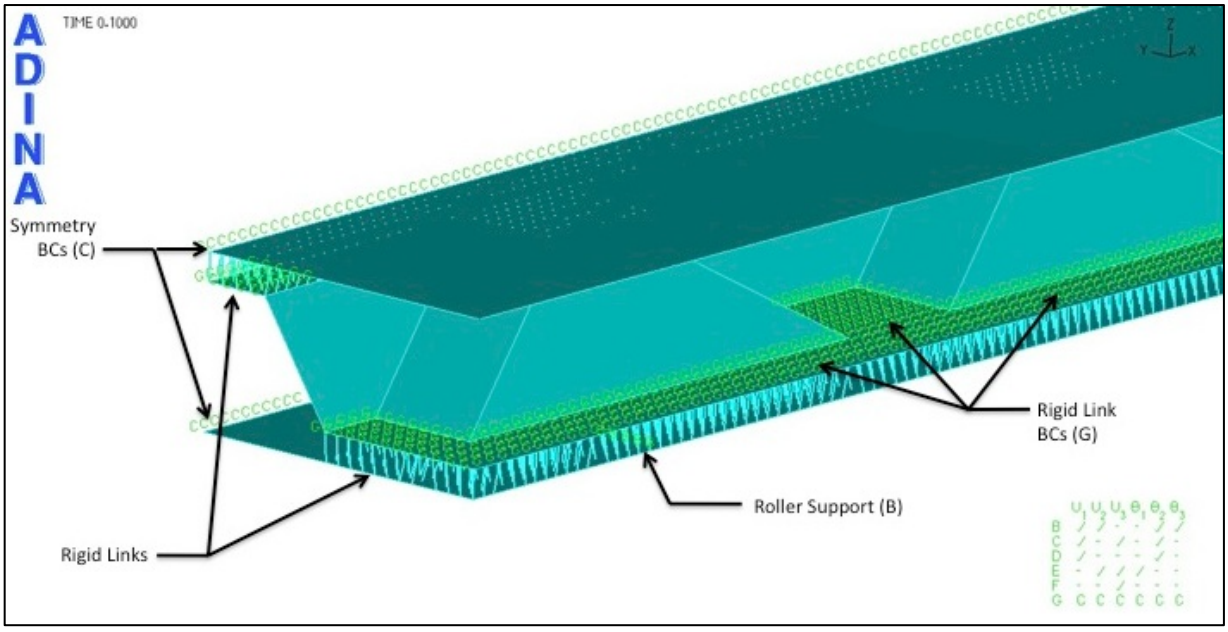

Figure 2.4.9: *Rigid links defined in FE model.*

2.4.4.6. Analysis Options:

Other analysis options that were utilized in this study were the use of automatic time stepping (ATS), no use of line searches, and the low-speed dynamic option. ATS helped with convergence in the solution. If no convergence occurred with the user-specified time step, the program automatically subdivided the time step until it reached convergence. In some cases, the time step size may have been increased to accelerate the solution (ADINA 2008). Line searches are typically used to reduce the number of iterations and have the ability to use bigger time steps to reduce overall solution time. However, in the case of this study, analysis typically ran quickly, therefore, line searches were not utilized. The low-speed dynamics option was a precautionary measure to help overcome any convergence difficulties with snap-through and snap-back that might have occurred.

2.5. Results and Discussion:

2.5.1. Thermal Properties Determined by Heat Flow Meter:

Thermal conductivity of the sandwich panel and OSB specimens tested was obtained from the Fox 304™ heat flow meter. Using specimen thickness and Equation 2.2.1, thermal resistance, R, was calculated for each. Near typical living conditions [12.5°C (54.5°F)] the wood-strand sandwich panel specimens had a mean R-value of 0.307 m^2-K/W (1.74 ft^2-hr-°F/Btu) compared to a mean R-value of 0.126 m^2-K/W (0.716 ft^2-hr-°F/Btu) for OSB specimens. OSB specimens tested in this study were validated by comparing to published ASHRAE (2009) values, where experimental R-values were

approximately 3% to 13% higher than published values (0.11 m^2-K/W for 9 mm to 11 mm OSB and 0.12 m^2-K/W for 12.7 mm OSB).

Table 2.5.1: *Summary of wood-strand sandwich panel and OSB panel thermal properties [1] (Note that R-values are for thickness of panel shown in the thickness column).*

		Thickness (mm)	Density (kg/m^3)	Thermal Conductivity, λ (W/m-K)	Thermal Resistance, R (m^2-K/W)	Mean Temp (°C)
Wood-Strand Panel	Mean	32.5	287	0.112	0.290	22.5
	Mean (US)	*1.28*	*17.9*	*0.778*	*1.65*	
	Std. Dev	0.916	5.27	0.003	0.006	
	% COV	2.8	1.8	2.5	2.2	
	Mean	32.5	287	0.106	0.307	12.5
	Mean (US)	*1.28*	*17.9*	*0.737*	*1.74*	
	Std. Dev	0.916	5.27	0.003	0.008	
	% COV	2.8	1.8	2.9	2.8	
OSB	Mean	11.7	652	0.095	0.124	22.5
	Mean (US)	*0.463*	*40.7*	*0.659*	*0.703*	
	Std. Dev	0.13	6.4	0.001	0.002	
	% COV	1.1	1.0	1.1	1.6	
	Mean	11.7	652	0.093	0.126	12.5
	Mean (US)	*0.463*	*40.7*	*0.647*	*0.716*	
	Std. Dev	0.13	6.4	0.001	0.003	
	% COV	1.1	1.0	1.1	2.4	

[1] U.S. units are in inches, pcf, Btu-in/ft^2-hr-°F, and ft^2-hr-°F/Btu respective to table

To determine if wood-strand sandwich panels are a viable solution to greater building envelope efficiency, the R-value for the sandwich panels was compared to R-values obtained by Kawasaki for typical building materials (OSB, plywood, and insulators) and his PSW in Figure 2.5.1. Data showed that the R-value of a 32 mm (1-1/4 in) wood-strand sandwich panel was 190% greater than 12.7 mm (1/2 in) OSB and plywood but approximately 45% of the 25 mm (1 in) insulators. When compared to Kawasaki's much thicker PSW [95 mm (3-3/4 in)] R-value for wood-strand sandwich panels was approximately 30% of Kawasaki's PSW. This shows that the PSW is an effectively better material to be utilized in building envelopes. However, once materials

were normalized by thickness in Figure 2.5.2, sandwich panels were comparable to Kawasaki's PSW. Therefore, a thicker sandwich panel [114 mm to 140 mm (4-1/2 in to 5-1/2 in)] incorporating two or three corrugated 3-D cores placed back to back and bonded to outer wood-strand faces and sandwiched by thick veneer sheets (Figure 2.5.3) may be a feasible solution to increase thermal performance of building envelopes.

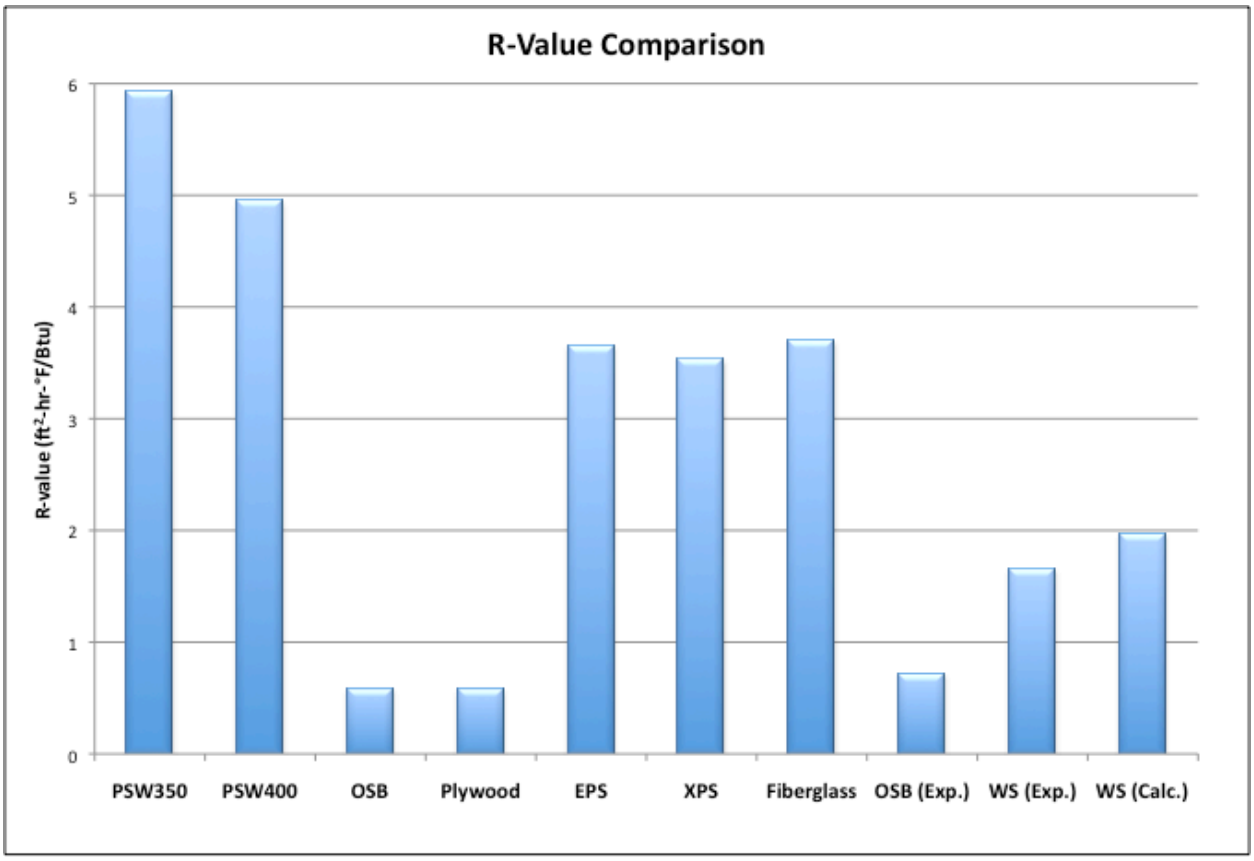

Figure 2.5.1: *R-values of wood-strand panels (WS), both experimental (Exp.) and calculated (Calc.), compared to Kawasaki's PSW, OSB, plywood, and commercial insulators (EPS, XPS, Fiberglass). OSB, plywood, and insulator values obtained from Kawasaki (2006) excluding OSB (Exp.) tested in this study. Given in U.S. units. 1R = 1 ft^2-hr-F / Btu = 0.176 m^2-K / W.*

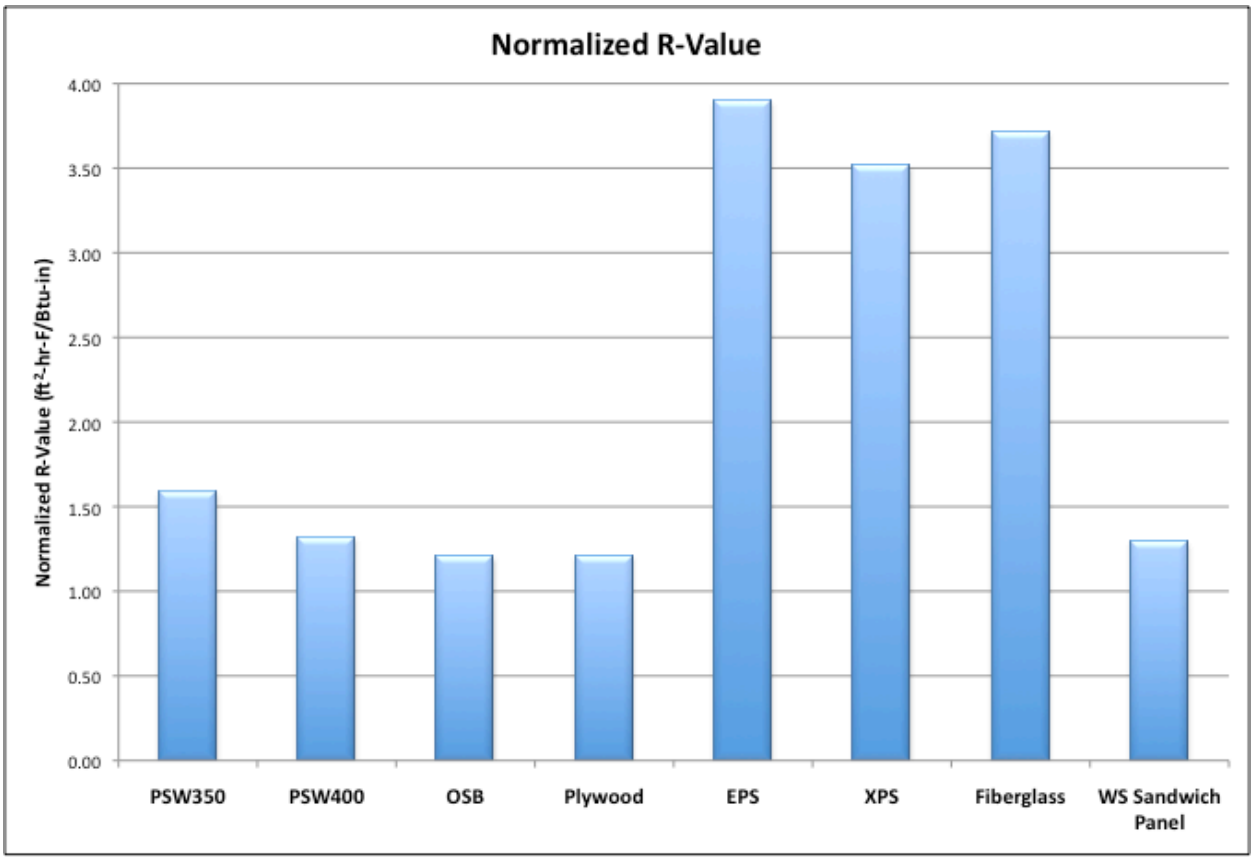

Figure 2.5.2: *R-values normalized by thickness and given in U.S. units. 1R = 1 ft^2-hr-F / Btu = 0.176 m^2-K / W.*

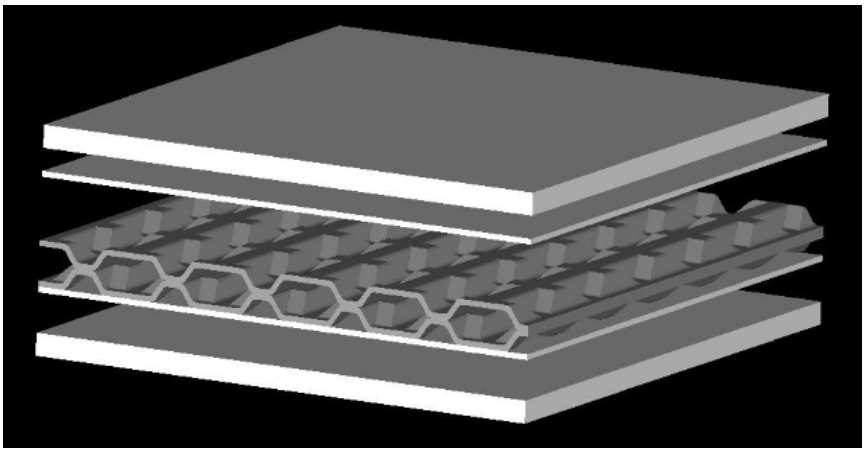

Figure 2.5.3: *Thicker sandwich panel construction. Utilizes multiple corrugated cores, thin wood-strand plies, and thick veneer panels. Shows individual components.*

2.5.2. Empirical Thermal Conductivity:

After conditioning [20°C (70°F) and 50% RH], the average density of the wood-strand sandwich panel specimens to be tested was determined to be approximately 288 kg/m^3 (18 pcf). Using the specimen SG of 0.288 and MC of approximately 9.2% a thermal conductivity of 0.0918 W/m-K (0.637 Btu-in/ft^2-hr-°F) was estimated from Equation 2.4.1 (Appendix B). In comparison to the R-value determined experimentally, sandwich panel results were within 19% at 22.5°C (72.5°F). However, when considering published thermal conductivities from the ASHRAE Handbook (2009), MacLean's equation does not work for OSB type materials such as the sandwich panels. The equation estimated a thermal conductivity of 0.154 W/m-K (1.069 Btu-in/ft^2-hr-°F) for OSB, which is 46% to 87% greater than ASHRAE values of 0.1058 W/m-K (0.734 Btu-in/ft^2-hr-°F) and 0.082 W/m-K (0.569 Btu-in/ft^2-hr-°F) for 12.7 mm (1/2 in) and 9 mm (0.354 in) OSB, respectively. Differences between empirically calculated estimations and experimental results from this study were due to densification that occurred during OSB manufacturing that could not be considered by MacLean in 1941. Therefore, MacLean's equation should not be used to estimate thermal conductivity.

2.5.3. Results of Mechanical Testing:

2.5.3.1. Flexure Tests:

Longitudinal flexural specimens typically failed from delamination at the interface between the 3-D core and the bottom ply (Figure 2.5.4). Delamination failure occurred prior to flexural failure due to lack of adequate bonding surface area. Weak (transverse) direction specimens failed due to local failures in the plies near the support bars or load

bars (Figure 2.5.5 a). However, one specimen with average thickness, density, and stiffness compared to other transverse specimens, failed under flexure (Figure 2.5.5 b) at 24% higher than the average specimen load [1390 N (313 lbs) compared to 1126 N (253 lbs)]. Bending stiffness results normalized by specimen width were 4% stiffer compared to Voth's (2009) results, showing no apparent advantage of an additional rib. Complete results for wood-strand sandwich panels are shown in Table 2.5.2 found in Section 2.5.3.3.

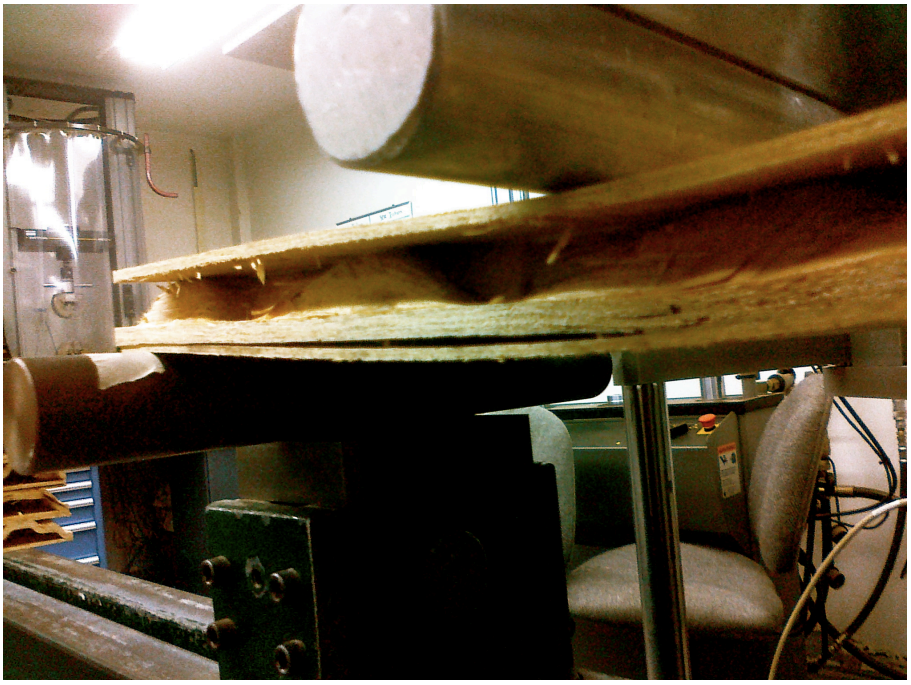

Figure 2.5.4: *Failure of longitudinal specimen. Note typical delamination failure as well as the occasional flexure failure in the core located below the load bar.*

(a) (b)

Figure 2.5.5: *(a) Typical local ply failure for transverse specimens. (b) Flexural failure in transverse specimen.*

2.5.3.2. Core Shear Flexure Tests:

Delamination failure at the interface between the 3-D core and the bottom ply often occurred simultaneously with crushing of the 3-D core at supports (Figure 2.5.6 a and b) in longitudinal core shear flexure specimens. Transverse specimens typically had local failures in the top or bottom plies (Figure 2.5.6 c and d) influenced by specimen geometry and test configuration. Results can be seen in Table 2.5.2.

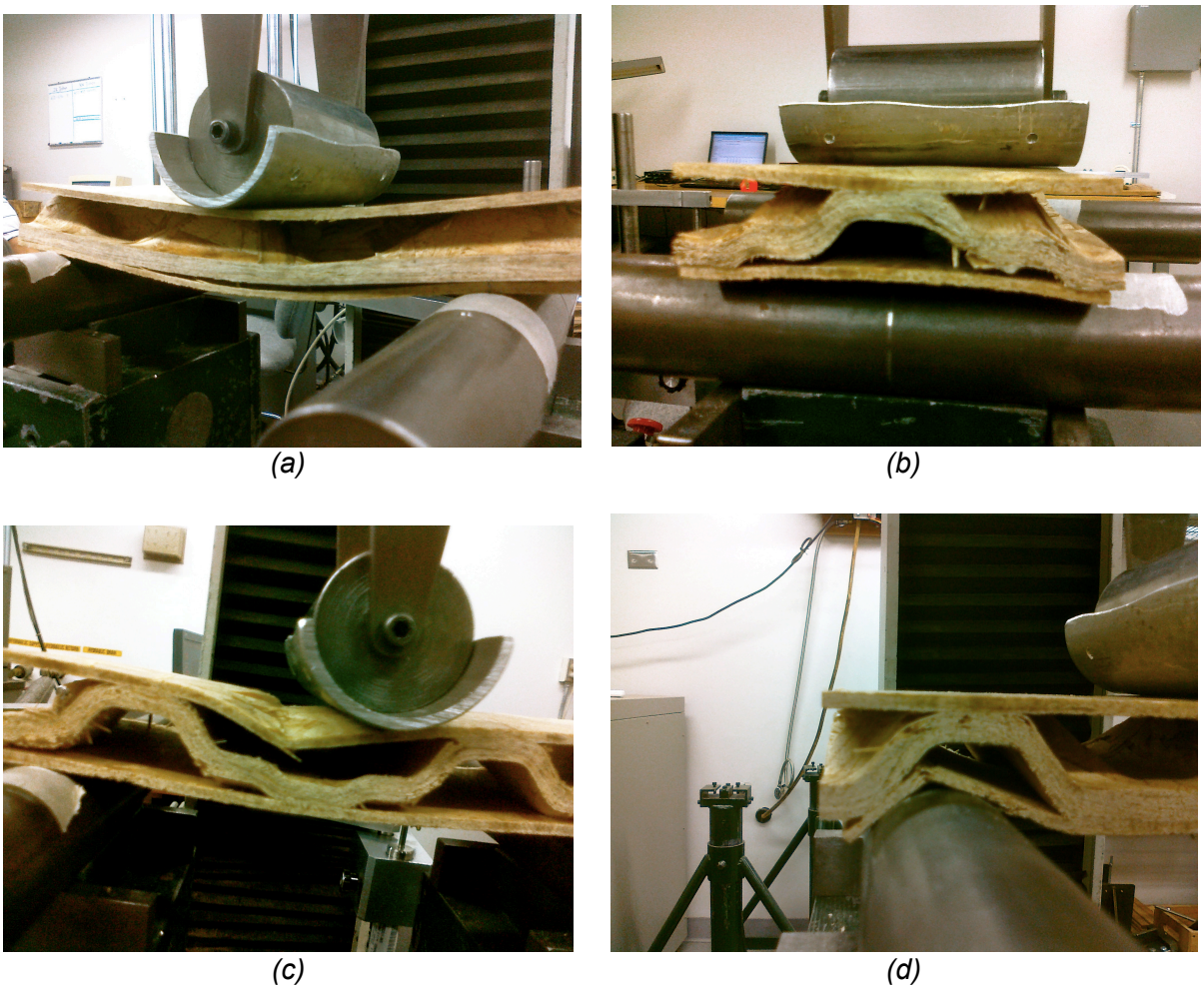

(a) *(b)*

(c) *(d)*

Figure 2.5.6: *(a) Delamination and (b) crushing at support in longitudinal specimens. (c) Top ply failure and (d) bottom ply failure in transverse specimens.*

2.5.3.3. Flatwise Compression Tests:

Compression specimens measuring 215 mm by 215 mm (8-1/2 in x 8-1/2 in) initially failed from delamination between the 3-D core and the bottom ply (Figure 2.5.7 a) caused by the core deforming outward under the load platen. Ultimate failure commonly occurred in the 3-D core or top ply failure at the edge of the load platen (Figure 2.5.7 b and c). The 108 mm by 108 mm (4-1/4 in x 4-1/4 in) specimens had similar delamination and 3-D core failures, which can be seen in Figure 2.5.7 d.

Additional bonding area found in larger specimens resulted in compressive strength 92% greater than that found by Voth (2009) and 149% stronger than that of smaller specimens from this study. As for compression modulus, values were not significantly different due to additional bonding surface. Compression modulus of larger specimens [215 mm (8-1/2 in)] was 14% greater than those of the smaller specimens tested by Voth (2009). When compared to the 108 mm (4-1/4 in) specimens tested in this study, compression modulus increased by 75%. A possible explanation for stiffer results could be delayed delamination between outer layers and the inner core due to larger specimen size, thus resulting in stiffer compression behavior.

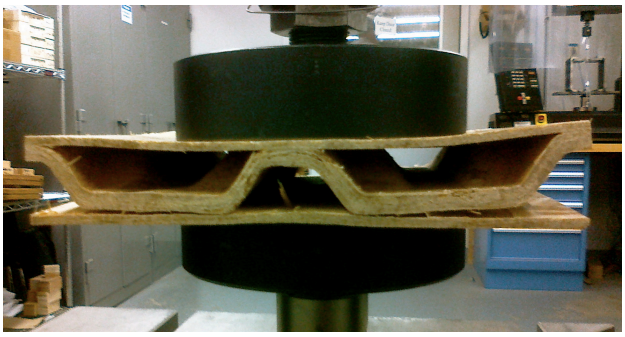

(a)

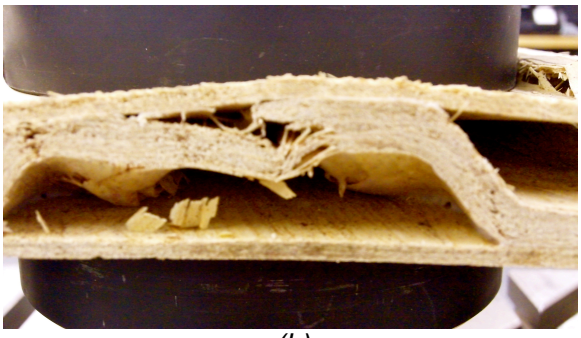

(b)

(c)

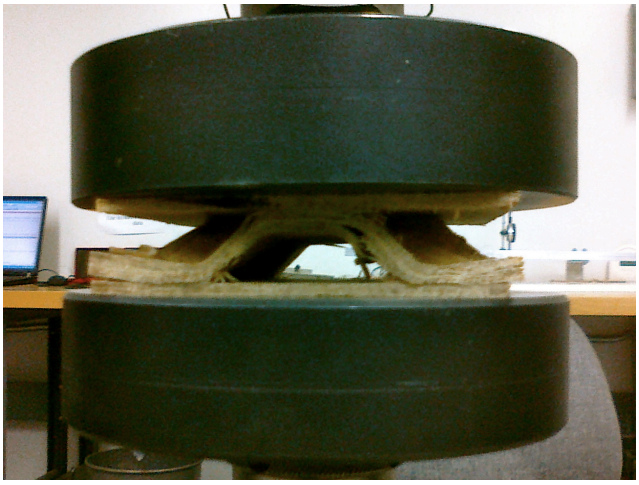

(d)

Figure 2.5.7: *(a) Delamination (b) core failure and (c) ply failure of 215 mm x 215 mm compression specimens. (d) Similar delamination and core failure in 108 mm x 108 mm specimens.*

Table 2.5.2: *Summary of wood-strand sandwich panel mechanical properties compared to results from Voth (2009)* [1]

			Beam Flexure Pmax (N)	Max Flexural Defl. (mm)	Bending Stiffness (N-m^2/m)	Core Shear Rigidity (N)	Core Shear Modulus (MPa)	Flatwise Comp. Strength (kPa)	Comp. Modulus (MPa)	Density (kg/m^3)
Wood-Strand Panel	Long.	Mean	3848	7.70	18757	89250	25.4	806	9.71	306
		Mean (US)	*865*	*0.303*	*166013*	*20064*	*3687*	*117*	*1408*	*19.1*
		Std Dev	1184	2.01	2398	19495	5.5	195	2.14	11
		COV%	30.8	26.1	12.8	21.8	21.8	24.2	22.0	3.5
	Trans.	Mean	1126	8.27	4435	17055	4.86	-	-	303
		Mean (US)	*253*	*0.325*	*39250*	*3834*	*705*	-	-	*18.9*
		Std Dev	173	1.12	302	6381	1.82	-	-	10
		COV%	15.3	13.5	6.8	37.4	37.4	-	-	3.3
Wood-Strand Panel (Voth)	Long.	Mean	2709	12.78	18078	41306	11.6	421	8.55	312
		Mean (US)	*609*	*0.503*	*160000*	*9286*	*1694*	*61.0*	*1240*	*19.5*
	Trans.	Mean	698	10.11	4768	18530	5.14	-	-	308
		Mean (US)	*157*	*0.398*	*42200*	*4165.7*	*751*	-	-	*19.2*

[1] Wood-Strand Panel represents 215 mm x 215 mm specimens while Wood-Strand Panel (Voth) represents 108 mm x 108 mm specimens.

2.5.4. Tensile Testing of Thin Plies:

Thin ply tensile specimens with wood-strands aligned perpendicular and 45° to the loading direction typically failed parallel to the strand orientation (Figure 2.5.8). Rather than failing in the bond between strands, specimens with strands aligned parallel to loading withstood higher loads and failed in strand tension. Tensile tests from flat ply coupons were also performed by Voth (2009) and Weight (2007). Differences in E values between the studies could be due to panel manufacturing variations, such as strand stiffness and orientation and voids in the panel. As the specimens are thin, any variation in strand deviations from the preferred direction will significantly influence the composite behavior, specifically since wood is anisotropic in nature. Because Voth (2009) did not determine shear modulus and Poisson's ratio, additional testing was conducted in this study to confirm Poisson's ratio and shear modulus values obtained by Weight (2007) along with providing a better representation of E.

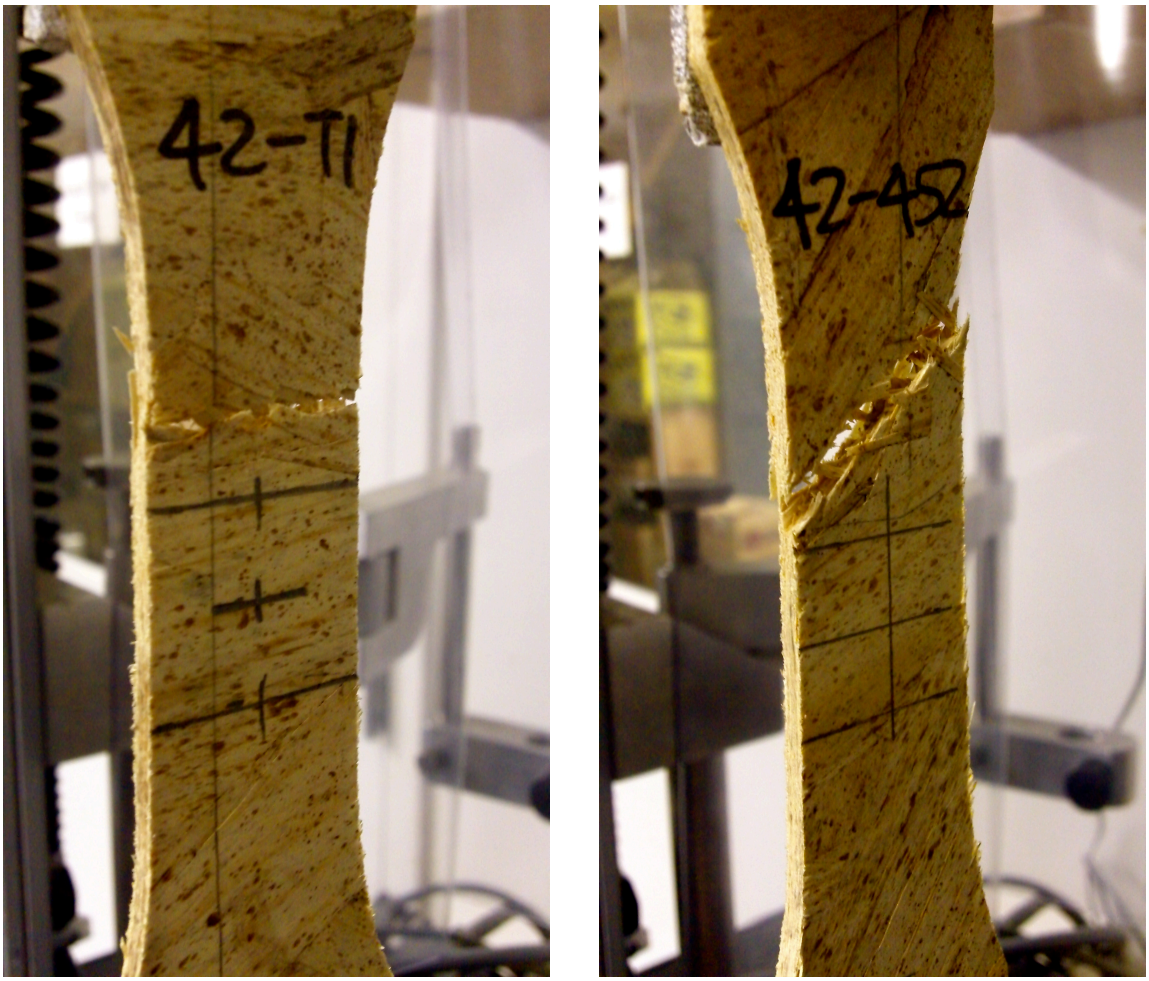

(a) (b)

Figure 2.5.8: *Failure of thin ply tensile specimens (a) perpendicular (90°) to load and (b) 45° to load.*

Excluding Voth's high values for transverse tensile strength and transverse E, results from this study were typically greater than results from Voth (2009) and Weight (2007). Specimen density was higher, but this is believed to have had a minor effect on increased values as normalizing data to a typical density of 640 kg/m^3 (40 pcf) still resulted in higher values. Once normalized, longitudinal tensile strength was 23% and 36% greater than results from Voth and Weight, respectively. Longitudinal E was 56% greater than Voth's results and similar to Weight's once normalized. Shear modulus

values, G_{ab}, compared to Weight's results, were significantly higher once normalized. A summary of various ply properties is shown in Table 2.5.3.

Table 2.5.3: *Summary of wood-strand ply properties from various studies* [1,2]

Study	Longitudinal		Transverse		θ = 45°		ν_{ab}	G_{ab} (MPa)	Density (kg/m^3)
	Tensile Strength (MPa)	E (MPa)	Tensile Strength (MPa)	E (MPa)	Tensile Strength (MPa)	E (MPa)			
Voth	31.0 (4500)	6370 (924000)	19.72 (2860)	5840 (847600)	-	-	-	-	668 (41.7)
Weight	30.8 (4470)	10890 (1579000)	3.27 (474)	1050 (152300)	6.03 (875)	2310 (335000)	0.358	1364 (197800)	730 (45.6)
White	43.4 (6300)	11290 (1638000)	7.29 (1057)	2320 (337000)	12.93 (1875)	6190 (898000)	0.379	5150 (746000)	759 (47.4)

[1] Subscript a and b denote longitudinal and transverse respectively. θ = 45° denotes wood strands aligned 45° from direction of loading.
[2] U.S. units (psi and pcf) shown in parentheses.

2.5.5. Finite Element Model:

After running the FE analysis, results were interpolated and manipulated such that when a deflection of 12.8 mm (0.503 in) (mean maximum flexural deflection found by Voth) occurred at the intersection of the two symmetry BCs, or center, the reaction at the roller support was summed and determined to be approximately 2660 N (598 lbs). This equates to a total sum of the reactions for flexure testing to be 5320 N (1196 lbs). As stated before, at a displacement of 12.8 mm (0.503 in), Voth (2009) recorded a mean maximum flexural load of 2710 N (609 lbs), which is significantly less than the predicted load by the FE model. However, since only linearly elastic material behavior was assumed in the FE model, the behavior after experimental material nonlinearity occurred cannot be compared.

Based on the material definition, to determine if the FE model successfully represented experimental testing, FE results should be compared to experimental

results in the linear region of the sandwich panel as shown in Figure 2.5.9. Experimental results were taken from Voth's five longitudinal flexure specimens at multiple displacements during the testing, averaged, and plotted versus load. The FE model displacement and load results were taken from each time step from the analysis and plotted with the experimental results.

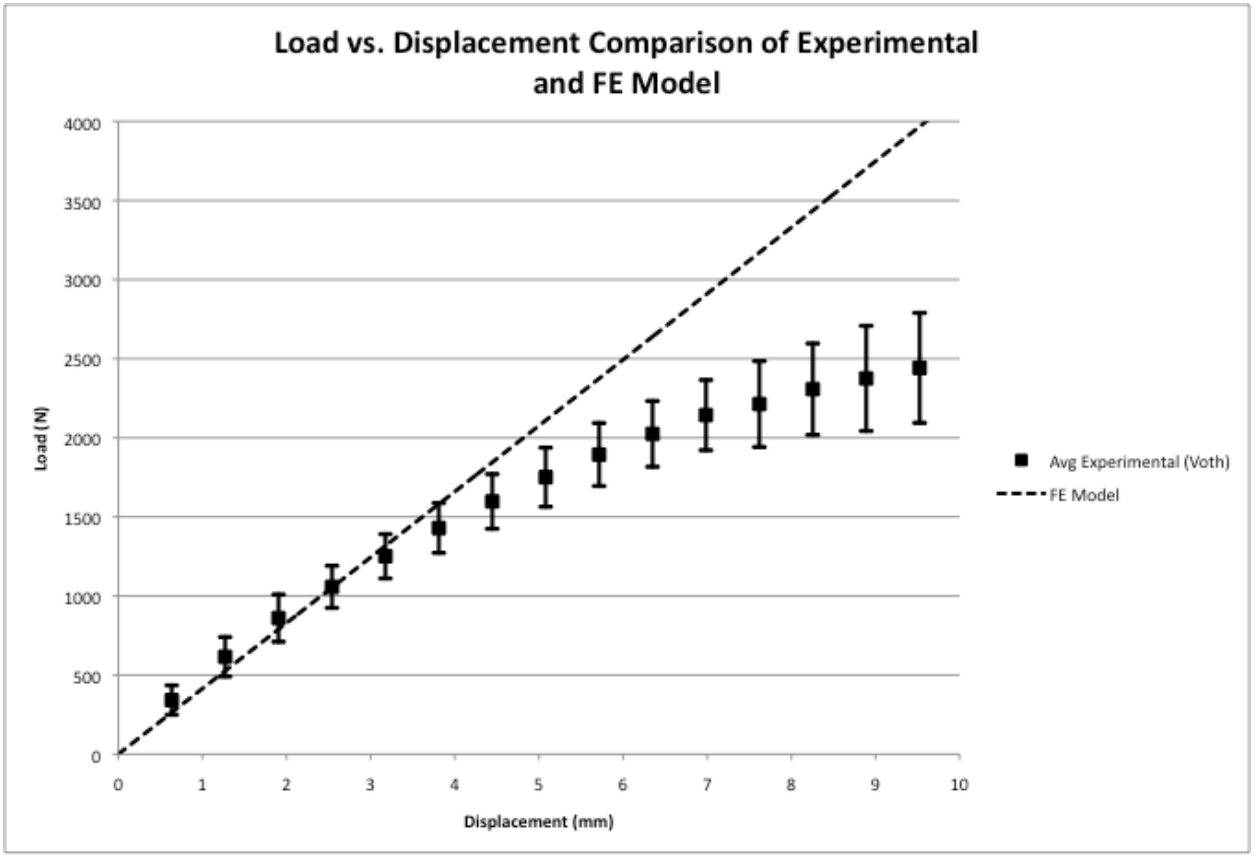

Figure 2.5.9: *Comparison between FE model and experimental results found by Voth. Error bars on experimental values based on standard deviation of experimental values.*

Figure 2.5.9 indicates that the FE model accurately represents the wood-strand sandwich panel within the linear region. Experimental values show that the linear region of the sandwich panel extends to a displacement of approximately 3.2 mm (0.125 in).

When displacement equals 3.2 mm (0.125 in), the FE model predicts a load of approximately 1320 N (296 lbs) compared to an experimental load of 1250 N (281 lbs). The FE model at this point falls within 5% of the experimental results as well as the standard deviation of 140 N (31.5 lbs). Table 2.5.4 shows the percentage difference between the FE results and the experimental results from Voth (2009) at various deflection points. Note that as deflection values climb out of the linear region (roughly 4.45 mm (0.175 in) and above), the percentage difference increases drastically. This indicates that the FE model only accurately represents experimental values within the linear region. Thus, nonlinear material behavior should be considered in future studies to accurately represent testing of specimens to failure. It was also observed that large deflection nonlinearity was not significant up to experimental failure as the FE model neither stiffened nor softened.

Table 2.5.4: *FE model results compared to experimental results.*

Deflection (mm)	FE Load (N)	Voth Load (N)	Percent (%)
0.635 (0.025)	263 (59.2)	342 (76.9)	23
1.27 (0.05)	526 (118)	616 (138)	14
1.905 (0.075)	790 (178)	860 (193)	8
2.54 (0.10)	1053 (237)	1058 (238)	0.4
3.175 (0.125)	1317 (296)	1251 (281)	5
3.81 (0.15)	1580 (355)	1430 (321)	11
4.445 (0.175)	1845 (415)	1598 (359)	15
5.08 (0.20)	2109 (474)	1751 (394)	20
5.715 (0.225)	2374 (534)	1894 (426)	25
6.35 (0.25)	2639 (593)	2025 (455)	30
6.985 (0.275)	2905 (653)	2143 (482)	36

Following its successful representation (linear region) of beam flexure testing by Voth (2009), the FE model was updated to represent sandwich panel specimens from this study. Material properties defined in the model were obtained from tensile testing of thin plies as discussed above. However, assumptions were made for Poisson's ratio and shear modulus based on published work and Weight's (2007) thesis.

Due to orthotropic material definitions within ADINA, the experimental value of Poisson's ratio (0.379) could not be used and also meet the material requirement shown in Equation 2.5.1. Experimental E values were used in conjunction with transversely

isotropic assumptions discussed in Section 2.4 to determine an allowable Poisson's ratio.

$$\nu_{ab}\nu_{bc}\cdot\left(\nu_{ac}\frac{E_a}{E_c}\right)<\frac{1}{2}\left(1-\nu_{ab}{}^2\frac{E_a}{E_b}-\nu_{bc}{}^2\frac{E_b}{E_c}-\nu_{ac}{}^2\frac{E_a}{E_c}\right) \qquad \text{(Equation 2.5.1)}$$

ν = Poisson's ratio

E = Young's modulus, MPa (psi)

Both ν_{ab} and ν_{ac} were assumed to be 0.3, thus making ν_{bc} equal to 0.125. Shear modulus was also noticeably high compared to Weight's value. A shear modulus value of approximately 710 MPa to 827 MPa (103000 psi to 120000 psi) is typical for solid lumber (Bodig and Jayne 1982), thus densification during manufacturing validates Weight's value of 1363 MPa (197800 psi) and that value was used for modeling. Table 2.5.4 displays properties used in FE modeling based on assumptions along with material properties obtained from tensile testing of thin plies.

Table 2.5.5: *Material properties representing flexure testing in this study* [1, 2]

	E_a[2] (MPa)	E_b[2] (MPa)	E_c (MPa)	ν_{ab}[3]	ν_{ac}	ν_{bc}	G_{ab}[3] (MPa)	G_{ac} (MPa)	G_{bc} (MPa)
FE Model	11290 (1638000)	2320 (337000)	2320 (337000)	0.3	0.3	0.125	1364 (197800)	1364 (197800)	1033 (149800)
Tensile Test	11290 (1638000)	2320 (337000)	2320 (337000)	0.3	0.3	0.125	4410 (639000)	4410 (639000)	1033 (149800)

[1] *FE Model values were used for FE modeling while properties from tensile testing are shown for comparison.*
[2] *U.S. units (psi) are given in parentheses.*

From using properties tabulated in Table 2.5.4, the FE model predicted a much stiffer flexural specimen than indicated from experimental results. After further analysis, it was determined that E_a significantly affects stiffness of the FE model and tensile testing of thin plies taken from the top ply of the panel flexure specimens examined earlier was executed to get a better representation of the material for the model. Because of bonding between the corrugated core and the outer plies, thin ply tensile specimens (taken from each flexure specimen) were limited to a width of 25 mm (1 in) and measured 254 mm (10 in) long.

Thin ply specimens obtained from sandwich panel outer plies resulted in a slightly lower mean E_a value [10250 MPa (1486000 psi)], but still predicted a stiffer sandwich panel. Figure 2.5.10 shows the upper and lower range of the FE model by plotting results from using the highest allowable E_a [11290 MPa (1638000 psi)] that met Equation 2.5.1 requirements [comparable to the highest recorded E of 11620 MPa (1686000 psi)] and the lowest E_a [6990 MPa (1014000 psi)]. Using the lower E value, results were within 17% and 27% of experimental results in the linear region. In measuring experimental deflections, crushing deformations in the specimen at the support bars (Figure 2.5.4) was not accounted for as the mid-span deflection was measured with respect to the base of the testing machine. This resulted in reduced stiffness of the tested specimens and larger difference compared to the predictions of the FE model.

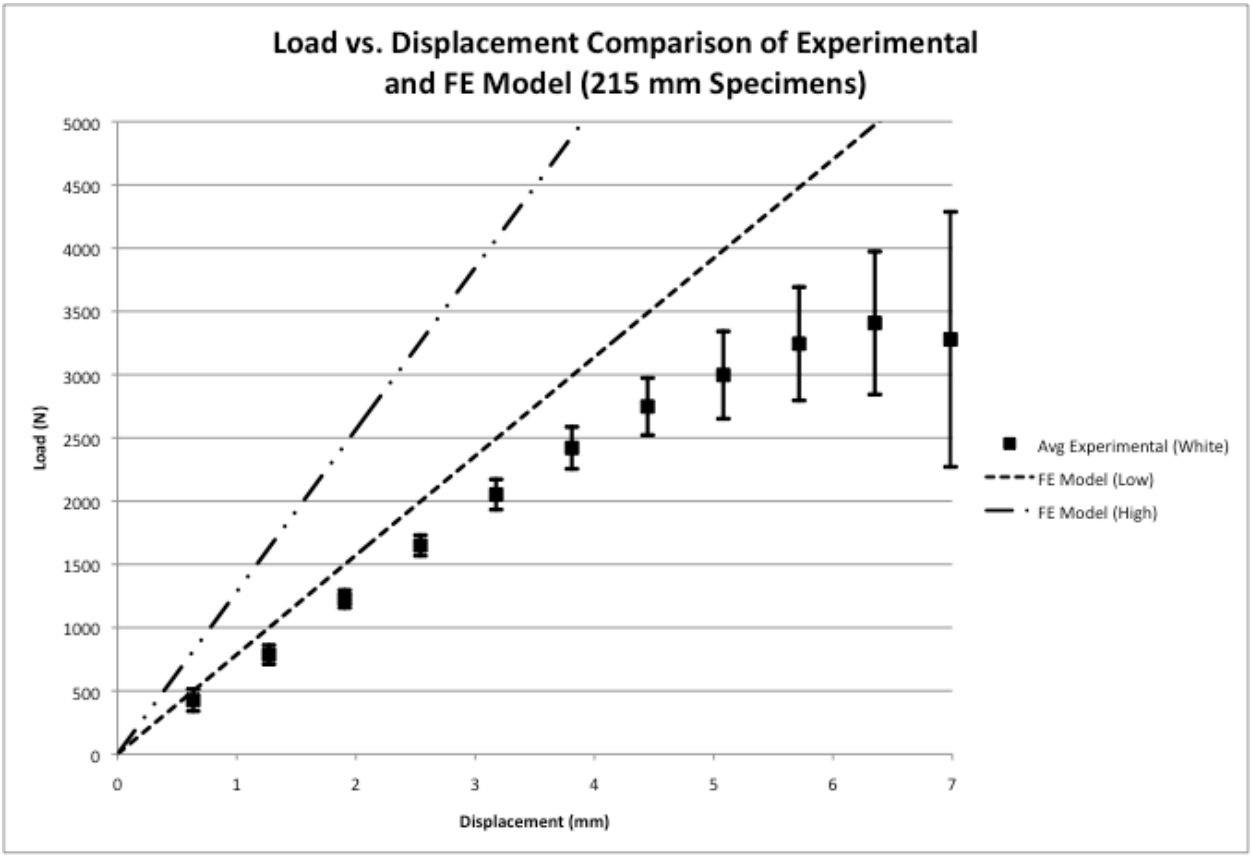

Figure 2.5.10: *FE model range compared to experimental results for 215 mm wide specimens. Error bars on experimental values are based on standard deviation of experimental values.*

2.6. Summary and Conclusions:

Sandwich panels (32 mm thick) had increased insulation properties compared to published values of OSB and plywood. However, after normalizing R-values of the sandwich panels and other commercial products by thickness, the sandwich panels were slightly better insulators (increase of 7%) compared to OSB and plywood and had lower properties than commercial insulators (approximately 35% of insulators). This is still beneficial for the sandwich panel as the R-value of the entire building envelope takes advantage of the increased R-value of the thicker sheathing. By replacing typical sheathing (OSB or plywood) with sandwich panels, a typical building envelope R-value

increased by a total of 0.190 m^2-K/W (1.082 ft^2-hr-°F/Btu). However, a strategy to further improve insulation properties of the sandwich panels must be considered to meet new energy code requirements, which will be discussed in the following chapter.

Wood-strand sandwich panels were considered a viable product based on mechanical properties compared to OSB and plywood (Voth 2009). Fabrication and reevaluation of sandwich panels (beam flexure, core shear flexure, and flatwise compression) in this study has proven that their performance can be replicated. It was also determined that an additional rib had no significant effect on bending stiffness when normalized by width (increase of 4% compared to Voth). Wood-strand sandwich panels continued to show an increase in bending stiffness (21%) compared to OSB, and when normalized by SG, bending stiffness increased 156%. These increases are extremely significant considering the reduced consumption of fiber and resin in producing the sandwich panels.

Development of an FE model allowed the evaluation of behavior of sandwich panels in flexure. The initial model, based on results from past work (Voth 2009), gave an accurate representation of flexural results within the linear region (within 0.4% to 15%), but future FE modeling should focus on the entire nonlinear performance until failure. Material properties of the outer thin plies were evaluated and used in the FE model to estimate behavior of the sandwich panels from this study. Due to strand orientation within the core and outer plies of panels, a large range of E values drastically affected accuracy of the FE model. By cutting tensile specimens from the thin plies of the flexure specimens, a better representation of experimental results was displayed, but values were still stiffer than experimental data. For better comparisons between the

FE model and experimental data, a yoke should be used to measure experimental deflection or the model should account for deformation at the supports. By using a yoke, deflection of beam flexure specimens will not include deformation at the supports, leading to stiffer specimens and yielding similar behavior as predicted by the FE model.

2.7. References:

ADINA R & D, Inc (2008). *ADINA Theory and Modeling Guide: Volume I: ADINA Solids & Structures. Report ARD 08-7.* Watertown, MA.

American Society of Heating, Refrigerating and Air-Conditioning Engineers, Inc. (2009). *ASHRAE Handbook – Fundamentals.* Atlanta, GA.

American Society of Testing Materials (1981). ASTM C518-76. Steady-State Thermal Transmission Properties By Means of the Heat Flow Meter. In: *1981 Annual book of ASTM standards.* ASTM, Philadelphia.

Bodig, J., Jayne, B.A. (1982). *Mechanics of Wood and Wood Composites.* New York, NY: Van Nostrand Reinhold Company Inc.

Cook, R. D., Malkus, D. S., Plesha, M. E., Witt, R. J. (2002). *Concepts and Applications of Finite Element Analysis* (4th ed.). Hoboken, NJ: John Wiley & Sons. Inc.

Davies, J.M. (2001). *Lightweight Sandwich Construction*. Malden, MA: Blackwell Science Ltd: Oxford.

Grandmont, J. F., Cloutier, A., Gendron, G., Desjardins, R. (2010). Wood I-Joist Model Sensitivity to Oriented Strandboard Web Mechanical Properties. *Wood and Fiber Science, 42* (3), 352-361.

Hunt, J. F. (2004). 3D Engineered Fiberboard: Finite Element Analysis of a New Building Product. *2004 International ANSYS Conference. Pittsburgh, PA, May 24-26, 2004.* USDA Forest Service, Forest Products Laboratory.

Hunt, J.F., Windandy, J.E. (2002). 3D Engineered Fiberboard: A New Structural Building Product, *6th European Panel Products Symposium. Llandudno, Wales. Oct. 9-11, 2002.* pp 106-117.

Kamke, F.A., Zylkowski, S.C. (1989). Effects of Wood-Based Panel Characteristics on Thermal Conductivity. *Forest Products Journal*, 39 (5), 19-24

Kawasaki, T., Kawai, S. (2006). Thermal Insulation Properties of Wood-Based Sandwich Panel For Use as Structural Insulated Walls and Floors. *Journal of Wood Science,* 52, 75-83.

Laser Comp, Inc. (1999-2011). Fox 200, Fox 300, Fox 304, and Fox 314 Instruments Manual. Saugus, MA.

MacLean, J.D. (1941). Thermal Conductivity of Wood. *Heating, Piping, and Air Conditioning.* 13:380-391.

Siau, J. F. (1995). *Wood: Influence of Moisture on Physical Properties*. Blacksburg, VA: Department of Wood Science and Forest Products, Virginia Polytechnic Institute and State University.

Voth, C. R. (2009). Lightweight Sandwich Panels Using Small-Diameter Timber Wood-Strand and Recycled Newsprint Cores. *Washington State University, Department of Civil and Environmental Engineering*.

Weight, S. W. (2007). A Novel Wood-Strand Composite Laminate Using Small-Diameter Timber. *Washington State University, Department of Civil and Environmental Engineering*.

Weight, S. W. & Yadama, V. (2008). Manufacture of Laminated Strand Veneer (LSV) Composite. Part 1: Optimization and Characterization of Thin Strand Veneers. *Holzforschung, 62(6),* 718-724.

White, N.B. (2011). Strategies For Improving Thermal and Mechanical Properties of Wood-Strand Composites With 3-D Core. M.S. Thesis. Chapter 1. *Washington State University, Department of Civil and Environmental Engineering.*

Zhu, E. C., Guan, Z. W., Rodd, P. D., Pope, D. J. (2005). Finite Element Modelling of OSB Webbed Timber I-Beams With Interactions Between Openings. *University of Brighton, School of the Environment, Brighton, UK*.

Chapter 3

Strategies for Improving Thermal and Mechanical Properties of Wood-Strand Sandwich Panels

3.1. Introduction:

The International Energy Conservation Code (IECC) is progressing toward more stringent energy performance requirements in an effort to encourage sustainability in the U.S. The IECC is calling for building energy performances to increase 30% from the 2006 code by 2012 and 50% in 2015 (Taylor 2011). This entails stricter building envelope R-value requirements (Figure 3.1.1 and Table 3.1.1). Building America, Federal Executive Orders, and the IECC make it vital for the wood and wood-based composite products industry to have high thermal performance in construction materials. This push to develop a more sustainable product while still meeting structural codes requires methods to increase thermal properties of wood-composites.

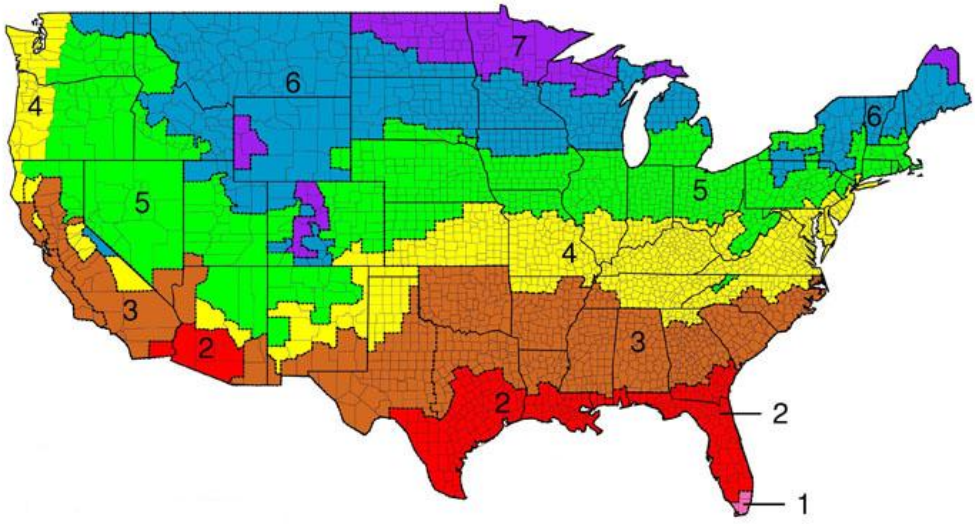

*Zone 1 includes Hawaii, Guam, Puerto Rico, and the Virgin Islands.
All of Alaska in Zone 7 except for the following Boroughs in Zone 8: Bethel, Dellingham, Fairbanks N. Star, Nome, North Slope, Northwest Arctic, Southeast Fairbanks, Wade Hampton, and Yukon-Koyukuk

Figure 3.1.1: *Zoned U.S. map with regard to thermal performance requirements.*

Table 3.1.1: *Current R-value requirements compared to future code requirements by zone* [1]

Zone	Wood-Frame Wall R-Value (2009)	Wood-Frame Wall R-Value (2012)
1		
2		
3	R13	R20
4 except Marine	R13	R20
5 and Marine 4		
6	R20	R20+5
7 & 8	R21	R20+5

[1] R-value conversion to S.I. units:
1R = 1 ft^2-hr-°F/Btu = 0.176 m^2-K/W

To meet the IECC's strict energy performance requirements, insulating type materials may be incorporated to enhance wood panel thermal performance. Structural insulated panels (SIPs) are large panels where a thick rigid foam plastic insulation core

is sandwiched between two OSB outer stress skins. SIPs range in thickness from 114 mm to 311 mm (4-1/2 in to 12-1/4 in), thus being much larger than the wood-strand sandwich panel discussed in Chapter 2 (White 2011). Similar to SIPs, use of rigid foam insulation can be beneficial when incorporated within the cavities of the 3-D core in the sandwich panel. Common sandwich panel core materials are rigid plastic foams with a closed cell structure that have critical core properties such as high thermal insulation, resistance to moisture absorption, favorable fire performance, and sound insulation (Davies 2001). The voids formed by the 3-D core in the sandwich panels allow for frequently used rigid foam plastics such as polyurethane/polyisocyanurate (PUR/PIR) and expanded or extruded polystyrene (EPS or XPS) to be incorporated for a possible increase in insulation. These common core materials, excluding EPS, contain a high percentage of closed cells (90%) such that the insulating material is enclosed between gas-tight facings. Gas diffusion and air infiltration are prevented (Davies 2001) and they maintain a high thermal resistance (R-value).

Radiant barriers are typically installed in residential attic spaces to reduce summer heat gain and winter heat loss by utilizing a highly reflective material that reflects radiant heat instead of absorbing it (U.S. Department of Energy 2010). Unlike the rigid foam insulators discussed above, a radiant barrier does not decrease the amount of heat flow via conduction or convection, but rather decreases heat transfer by radiation. Radiant heat from the sun is the primary source of heating the roof of a building, which results in a large amount of heat traveling via conduction through the roofing materials to the attic side of the roof. The hot underside of the roof radiates the gained heat onto cooler attic surfaces, such as air ducts and the attic floor. A radiant

barrier reduces this radiant heat transfer to other surfaces in the attic (U.S. Department of Energy 2010).

Emissivity and reflectivity determine effectiveness of radiant barriers, where emissivity is the ratio of radiant heat leaving, or being emitted by, a surface to that of a black body at the same temperature and area (U.S. Department of Energy 2010). Emissivity is denoted as a number between 0 and 1 with higher numbers representing greater emittance. Reflectivity is the opposite of emissivity, where it is the ratio of reflected heat to that of the black body under similar conditions. Commercial radiant barriers typically have an emissivity of 0.03 to 0.05. This corresponds to a reflectivity of 0.95 to 0.97, commonly referred to as 95% to 97%, and represents a low amount of heat being emitted from building materials into the living space or attic.

Radiant barriers excel in thermal performance when the temperature difference between the exterior surface and interior surface is large. They are also more effective in hot climates than cool climates, especially when cooling air ducts are located in the attic. Studies have shown that radiant barriers can lower cooling costs between 5% and 10% when used in a warm, sunny climate and may even allow for a smaller air conditioning system (U.S. Department of Energy 2010). Radiant barrier use in cool climates, however, prevents heat loss during winter nights, but also prevents favorable heat gain during the day. In these cooler climates, additional insulation may be more cost effective than a radiant barrier, showing that climate shall be considered when utilizing a radiant barrier within wood-strand sandwich panels.

Foam will provide the insulation, whereas the corrugated wood-strand core offers more structural support than the foam core of a SIP. Low emissivity of radiant barriers reducing undesired heat transfer through the building envelope makes incorporation of a radiant barrier within the sandwich panel a possible option. When placed in the core without foam to allow airflow, a radiant barrier may reduce heat transfer and increase energy efficiency of panels. Inclusion of rigid foam in the cavities may also increase structural performance of the sandwich panel by providing lateral support to the core and outer plies. No tests have been conducted, as per the author's knowledge, on thermal properties of lightweight wood-strand sandwich panels with or without insulating material. The following study provides insight into the influence of insulating material included in cavities of sandwich panels on their thermal properties and compares their performance against currently used building sheathing materials.

3.2. Objectives:

The goal of this study was to establish strategies to improve the thermal properties of the wood-strand sandwich panels in anticipation of their use in residential building envelopes for reduced consumption of operational energy. Since incorporation of insulation foam, especially rigid foam, may also provide better structural performance, mechanical properties of panels with foam were evaluated as well. Objectives to achieve the goal are listed as follows:

- Incorporate commercially produced materials (foam insulation and radiant barrier) into the cavities of wood-strand sandwich panels.

- Evaluate thermal properties for the wood-strand sandwich panel with incorporated materials.
- Determine thermal resistance for typical wall construction utilizing these panels.
- Determine any mechanical advantages resulting from inclusion of foam in panel cavities through evaluation of mechanical properties of wood-strand sandwich panel filled with rigid foam insulation in voids created by the 3-D core geometry.

3.3. Methods:

3.3.1. Incorporated Materials:

3.3.1.1. Rigid Foam:

To determine the effects of rigid foam on thermal and mechanical properties of wood-strand sandwich panels, a spray rigid foam called Foam it Green® was incorporated within the air voids developed by the 3-D core geometry as seen in Figure 3.3.1. Foam it Green® also contains a high (97%) closed cell structure compared to the other rigid foams. Energy efficiency benefits of Foam it Green® can be seen from the claimed R-value of 0.0464 m^2-K/W-mm (6.7 ft^2-hr-°F/Btu per inch) or 6.48 m^2-K/W (36.9 ft^2-hr-°F/Btu) for use in a 2x6 stud wall, compared to the R-value of 3.70 m^2-K/W (20.8 ft^2-hr-°F/Btu) for 140 mm (5-1/2 in) thick batt insulation (American Society of Heating, Refrigerating, and Air-Conditioning Engineers 2009). Aside from desired thermal insulation and closed cell content, Foam it Green® also advertises that it meets the E-84 Class 1 fire retardant requirements, provides an air and moisture barrier, resists pests and mold, reduces noise, does not hold water, and acts as a rigid structural support with a parallel compressive strength of 95.1 kPa (13.8 psi) (Guardian Energy

Technologies n.d.). While this may be a relatively low compressive strength compared to the wood-strand sandwich panel as a whole, when utilized within the air voids formed by the 3-D core, the rigid support may work well as a lateral support to resist core buckling.

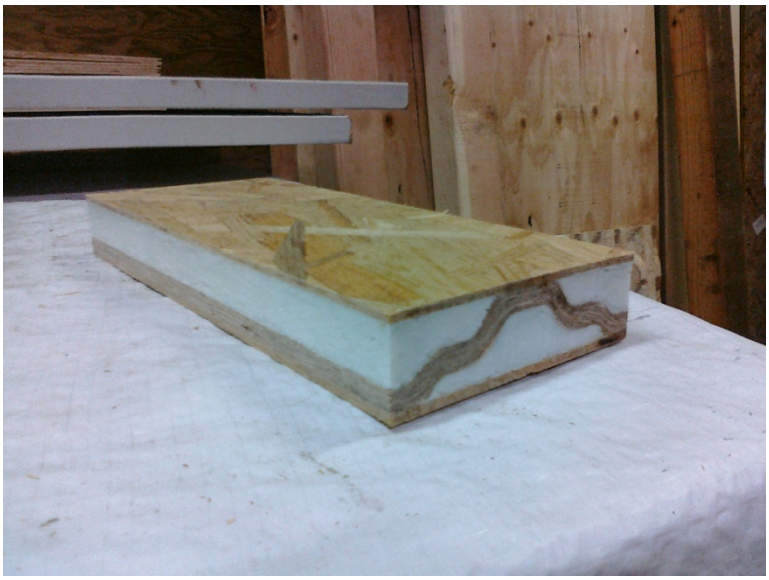

Figure 3.3.1: *Foam it Green® incorporated within air voids created by the 3-D core for a typical shear specimen.*

3.3.1.2. Radiant Barrier:

Radiant barriers are available as a reflective foil, reflective metal roof shingles, or reflective laminated roof sheathing. AtticFoil®, a reflective foil radiant barrier, was incorporated with the wood-strand sandwich panel in this study. An aluminum foil type material is typically used as the reflective material for radiant barriers, since it has a desired emittance of 0.03 to 0.05 (American Society of Heating, Refrigerating and Air-Conditioning Engineers 2001). This can be compared to aluminum paint or typical building materials such as wood, masonry, and nonmetallic paints as shown in Table 3.3.1. These are ideal values where dust accumulation and other factors that may

decrease effectiveness are not taken into account. R-values can be estimated for air spaces based on effective emittance values from Table 3.3.1. Table 3.3.2 shows R-values for a 19 mm (3/4 in) air gap, which coincides with the approximate air gap in the sandwich panel. Values shown represent a vertical position of air space and horizontal heat flow corresponding with wall installation. Wood-strand sandwich panels in roof or floor construction will also have similar effects and values can be obtained from the ASHRAE Handbook – Fundamentals (2009).

Table 3.3.1: *Emittance Values of Surfaces and Effective Emittance of Air Space* [1, 2]

	Average Emittance ε	**Effective Emittance, ε_{eff}, of Air Space. One Surface Foil; Other, 0.90**
Aluminum foil, bright	0.05	0.05
Aluminum paint	0.50	0.47
Building materials - wood, paper, masonry, nonmetallic paints	0.90	0.82

[1] These values apply in the 4 to 40 μm range of the electromagnetic spectrum.
[2] Values taken from ASHRAE Handbook – Fundamentals 2001.

Table 3.3.2: *Thermal Resistance, R-value, of Plane Air Spaces, ft^2-hr-°F/Btu [1,3]*

Air Space		19 mm (3/4 in) Air Space			Increase With Radiant Barrier Use[4] (%)
Mean Temp.[2] (°C)	Temp. Diff.[2] (°C)	Effective Emittance, ε_{eff}			
		0.03	0.05	0.82	
32 (90)	-12 (10)	3.50	3.24	0.84	386
10 (50)	-1 (30)	2.91	2.77	0.94	295
10 (50)	-12 (10)	3.70	3.46	1.01	343
-18 (0)	-7 (20)	3.14	3.02	1.18	256
-18 (0)	-12 (10)	3.77	3.59	1.26	285
-46 (-50)	-7 (20)	2.90	2.83	1.39	204
-46 (-50)	-12 (10)	3.72	3.60	1.56	231

[1] Values taken from ASHRAE Handbook – Fundamentals 2001
[2] Temperatures in parentheses are in Fahrenheit
[3] R-value conversion to S.I. units: 1R = 1 ft^2-hr-°F/Btu = 0.176 m^2-K/W
[4] Effective emittance assumed to be 0.05 and compared to an effective emittance of 0.82

3.3.2. Material Installation:

3.3.2.1. Rigid Foam:

Trial installations by spraying rigid foam insulation into the 3-D core air voids both prior to and after ply bonding determined that installation would be easiest and most economical if sprayed after ply bonding. Foam insulation was sprayed into the panel cavities from each end with a trial sandwich panel and cut to ensure consistent foam distribution as shown in Figure 3.3.2. Successful trials of spraying from each end of shorter specimens led to typical installation for test specimens with lengths of approximately 370 mm (14-1/2 in) and shorter. Longer sandwich panels, with length of approximately 740 mm (29 in), were filled with foam insulation by attaching tubing to the end of the nozzle as shown in Figure 3.3.3. This ensured foam distribution along the entire length of the cavity where spraying from each end may not reach the middle of the specimen.

(a) (b)

Figure 3.3.2: *(a) Ply removed showing even foam expansion. (b) End and longitudinal cuts showing consistent foam distribution.*

(a) (b)

Figure 3.3.3: *(a) Tubing attached to end of nozzle. (b) Typical foaming result of longer specimens prior to trimming.*

While cutting sandwich panels to final specimen dimensions, specimens filled with foam insulation from each end were found not to have foam consistently in the middle of the specimen. Only specimen perimeters could be observed, therefore, detection of foam in the center of specimens could not be determined. Visible voids without foam received additional foam to fill air voids as shown in Figure 3.3.4.

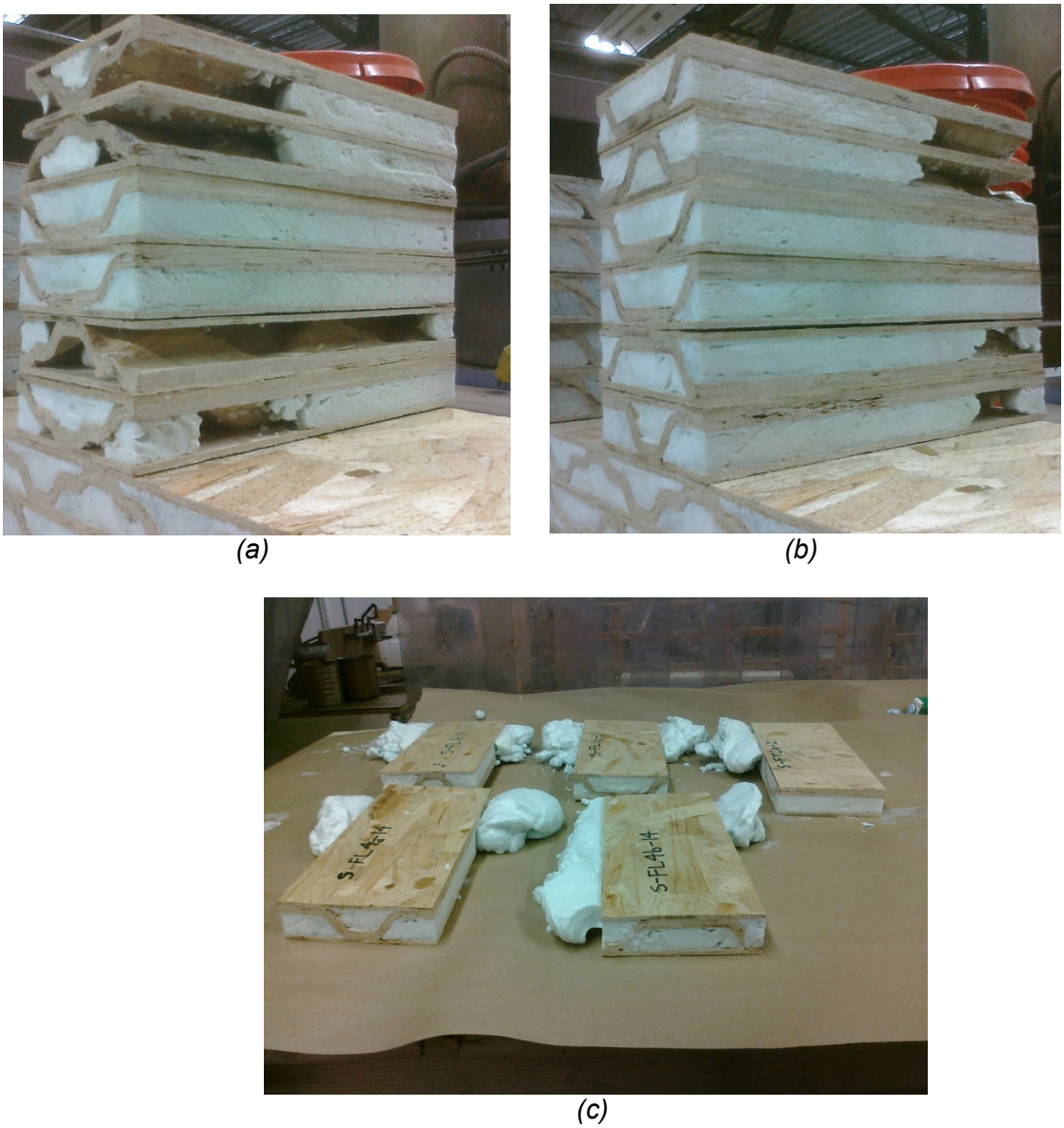

(a) *(b)*

(c)

Figure 3.3.4: *(a) Voids discovered in test specimens. (b) Opposite sides of same test specimens with voids. (c) Additional foam placed due to voids discovered.*

3.3.2.2. Radiant Barrier:

Radiant barriers are commonly installed by stapling the radiant barrier to structural framing or sheathing as shown in Figure 3.3.5. Staples would induce thermal bridging because of the thin nature of the sandwich panel; therefore a spray adhesive was used to apply the radiant barrier. AtticFoil® perforated radiant barrier was incorporated within the wood-strand sandwich panel cavities based on wall and roof installation recommendations to allow moisture from within the building to escape. This prevents the radiant barrier from acting as a vapor barrier and causing unwanted moisture to condense. Rare instances of water freezing and sealing the small holes may still be an issue in cold climates, indicating that use in cold climates not only has low cost efficiency, but also results in undesirable moisture. (U.S. Department of Energy 2010). An air gap of 19 mm to 25.4 mm (3/4 in to 1 in) minimum must also be present on one side of the radiant barrier such that no conduction occurs while preventing radiant heat transfer.

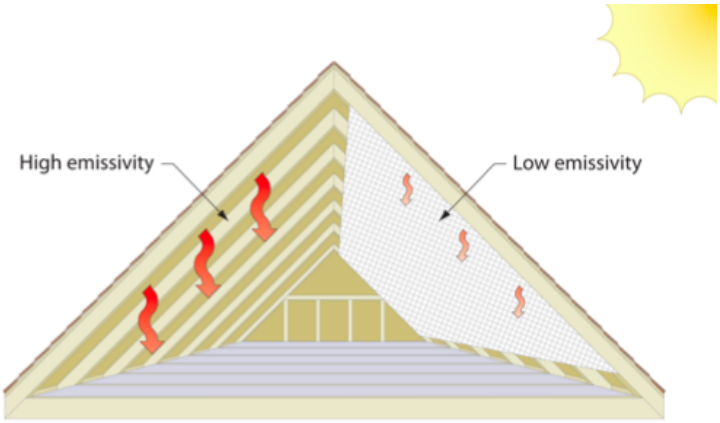

Figure 3.3.5: *Typical radiant barrier installation at roof framing (U.S. Department of Energy 2010).*

By installing the radiant barrier on one of the plies and within the cavity of the 3-D core as shown in Figure 3.3.6, the air gap requirement was met. When applied to the 3-D core, the 3-D core was sprayed with adhesive followed by placing of the radiant barrier. Adhesive was detected on the ribs of the 3-D core, which was later removed during typical sanding prior to sandwich panel bonding. For ply application, adhesive was applied to radiant barrier strips and placed on the ply. During panel bonding, modified MDI resin was applied to the 3-D core as described previously by White (2011) and placed on the ply with the radiant barrier, being careful not to inadvertently get MDI on the radiant barrier, thus making it less effective. Typical radiant barrier installation within the sandwich panel can be seen in Figure 3.3.7. In application, the panel should be used such that the radiant barrier should face outward and away from interior space. This can be an effective method of improving thermal efficiency of rain screen walls.

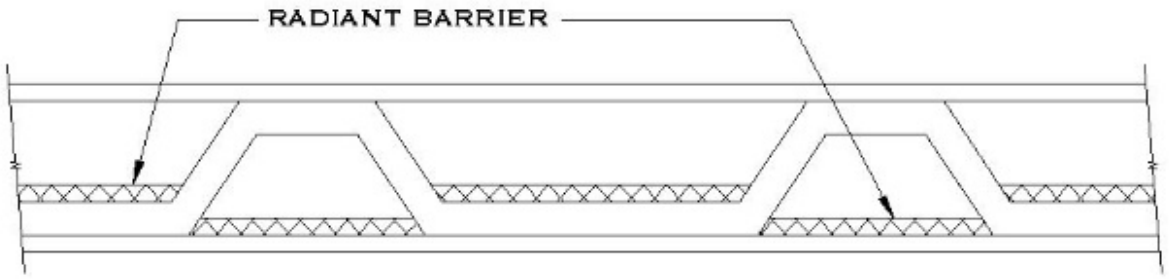

Figure 3.3.6: *Radiant barrier installation within wood-strand sandwich panels.*

Figure 3.3.7: *Typical installation of radiant barrier.*

3.3.3. Specimen Tests:

3.3.3.1. Thermal Tests:

Thermal conductivity, λ, for wood-strand sandwich panels with incorporated materials (rigid foam and radiant barrier) was determined in a similar manner as described previously by the author (White 2011). Six specimens in total of the same size and conditioning as before were tested, where three had rigid foam insulation within the core cavity and three had a radiant barrier adhered on both the 3-D core and one of the plies as discussed earlier. Specimens with incorporated materials were tested consistent with the plain sandwich panels by placing the three longitudinal ribs upright and along the left wall of the heat flow meter chamber as shown in Figure 3.3.8. This allowed for the radiant barrier to be near the hot plate with the air gap on the cold side of the radiant barrier similar to typical attic installation for radiant barriers in warm

climates. Thermal resistance, R, was calculated and compared to commercial products and sandwich panels from Chapter 2.

(a) (b)

Figure 3.3.8: *(a) Foam incorporated wood-strand sandwich panel. (b) Radiant barrier incorporated sandwich panel. Note the radiant barrier on bottom near the hot plate.*

3.3.3.2. Mechanical Tests:

Beam flexure, core shear in flexure, and flatwise compression properties of wood-strand sandwich panels with foam were determined following the methods described for sandwich panels with unfilled cavities (White 2011) (Figure 3.3.9). No mechanical testing was performed on specimens with radiant barrier, as no mechanical advantage could be perceived. Bending stiffness, core shear rigidity, and core shear modulus were calculated and compared to results from Chapter 2.

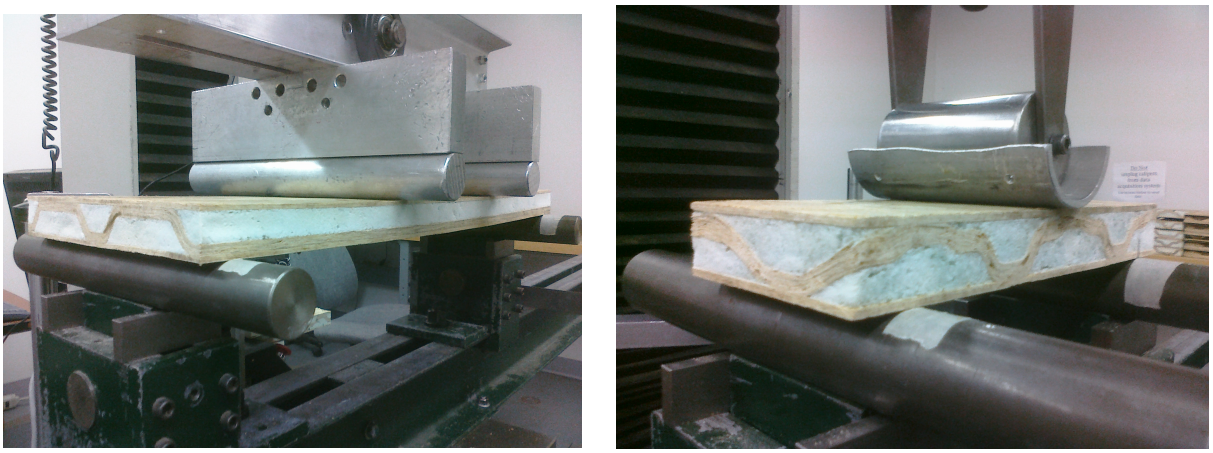

(a) *(b)*

Figure 3.3.9: *(a) Longitudinal flexure test showing foam. (b) Transverse core shear flexure test.*

Flatwise compression specimens with foam incorporated were tested similar to the specimens without foam mentioned in Chapter 2 (White 2011), with five 108 mm by 108 mm (4-1/4 in x 4-1/4 in) and five 215 mm by 215 mm (8-1/2 in x 8-1/2 in) specimens. Trial testing determined that the compressive nature of the foam stiffened the panel after the wood-strand component of the panel failed. Specimens were loaded to the maximum displacement of the sandwich panels without foam [11 mm (0.434 in) for the larger specimen] to guarantee failure. This ensured that compressive strength results could be compared between specimens with and without foam at similar displacements. Compressive strength and compressive modulus were calculated at the average displacement [8.4 mm (0.3296 in)] of the sandwich panel without foam and the approximate wood-strand failure.

3.4. Results and Discussion:

3.4.1. Thermal Properties Determined by Heat Flow Meter:

With a mean temperature of 22.5°C (72.5°F), the R-value for the radiant barrier wood-strand sandwich panel was 0.398 m^2-K/W (2.25 ft^2-hr-°F/Btu). Foam, with an R-value of 0.663 m^2-K/W (3.76 ft^2-hr-°F/Btu), significantly improved insulation efficiency. Specimens with a mean temperature of 12.5°C (54.5°F) resulted in slightly lower thermal resistance. To validate experimental results, thermal resistance was estimated for the sandwich panel with foam and radiant barrier using thermal conductivity [mean temperature of 24°C (75°F)] and thickness of each component (ply, core, foam, and ply) as shown in Appendix C. Assuming 19 mm (3/4 in) of consistent foam thickness, the R-value was estimated to be 1.0 m^2-K/W (5.68 ft^2-hr-°F/Btu). However, the foam did not always have constant thickness and dropped as low as 14 mm (0.553 in). This resulted in an R-value of 0.813 m^2-K/W (4.62 ft^2-hr-°F/Btu). R-value of the air gap was used while estimating radiant barrier effects in addition to ply and core values. This resulted in an R-value of 0.602 m^2-K/W (3.42 ft^2-hr-°F/Btu) assuming a constant air gap of 19 mm (3/4 in). Experimental results for the sandwich panel with foam was approximately 66% and 81% of the estimated values for 19 mm (3/4 in) and 14 mm (0.553 in) of foam respectively and radiant barrier R-value was 66% of the estimated value. Thermal bridging that occurred experimentally was not taken into consideration for the estimated values, resulting in the higher estimates. Thermal conductivity and thermal resistance results compared to the plain wood-strand sandwich panels and OSB panels tested in Chapter 2 (White 2011) are displayed in Table 3.4.1.

Table 3.4.1: *Summary of thermal properties for wood-strand sandwich panels and OSB [1] (R-values correspond to the stated thickness of the materials)*

		Thickness (mm)	Density (kg/m^3)	Thermal Conductivity, λ (W/m-K)	Thermal Resistance, R (m^2-K/W)	Mean Temp (°C)
Wood-Strand Panel	Mean	32.5	287	0.112	0.290	22.5
	Mean (US)	*1.28*	*17.9*	*0.778*	*1.65*	
	Std. Dev	0.916	5.27	0.003	0.006	
	% COV	2.8	1.8	2.5	2.2	
	Mean	32.5	287	0.106	0.307	12.5
	Mean (US)	*1.28*	*17.9*	*0.737*	*1.74*	
	Std. Dev	0.916	5.27	0.003	0.008	
	% COV	2.8	1.8	2.9	2.8	
Wood-Strand Panel w/ Radiant Barrier	Mean	32.9	294	0.083	0.398	22.5
	Mean (US)	*1.29*	*18.4*	*0.574*	*2.25*	
	Std. Dev	1.027	11.90	0.002	0.022	
	% COV	3.1	4.0	2.4	5.4	
	Mean	32.9	294	0.080	0.413	12.5
	Mean (US)	*1.29*	*18.4*	*0.553*	*2.34*	
	Std. Dev	1.027	11.90	0.001	0.020	
	% COV	3.1	4.0	1.8	4.9	
Wood-Strand Panel w/ Foam	Mean	32.3	311	0.049	0.663	22.5
	Mean (US)	*1.27*	*19.4*	*0.339*	*3.76*	
	Std. Dev	0.880	11.50	0.004	0.041	
	% COV	2.7	3.7	7.3	6.2	
	Mean	32.3	311	0.047	0.694	12.5
	Mean (US)	*1.27*	*19.4*	*0.324*	*3.94*	
	Std. Dev	0.880	11.50	0.004	0.045	
	% COV	2.7	3.7	7.6	6.4	
OSB	Mean	11.7	652	0.095	0.124	22.5
	Mean (US)	*0.463*	*40.7*	*0.659*	*0.703*	
	Std. Dev	0.13	6.4	0.001	0.002	
	% COV	1.1	1.0	1.1	1.6	
	Mean	11.7	652	0.093	0.126	12.5
	Mean (US)	*0.463*	*40.7*	*0.647*	*0.716*	
	Std. Dev	0.13	6.4	0.001	0.003	
	% COV	1.1	1.0	1.1	2.4	

[1] US units are given in inches, pcf, Btu-in/ft^2-hr-°F, and ft^2-hr-°F/Btu

Experimental R-values at a mean temperature of 22.5°C (72.5°F) were compared to commercial products such as OSB, plywood, insulators (EPS, XPS, and fiberglass), and SIPs as seen in Figure 3.4.1. SIPS had thicknesses of 114 mm, 165 mm, and 210 mm (4-1/2 in, 6-1/2 in, and 8-1/4 in) and had an EPS core. Once normalized by thickness (Figure 3.4.2), the wood-strand sandwich panels were better represented when compared to the much thicker SIPs. R-values for normalized sandwich panels,

panels with radiant barrier, and panels with foam increased 7%, 45%, and 147%, respectively, from common sheathing material (OSB/plywood). However, these normalized results may be misleading since material thickness benefits the building envelope as a whole. Greater thermal advantages can be seen when comparing 32 mm (1-1/4 in) sandwich panels to 12.3 mm (0.484 in) OSB/plywood. Wood-strand sandwich panels then increase R-value by 190% while the addition of radiant barrier or foam increase R-value by 297% and 562%, respectively.

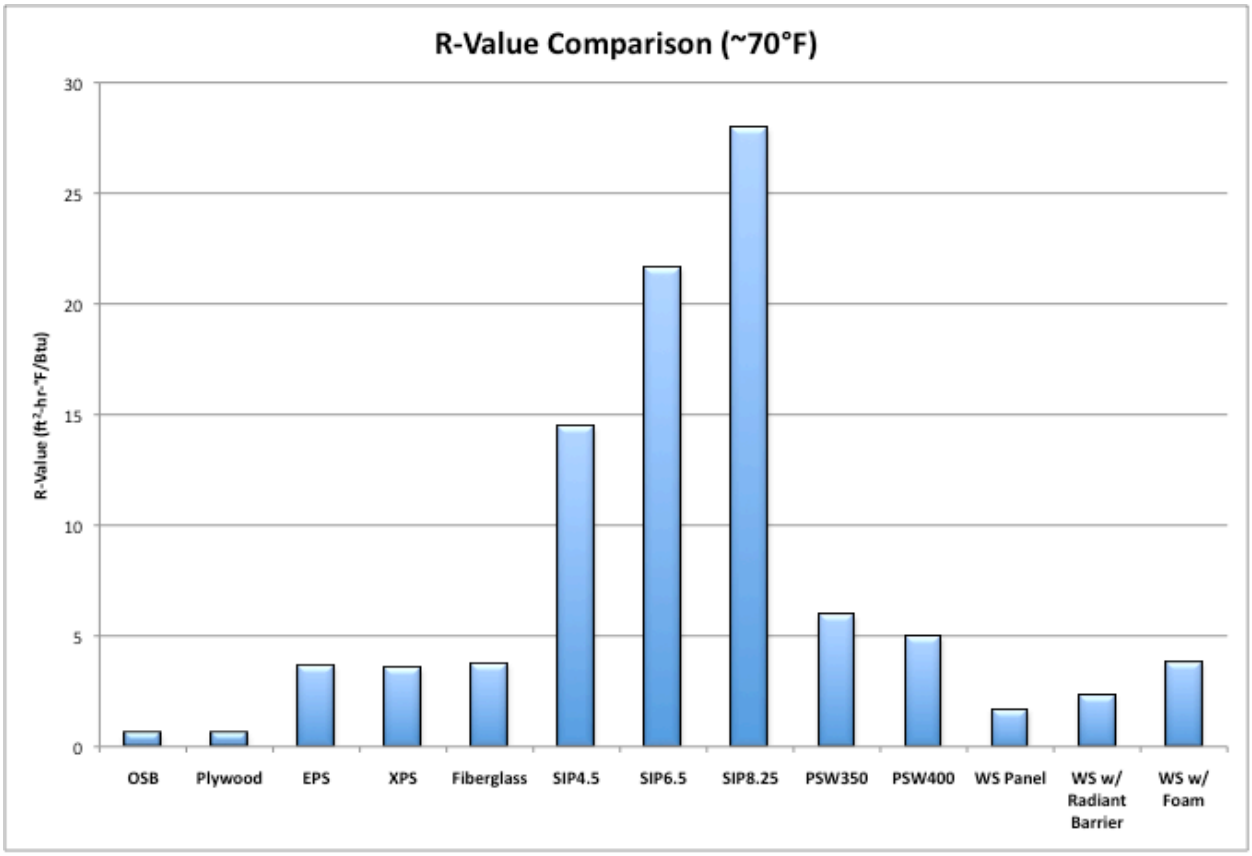

Figure 3.4.1: *R-values for commercial products and wood-strand (WS) sandwich panels. R-value conversion to S.I. units: 1R = 1 ft^2-hr-°F/Btu = 0.176 m^2-K/W. SIPs denoted by inch thickness.*

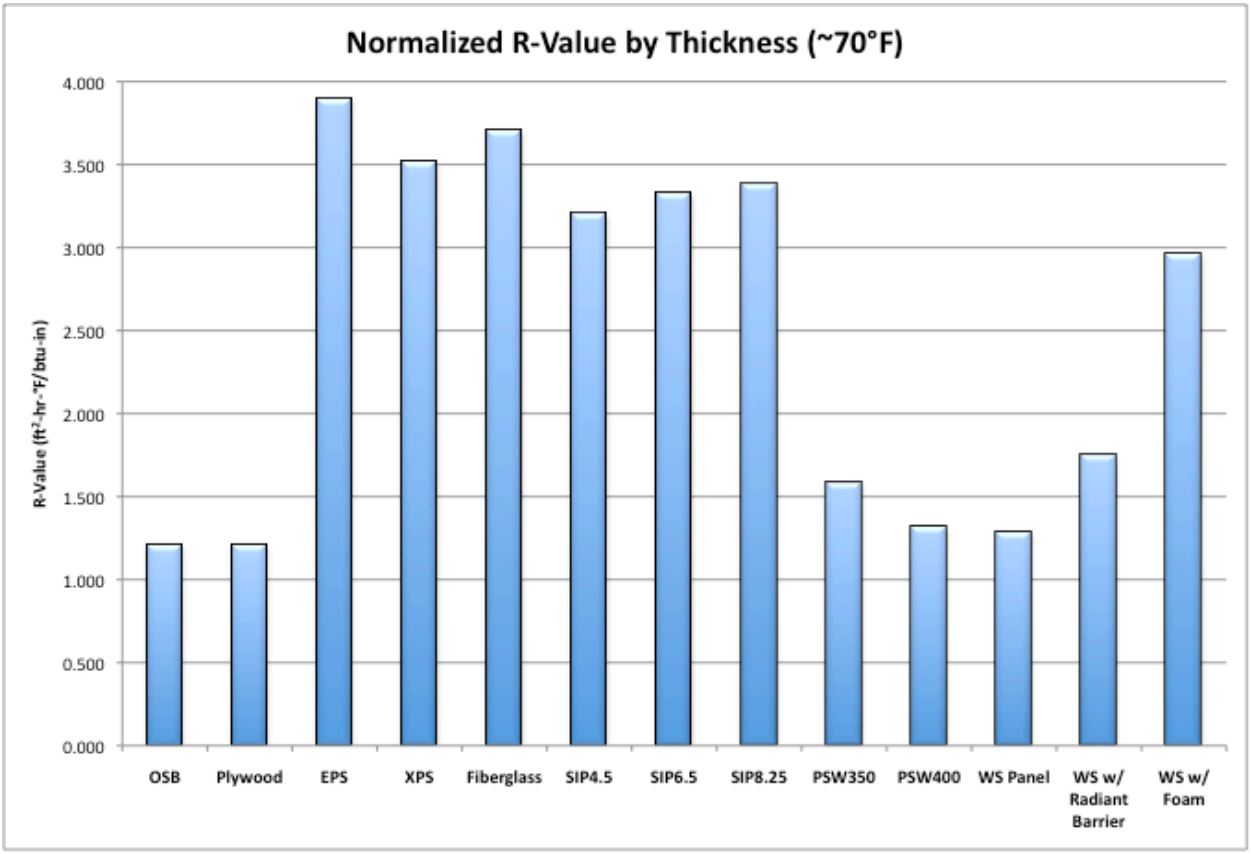

Figure 3.4.2: *R-values normalized by thickness for commercial products and wood-strand (WS) sandwich panels. R-value conversion to S.I. units: 1R = 1 ft^2-hr-°F/Btu = 0.176 m^2-K/W. SIPs denoted by inch thickness.*

3.4.2. Mechanical Tests:

3.4.2.1. Flexure Tests:

Longitudinal flexural specimens with foam typically failed due to delamination between the core and top or bottom ply as shown in Figure 3.4.3 a. Occasional buckling occurred in the top ply at one of the load bars as seen in Figure 3.4.3 b. Failure due to tension in the bottom ply often took place in transverse specimens, but occasionally failed due to top ply buckling. Both failures are shown in Figure 3.4.3 c and d.

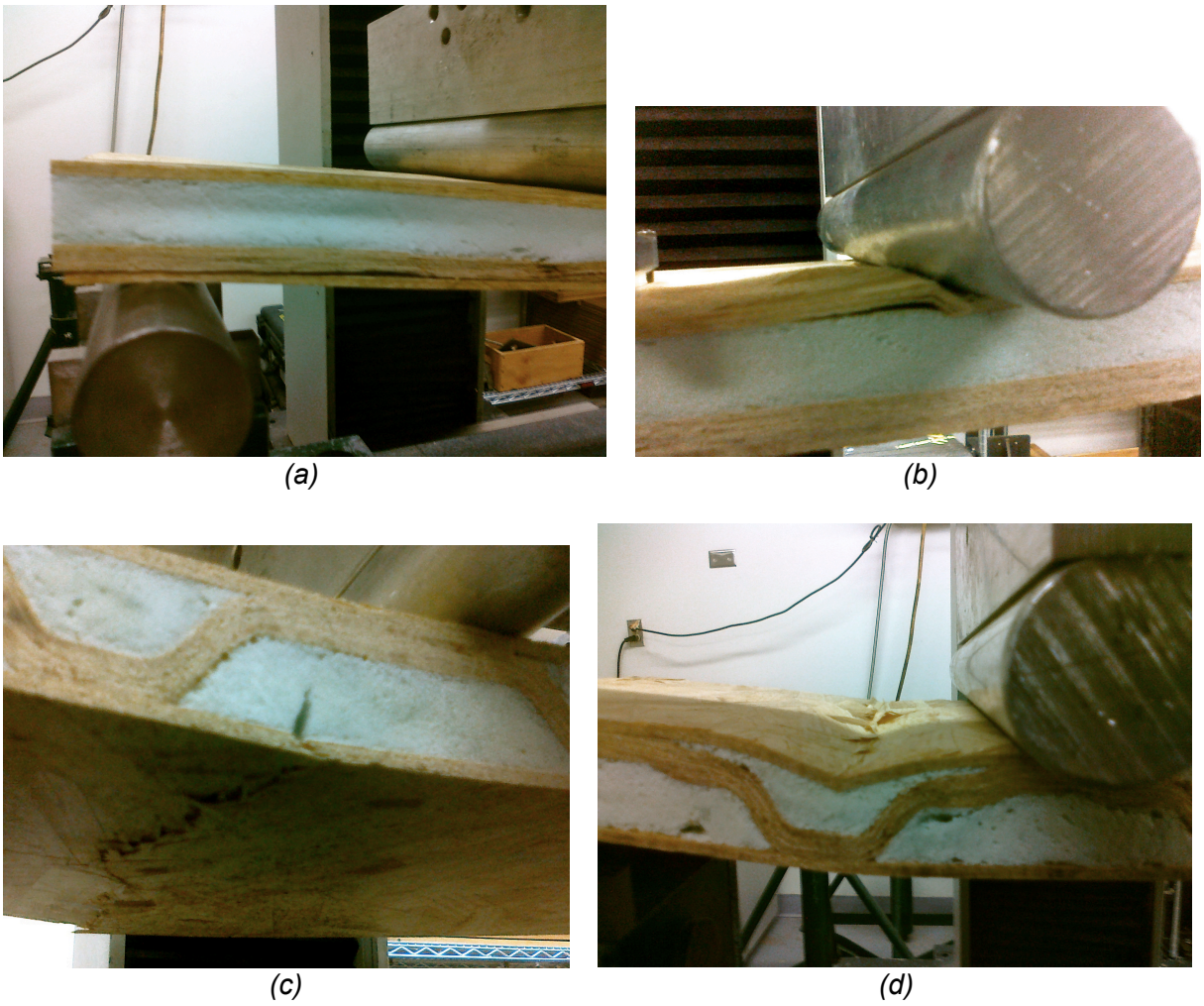

Figure 3.4.3: *(a) Longitudinal flexural specimen failure between core and bottom ply. (b) Top ply buckling for longitudinal specimen. (c) Transverse flexural specimen failing in bottom ply tension. (d) Top ply buckling of transverse specimen.*

Longitudinal and transverse specimens showed increased strength and stiffness with the addition of foam compared to wood-strand sandwich panels without foam. Figure 3.4.4 shows typical load versus deflection behavior for wood-strand sandwich panels and displays increased bending stiffness with the addition of foam within core cavities. Density of the panel remained low as it increased only 7%. Compared to OSB and plywood of similar thickness (Figure 3.4.5) wood-strand sandwich panels with foam were much stiffer. Sandwich panels previously tested by Voth (2009) were also included

for comparison (they behaved similar to ones fabricated and tested by the author as they are of the same type). Greater advantages of lightweight sandwich panels with foam are shown in Figure 3.4.6 once bending stiffness was normalized by SG. Ultimate load, maximum deflection, and bending stiffness results are tabulated in Table 3.4.2.

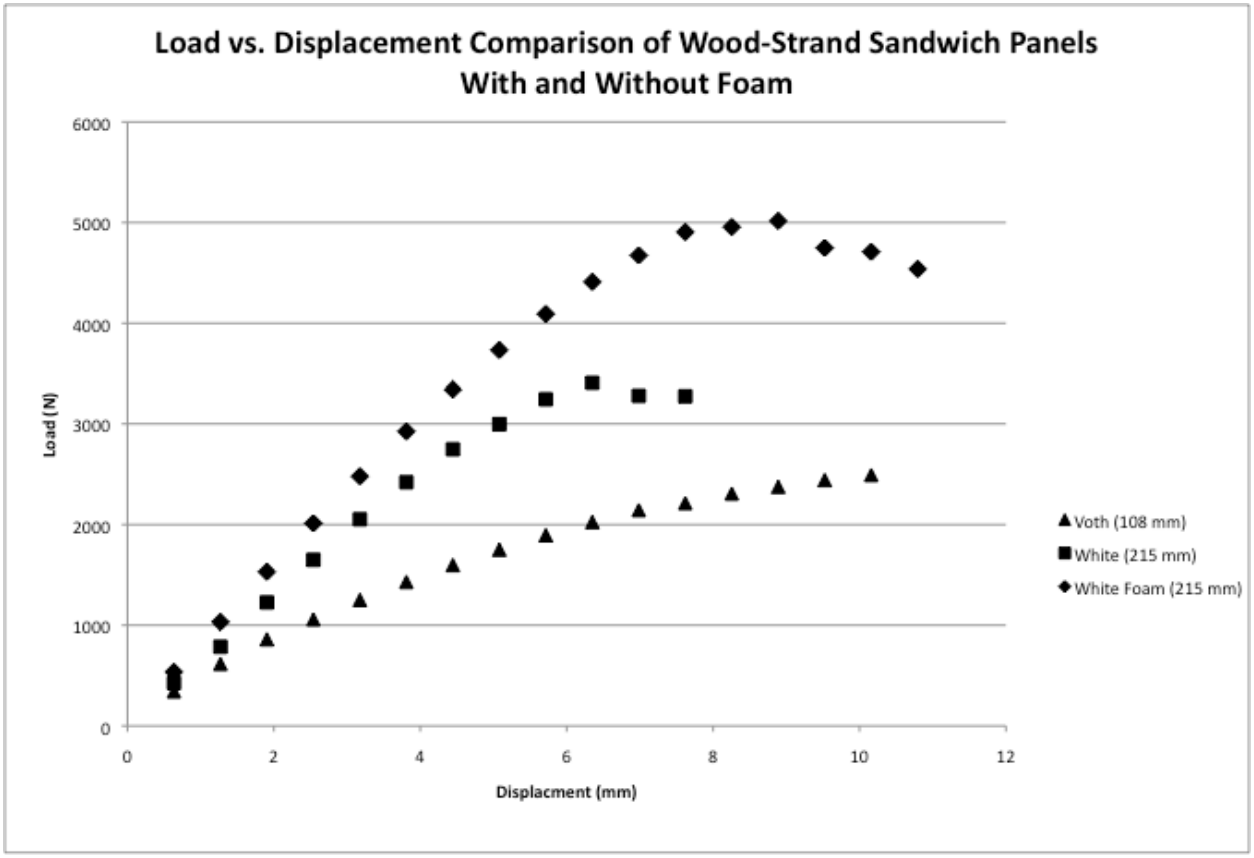

Figure 3.4.4: *Load versus displacement of sandwich panels with and without foam.*

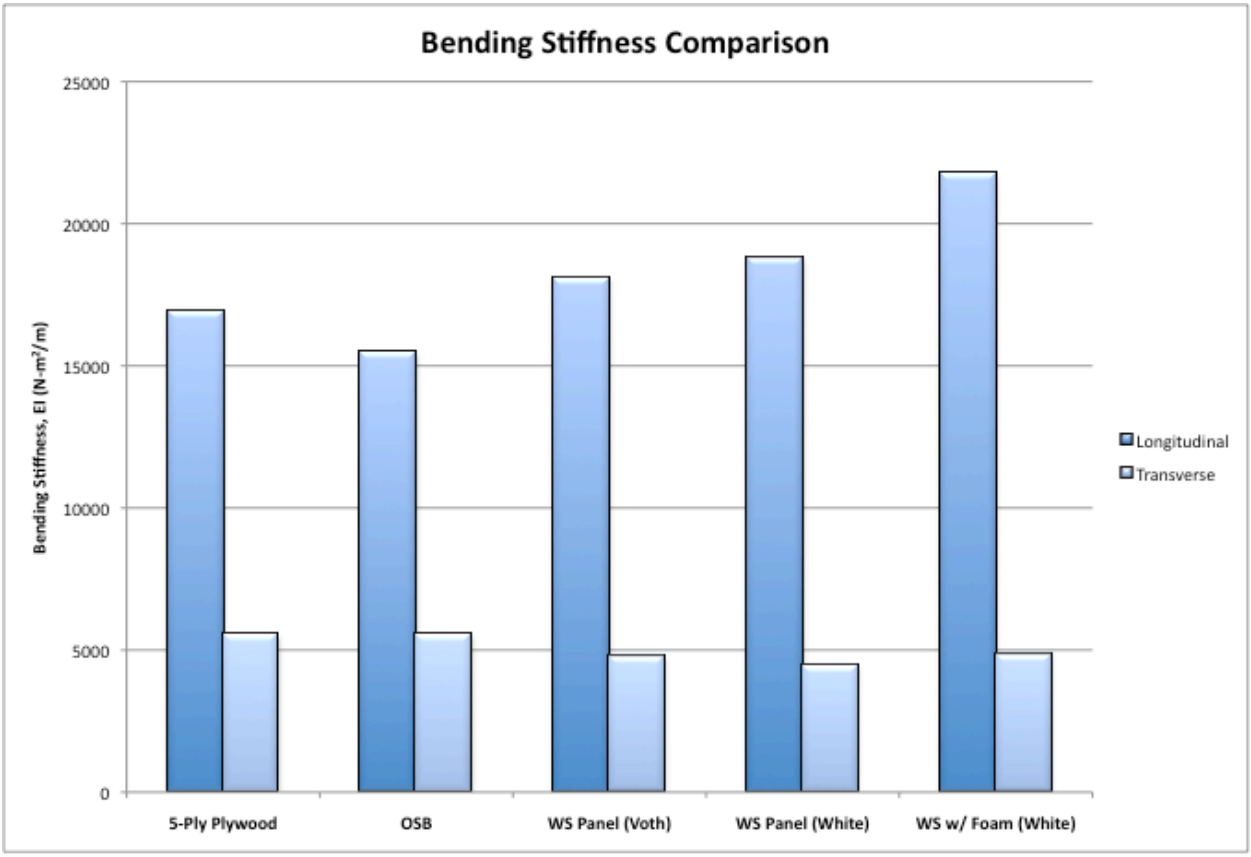

Figure 3.4.5: *Bending stiffness for wood-strand sandwich panels with and without foam, OSB, and plywood.*

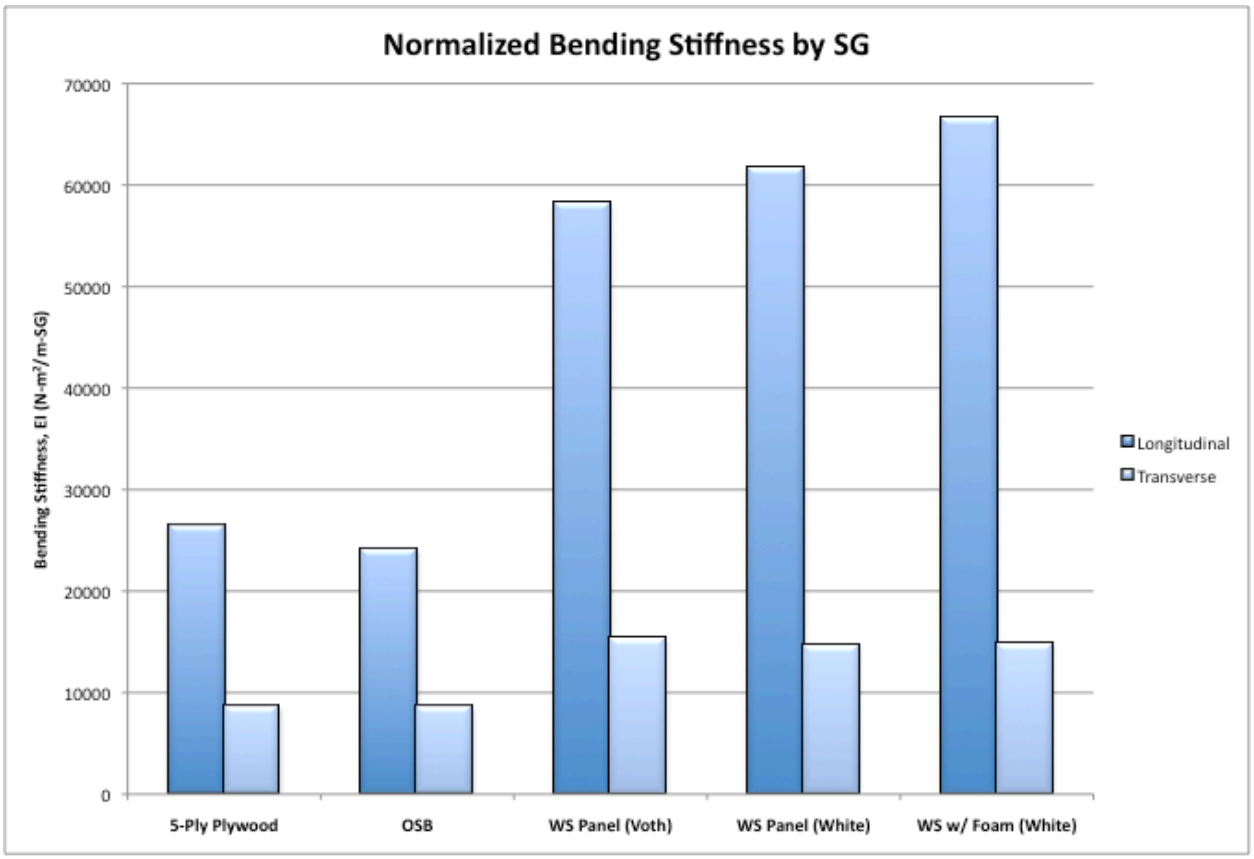

Figure 3.4.6: *Normalized bending stiffness for wood-strand sandwich panels with and without foam, OSB, and plywood.*

3.4.2.2. Core Shear Flexure Tests:

Delamination failure at the interface between the 3-D core and the bottom ply and failure in tension in the bottom ply were common for longitudinal core shear flexure specimens (Figure 3.4.7 a). Transverse specimens tended to fail in bottom ply tension as the foam helped reduce local ply failures found at load and support bars in transverse core shear flexure specimens without foam (Figure 3.4.7 b and c). By slightly increasing density with the addition of foam, transverse specimen strength and core shear modulus increased drastically. Foam resisted local failures, thus improved results by leading to more desirable global failures. Longitudinal specimen results stayed

approximately the same for panels fabricated in this study. However, when compared to results of a previous study on wood-strand sandwich panels without foam by Voth (2009), specimens with and without foam resulted in higher core shear modulus in the longitudinal direction (Figure 3.4.8). Higher ply density may be the reason for this large increase. Core shear rigidity and core shear modulus are displayed in Table 3.4.2.

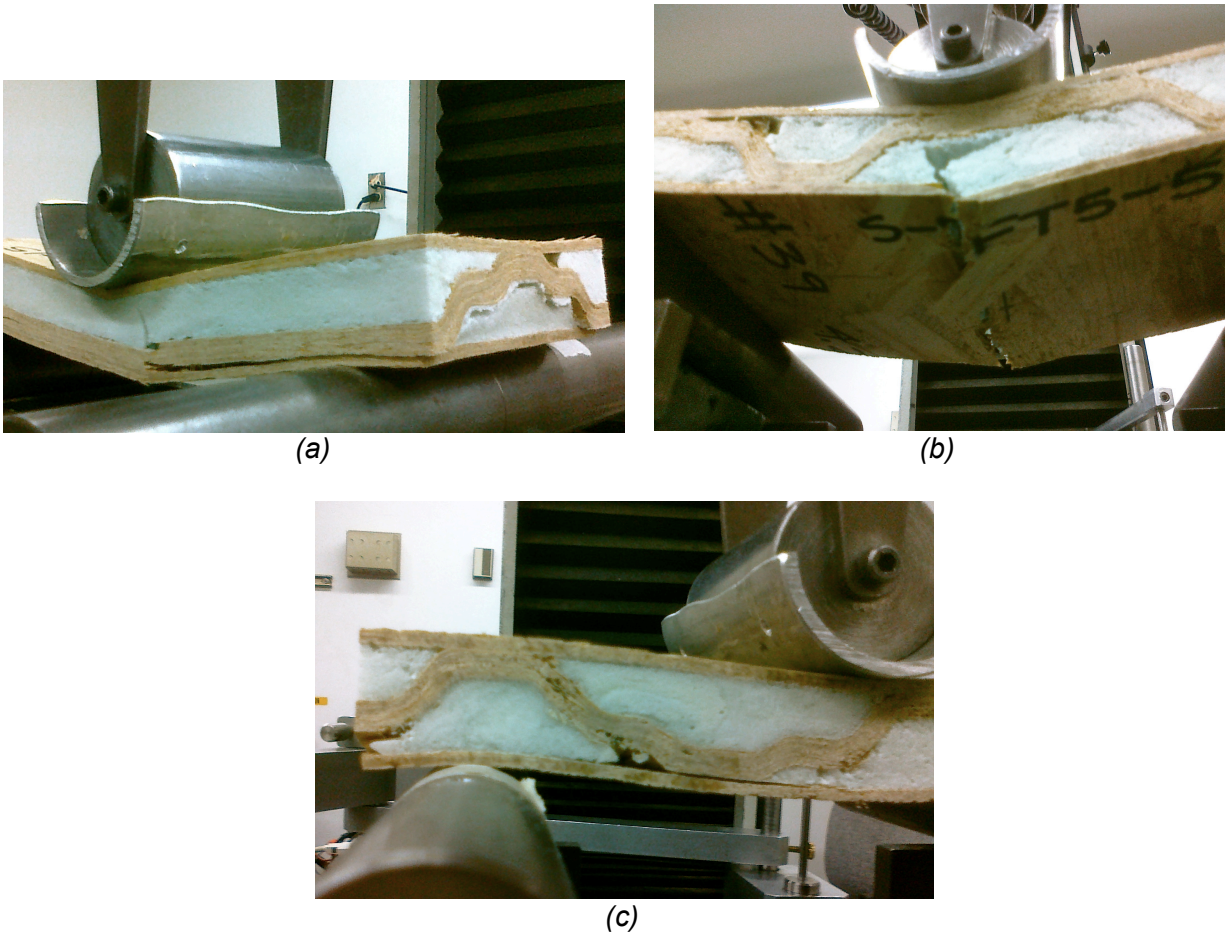

(a) *(b)* *(c)*

Figure 3.4.7: *(a) Delamination and flexure failure in longitudinal core shear specimen, (b) Bottom ply tension failure in transverse core shear specimen, and (c) delamination failure in transverse core shear specimen.*

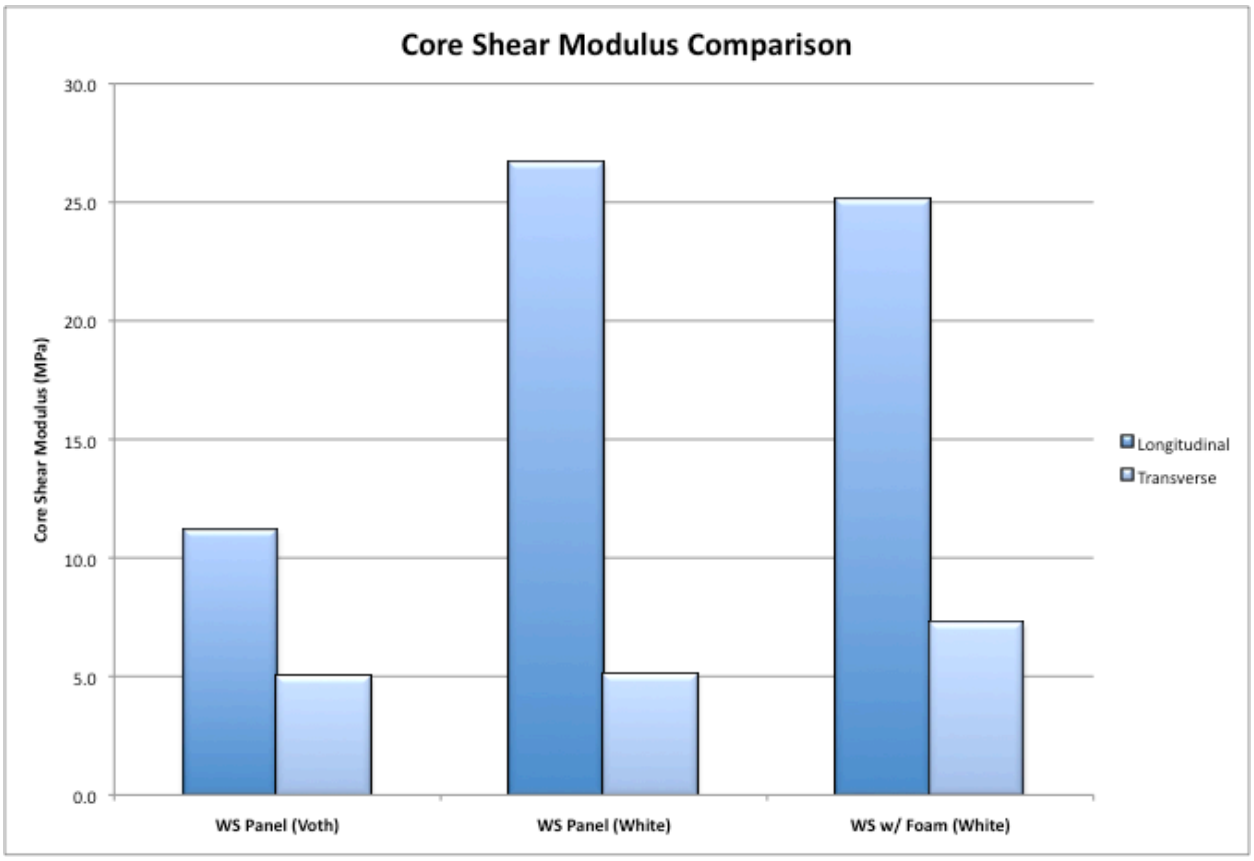

Figure 3.4.8: *Core shear modulus comparison. Sandwich panels without foam (Voth and this study) were normalized to a density of 310 kg/m^3. Sandwich panels with foam had a density of 326 kg/m^3.*

3.4.2.3. Flatwise Compression Tests:

Inclusion of rigid foam in the core prevented an ultimate failure and appeared to stiffen the panel in compression as shown in Figure 3.4.9. Failure of the wood-strand component was taken from the load versus displacement graph prior to signs of stiffening (Figure 3.4.10). 108 mm (4-1/4 in) and 215 mm (8-1/2 in) square specimens failed in crushing of the core and delamination at the interface between core and ply similar to sandwich panels without foam. These failures shown in Figure 3.4.11 became exaggerated as specimens continued to be loaded while foam resisted load.

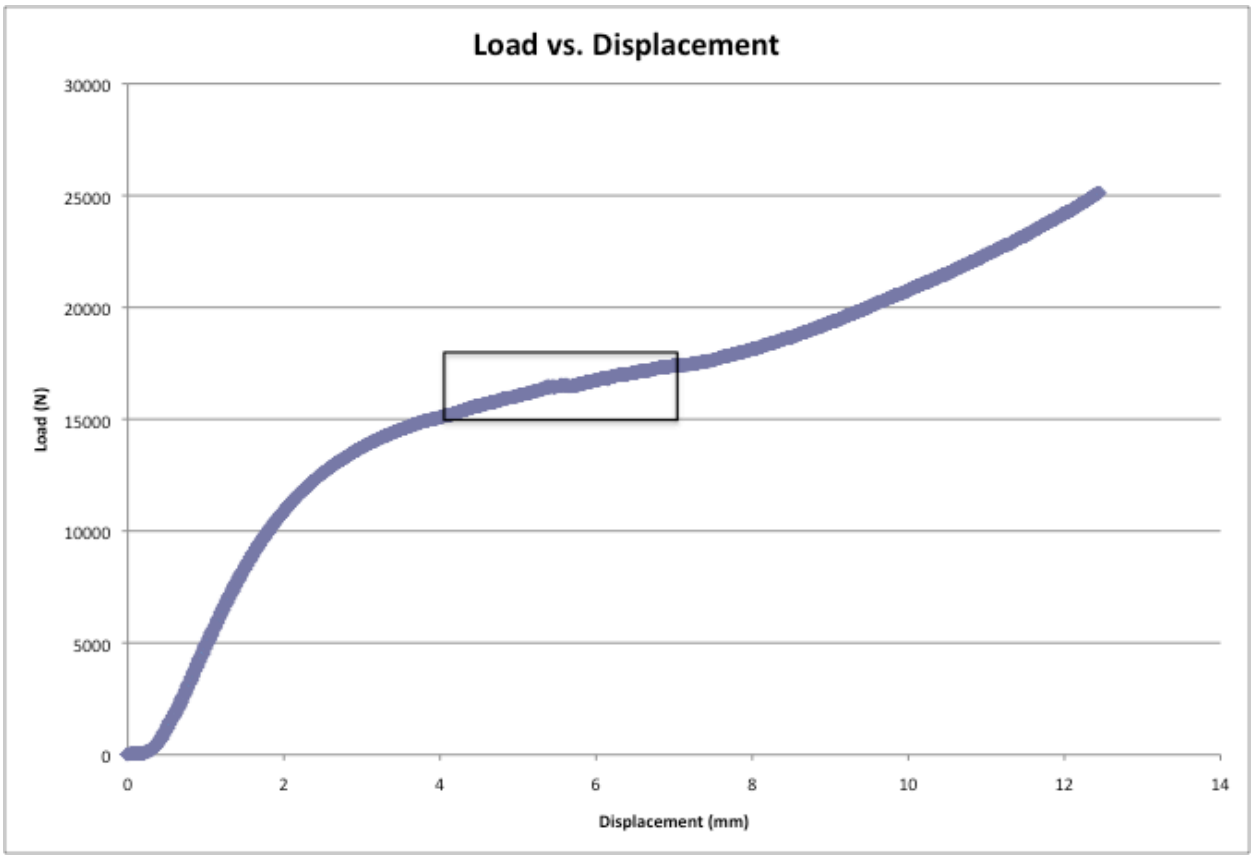

Figure 3.4.9: *Load versus displacement showing specimen stiffening. Box represents portion graphed in Figure 3.4.10.*

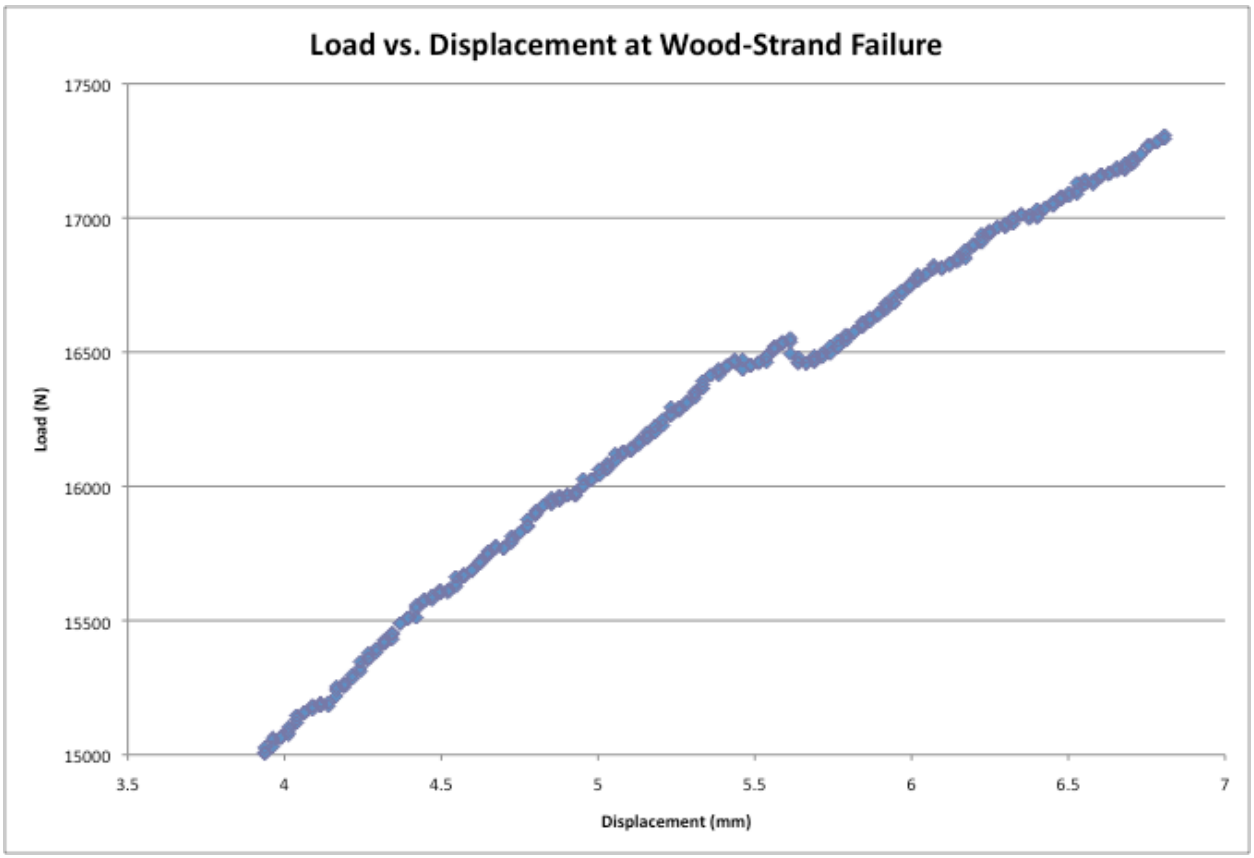

Figure 3.4.10: *Load versus displacement zooming in at wood-strand failure.*

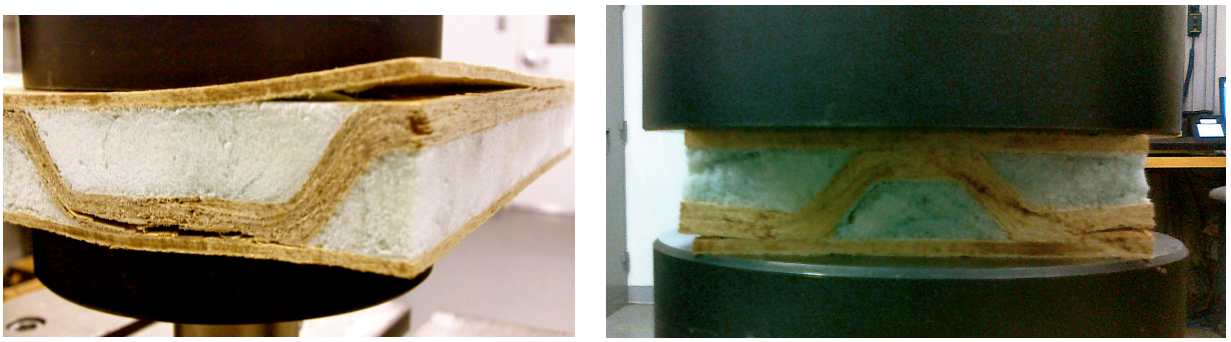

(a) *(b)*

Figure 3.4.11: *(a) Delamination failure in 215 mm x 215 mm specimen at wood-strand failure prior to stiffening caused by foam. (b) Delamination failure in 108 mm x108 mm specimen at wood-strand failure.*

By increasing density only 10% with foam, strength and compression modulus increased by 50% and 83%, respectively, for 108 mm (4-1/4 in) and 29% and 50%, respectively, for 215 mm (8-1/2 in) square specimens. Compressive strength and compression modulus comparisons including results from Voth (2009) and the small and large specimens from this study can be seen in Figure 3.4.12 and Figure 3.4.13. Table 3.4.2 presents compressive strength and compression modulus results.

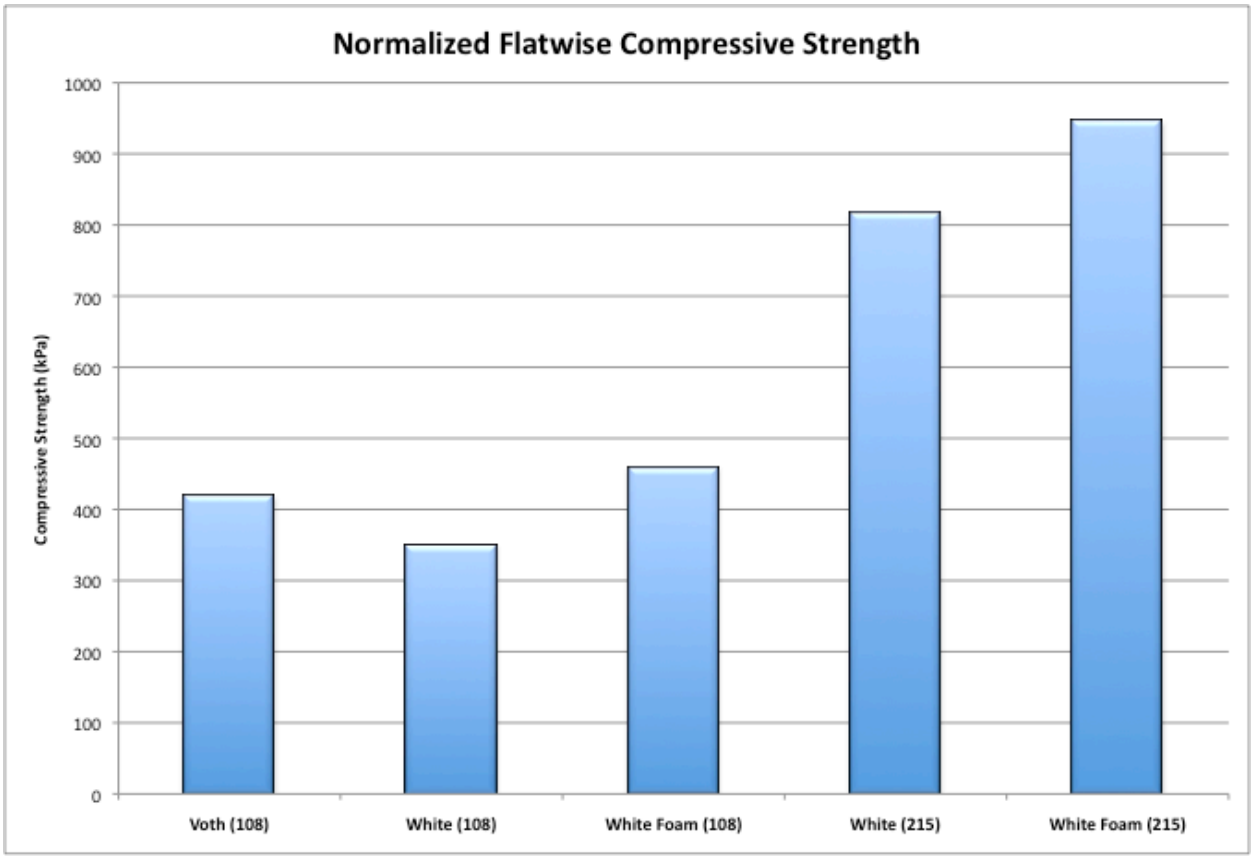

Figure 3.4.12: *Compressive strength of wood-strand sandwich panels with and without foam. 108 represents 108 mm x 108 mm specimens and 215 represents 215 mm x 215 mm specimens. Normalized to a density of 310 kg/m^3.*

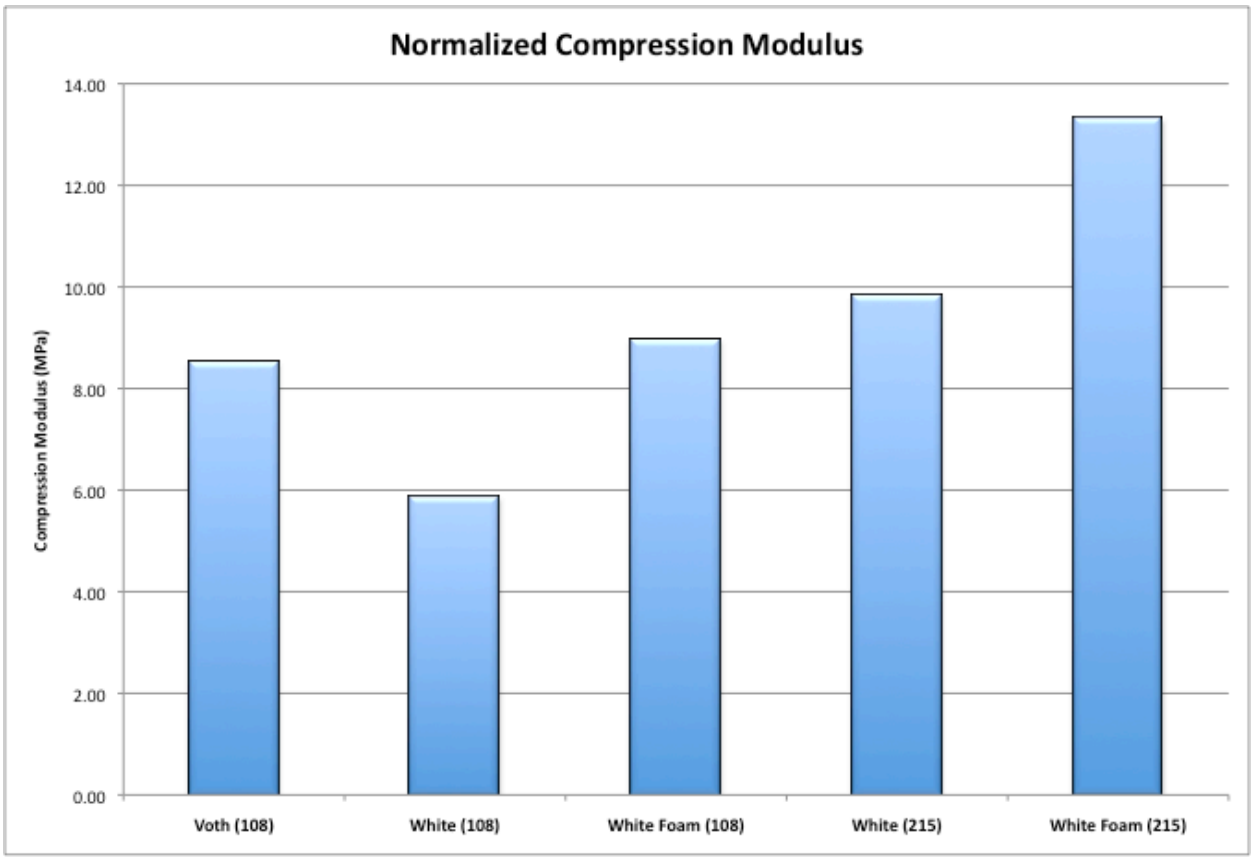

Figure 3.4.13: *Compression modulus of sandwich panels with and without foam. Normalized to 310 kg/m^3.*

Table 3.4.2: *Summary of wood-strand sandwich panel properties* [1,2]

			Beam Flexure Pmax (N)	Max Flexural Defl. (mm)	Bending Stiffness ($N\text{-}m^2/m$)	Core Shear Rigidity (N)	Core Shear Modulus (MPa)	Flatwise Comp. Strength (kPa)	Comp. Modulus (MPa)	Density (kg/m^3)
Wood-Strand Panel	Long.	Mean	3848	7.70	18757	89250	25.4	806	9.71	306
		Mean (US)	*865*	*0.303*	*166013*	*20064*	*3687*	*117*	*1408*	*19.1*
		Std Dev	1184	2.01	2398	19495	5.5	195	2.14	11
		COV%	30.8	26.1	12.8	21.8	21.8	24.2	22.0	3.5
	Trans.	Mean	1126	8.27	4435	17055	4.86	-	-	303
		Mean (US)	*253*	*0.325*	*39250*	*3834*	*705*	-	-	*18.9*
		Std Dev	173	1.12	302	6381	1.82	-	-	10
		COV%	15.3	13.5	6.8	37.4	37.4	-	-	3.3
Wood-Strand Panel With Foam	Long.	Mean	5159	9.07	21739	88380	25.1	1037	14.59	332
		Mean (US)	*1160*	*0.357*	*192410*	*19869*	*3645*	*150*	*2117*	*20.7*
		Std Dev	521	1.06	1341	22737	6.4	189	1.01	14
		COV%	10.1	11.7	6.2	25.7	25.3	18.2	6.9	4.2
	Trans.	Mean	1601	11.35	4850	25347	7.24	-	-	324
		Mean (US)	*360*	*0.447*	*42928*	*5698*	*1050*	-	-	*20.2*
		Std Dev	451	2.69	684	1361	0.44	-	-	6
		COV%	28.2	23.7	14.1	5.4	6.1	-	-	1.8
Wood-Strand Panel (Voth)	Long.	Mean	2709	12.78	18078	41306	11.6	421	8.55	312
		Mean (US)	*609*	*0.503*	*160000*	*9286*	*1694*	*61.0*	*1240*	*19.5*
	Trans.	Mean	698	10.11	4768	18530	5.14	-	-	308
		Mean (US)	*157*	*0.398*	*42200*	*4165.7*	*751*	-	-	*19.2*

[1] US units are shown in lb, in, $lb\text{-}in^2/in$, lb, psi, psi, psi, and pcf respectively.
[2] Compression results are for 215 mm x 215 mm specimens.

Larger square specimens [215 mm (8-1/2 in)] with foam were compared to specimens without foam at the average displacement [8.4 mm (0.3296 in)] of plain wood-strand specimens for a better comparison because of the stiffening properties of the foam. Foam filled specimens yielded increased compressive strength [1114 kPa (162 psi)] compared to specimens without foam [806 kPa (117 psi)]. Obtaining compressive strength at a defined displacement also showed a slight difference in results for foam specimens. Wood-strand failure for specimens with foam incorporated was estimated to occur at a displacement of 5.3 mm (0.208 in) with a compressive strength of 1037 kPa (150 psi). When these same specimens were analyzed at the average deflection at failure for specimens without foam [8.4 mm (0.3296 in)], compressive strength was found to increase to 1114 kPa (162 psi). This was a result of

the defined displacement correlating with the stiffened portion of the load versus displacement graph.

3.5. Building Envelope Thermal Resistance:

Changes in the energy code requiring better insulation properties by region, make it key to analyze the effect of wood-strand sandwich panels on the thermal resistance of a building envelope. Calculations shown in Appendix D estimated the R-value for a wall cross-section by calculating the R-values for each component and combining them the same way as electrical resistances. Thermal resistances through both the stud and insulation were calculated and occur in parallel as shown in Figure 3.5.1.

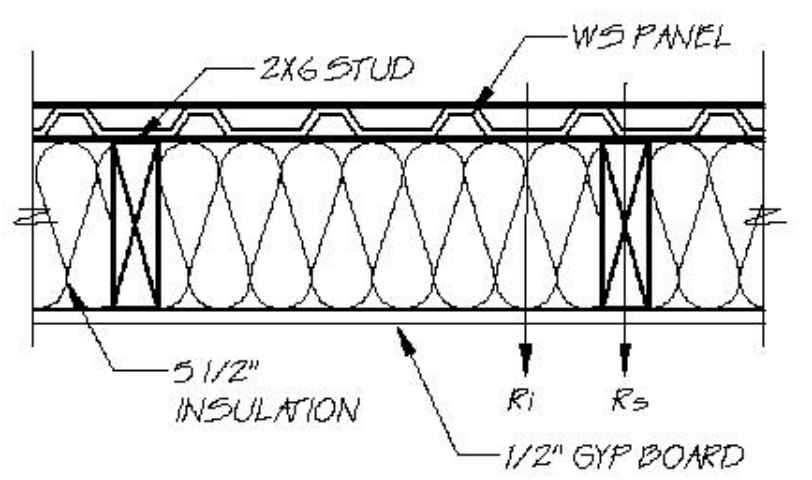

Figure 3.5.1: *Parallel thermal resistance through wall. R_i and R_s represent resistance through insulation and stud, respectively.*

Analysis was based upon only exterior sheathing, studs, insulation, and gypsum board. Only exterior sheathing varied where 12.7 mm (1/2 in) OSB, 19 mm (3/4 in) OSB, wood-strand sandwich panel, sandwich panel with radiant barrier, and sandwich panel with foam were analyzed. By replacing 12.7 mm (1/2 in) OSB or 19 mm (3/4 in) OSB sheathing with the wood-strand sandwich panel, the wall R-value increased slightly (~5%). The greatest difference occurred when sandwich panels with foam was introduced; it predicted an increase in wall R-value by 20% compared to 12.7 mm OSB. Figure 3.5.2 compares the different types of sheathing analyzed.

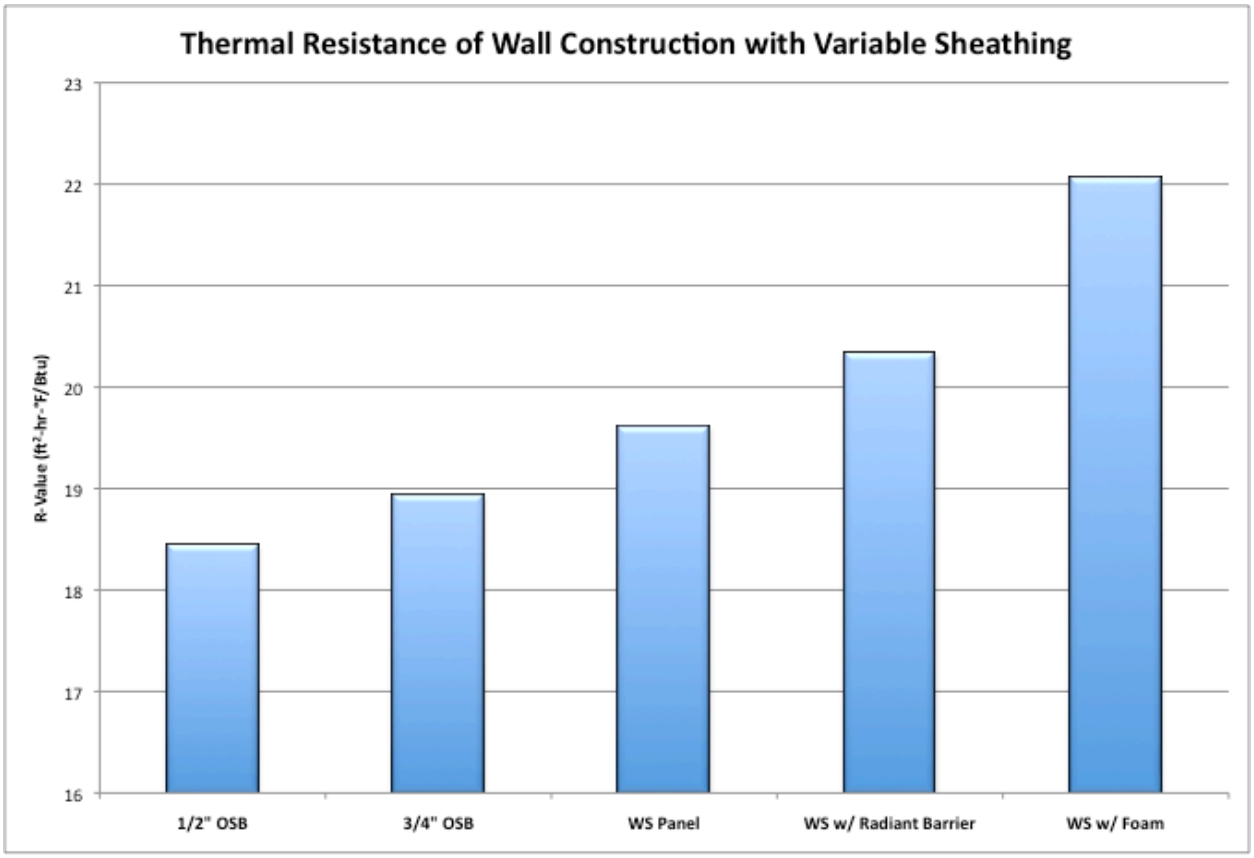

Figure 3.5.2: *R-values for typical wall construction. Only exterior sheathing varied. R-value conversion to S.I. units: 1R = 1 ft^2-hr-°F/Btu = 0.176 m^2-K/W.*

3.6. Summary and Conclusions:

Strategies to improve thermal efficiencies of wood-strand sandwich panels were discussed and implemented. Inclusion of rigid foam within the cavities of the panel showed significant improvements in thermal properties as well as structural properties, whereas inclusion of radiant barrier only improved thermal properties. Although results were successful with foam integration, future studies incorporating foam into sandwich panel voids should use tubing when placing foam manually as discussed earlier. Any air voids within specimens would result in lower mechanical results. By using tubing, even foam distribution is ensured throughout specimens.

Greatest thermal resistance was found in panels with foam by increasing R-value by 128%. Replacing OSB sheathing with wood-strand sandwich panels without foam estimated an improvement in thermal resistance of the building envelope by 6% and 4% (compared to 12.7 mm (1/2 in) OSB and 19 mm (3/4 in) OSB). These minor improvements may not outweigh conventional practices. However, once foam was integrated, increases of 20% and 17% were found when compared to 12.7 mm and 19 mm OSB. Increases in flexural strength of 34% and 42% for longitudinal and transverse specimens with foam compared to panels without foam (White 2011) display further advantages of foam. Bending stiffness also increased 16% and 9% for longitudinal and transverse specimens, respectively. Inclusion of foam prevented local failure in core shear flexure specimens, while improving sandwich panel shear strength by 35% and core shear modulus 62%. Not only does the sandwich panel with foam increase energy efficiency, but it also improves mechanical aspects of a sheathing material, thus making it a feasible method to improve sandwich panel construction. Inclusion of foam created

continuous support within the panel, which prevented any possible core wall buckling along with preventing localized buckling of outer plies. Results of this study strongly support developing panelized wall systems with wood-strand sandwich panels where inclusion of several corrugated layers within the core (Figure 3.6.1) with selected cavity layers filled with foam for insulation and others left unfilled for functional purposes (running electrical wires or plumbing) could provide thermally, structurally, and functionally efficient wall systems for future residential buildings. Hollow sandwich panel can also be used effectively for rain screen systems, where performance can be further improved by inclusion of radiant barrier within the cavities of the panel.

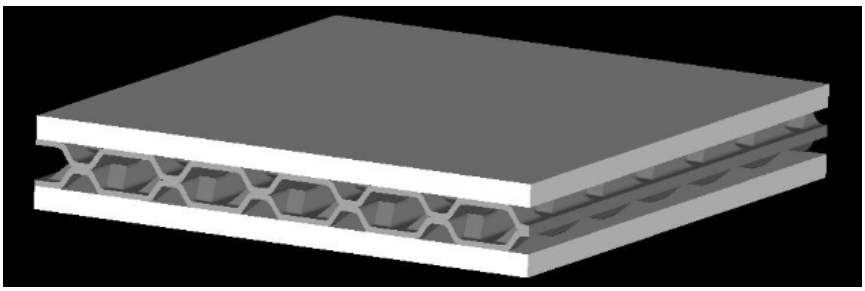

Figure 3.6.1: *Possible panelized wall system utilizing wood-strand sandwich panel research.*

3.7. References:

American Society of Heating, Refrigerating and Air-Conditioning Engineers, Inc. (2001). *ASHRAE Handbook – Fundamentals.* Atlanta, GA.

American Society of Heating, Refrigerating and Air-Conditioning Engineers, Inc. (2009). *ASHRAE Handbook – Fundamentals.* Atlanta, GA.

Davies, J.M. (2001). *Lightweight Sandwich Construction*. Malden, MA: Blackwell Science Ltd: Oxford.

Guardian Energy Technologies (n.d.). Specifications. Retrieved from http://www.sprayfoamdirect.com

Taylor, T.Z. (2011). *DOE's Involvement in Residential Energy Codes* [PowerPoint slides]. Retrieved from apps1.eere.energy.gov/.../webinar_residential_energycodes_20110222.pdf

U.S. Department of Energy. (2010). *Radiant Barriers. Energy Savers.* Retrieved January 19, 2011 from U.S. Department of Energy: http://www.energysavers.gov/your_home/insulation_airsealing/index.cfm/mytopic=11680

Voth, C. R. (2009). Lightweight Sandwich Panels Using Small-Diameter Timber Wood-Strand and Recycled Newsprint Cores. M.S. Thesis. *Washington State University, Department of Civil and Environmental Engineering*.

White, N.B. (2011). Strategies For Improving Thermal and Mechanical Properties of Wood-Strand Composites With 3-D Core. M.S. Thesis. Chapter 2. *Washington State University, Department of Civil and Environmental Engineering.*

Chapter 4

Project Summary and Conclusions

Successful mechanical results such as similar or better bending stiffness compared to OSB and plywood have confirmed that wood-strand sandwich panels are a viable option for residential building sheathing, thus thermal properties of the sandwich panels were obtained and presented. Thermal insulating properties were analyzed and compared to typical building envelope materials in an effort to create a more sustainable, energy efficient sheathing meeting both structural and energy codes. FE modeling of sandwich panels was also utilized to aid in future redesigning of sandwich panel core geometry and layer materials.

The FE model using existing data accurately (within 0.4% to 15%) represented the sandwich panels within the linear elastic region, while the model from this study was not as successful (lower range of strong direction E used in the FE model led to a prediction of stiffness that was 17% to 27% larger than that of the flexural specimen within the linear region).

Insulating properties served as metrics to evaluate energy efficiency of wood-strand sandwich panels when used as a sheathing material. Results were compared to typical building envelope materials (OSB, plywood, SIPs, etc.). Panels that are 32 mm (1-1/4 in) thick showed increased thermal resistance (R-value) by 190% compared to 12.3 mm (0.484 in) OSB/plywood. When normalized by thickness (i.e. per inch), the R-value of wood-strand sandwich panels increased 7% compared to the same

OSB/plywood. These increases in insulating properties correlate to a 6% increase in overall building envelope R-value when substituting the wood-strand sandwich panel for 12.7 mm (1/2 in) OSB. However, inclusion of rigid foam insulation or radiant barrier within the wood-strand sandwich panel cavities significantly improved thermal properties of the sandwich panels. By incorporating foam, R-value increased 562% compared to 12.3 mm (0.484 in) OSB and 147% when normalized by thickness. Radiant barrier incorporated within cavities did not have as great a return as foam, but still increased R-value 297% compared to that of OSB and 45% when normalized. Hypothetical wall R-value in a typical building envelope saw increases of 20% and 10% when sandwich panels incorporating foam and radiant barrier materials were used in place of 12.7 mm (1/2 in) OSB. Therefore, it is highly possible to design more energy efficient sheathing material using sandwich panels with effective insulation or thermal barrier materials included in their cavities, thus having a potential to cut down on operational energy costs of buildings.

Mechanical testing of sandwich panels also created a control to compare sandwich panels with rigid foam insulation within core cavities to those without insulation along with comparison to an FE model. By placing rigid foam within the sandwich panel cavities, mechanical properties improved with small increases in density (5% to 10%). Increases of 34% in bending strength and 16% in stiffness were evident when compared to sandwich panels without foam. Added support from the foam improved compressive strength of the sandwich panels by 29% and compression modulus by 50% compared to specimens without foam.

Viability of sandwich panels with foam should also be considered when readily available SIPs produce a high energy efficient building envelope material. Wood-strand sandwich panels with foam are comparable (90% of SIP R-values) when normalized by thickness. However, thicker SIP construction [114 mm (4-1/2 in) to 210 mm (8-1/4 in) SIPs] boosts efficiency with R-values ranging from 283% to 642% greater than sandwich panels with foam. This suggests that for wood-strand sandwich panels to be competitive with SIP construction, a thicker, panelized construction (similar to cross-laminated timber and SIPs) involving multiple core layers must be developed. Before wood-strand sandwich panels can become available commercially, more work must be done to prove that the sandwich panels are truly a viable building envelope material. Next steps in development are as follows:

- Development of an FE model defining nonlinear material properties to represent experimental results beyond the linear region. The model should also consider geometric nonlinearities in reducing its stiffness. This development will allow more complete predictions of flexure testing of sandwich panels.
- Analysis of panelized construction utilizing multiple corrugated cores, thin wood-strand plies, and thick veneer timber. Panelized construction will decrease construction time while corrugated cores filled with foam provide strength and insulation.
- Analysis of connections for wood-strand sandwich panels for wall and floor/roof applications. The corrugated core creates issues with respect to typical sheathing nailing and an innovative solution must be found. Connection systems used in

other 3-D panels can be tested and adopted for the wood-strand sandwich panels.

- Examination of wood-strand sandwich panels as sheathing resisting lateral loads. To replace OSB and plywood as sheathing, sandwich panels must resist lateral loads in shear walls and diaphragms.

Appendix A

Strand and Resin Amount Calculations

Wood Strand 3-D Core Calculations:

Panel width =	26 in
Panel length =	36 in
Panel thickness =	0.25 in
Panel volume =	234 in^3
Panel density =	40 pcf
Panel weight =	5.42 lbs
Wood and resin waste factor =	1.10

PF resin content	8%
PF resin solid content	55.70%
Solids weight of the resin	0.40 lbs
Liquid weight of the resin	0.32 lbs
Resin weight (solid + liquid)	0.72 lbs
Resin (considering waste factor)	0.79 lbs → 359 g (Amount of PF resin in mixer)

Oven dry wood weight	5.02 lbs
Actual wood MC	5%
Desired wood MC	5%
Water in wood	0.25 lbs
Wood with moisture	5.27 lbs
Wood with MC & waste factor	5.79 lbs → 2628 g (Amount of wood in mixer)

Final wood MC in panel	11%

Amount of total resin & wood for press	5.99 lbs → 2715 g

Wood Strand Ply Calculations:

Panel width =	27 in
Panel length =	36 in
Panel thickness =	0.125 in
Panel volume =	121.5 in^3
Panel density =	40 pcf
Panel weight =	2.81 lbs
Wood and resin waste factor =	1.10

PF resin content	8%
PF resin solid content	55.70%
Solids weight of the resin	0.21 lbs
Liquid weight of the resin	0.17 lbs
Resin weight (solid + liquid)	0.37 lbs
Resin (considering waste factor)	0.41 lbs → 187 g (Amount of PF resin in mixer)

Oven dry wood weight	2.60 lbs
Actual wood MC	4.2%
Desired wood MC	4.2%
Water in wood	0.11 lbs
Wood with moisture	2.71 lbs
Wood with MC & waste factor	2.98 lbs → 1354 g (Amount of wood in mixer)

Final wood MC in panel	11%

Amount of total resin & wood for press	3.09 lbs → 1400 g

Appendix B

Empirical Thermal Conductivity Calculations

Define thickness (in.), density (pcf), and moisture content (%) of panel

$t := 1.25$

$density := 19.5$

$MC := 9.2$

Calculate specific gravity of panel

$$SG := \frac{density}{62.4}$$

$SG = 0.313$

Calculate transverse thermal conductivity in S.I. units

$Ktm := SG \cdot (0.2 + 0.0038 \cdot MC) + 0.024$

$Ktm = 0.097$ W/m K

Convert thermal conductivity from S.I. to U.S. units

$Kt := Ktm \cdot 6.94$

$Kt = 0.676$ Btu in/(ft^2 hr F)

Calculate thermal resistance of panel

$$R := \frac{t}{Kt}$$

$R = 1.849$ ft^2 hr F/Btu

Appendix C

R-Value Estimation Calculations

Thermal conductivity, k, defined in U.S. units (Btu-in/ft^2-hr-F)
Thickness, t, defined in U.S. units (in)
Thermal resistance, R, in U.S. units (ft^2-hr-F/Btu)

$kply := 0.9022$

$tply := 0.125$

$kcore := 0.9022$

$tcore := 0.25$

$Rfoam := 6.7$

$tfoam := 0.75$

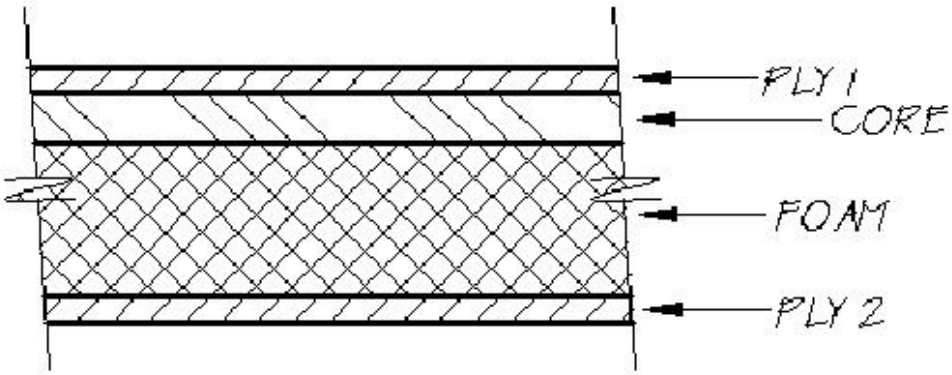

$$kfoam := \frac{1}{Rfoam} = 0.149$$

$$Rply1 := \frac{tply}{kply} = 0.139 \qquad Rply2 := \frac{tply}{kply} = 0.139$$

$$Rcore := \frac{tcore}{kcore} = 0.277 \qquad Rfoam := \frac{tfoam}{kfoam} = 5.025$$

$$Rtotal := Rply1 + Rcore + Rfoam + Rply2 = 5.579$$

Appendix D

Wall R-Value Calculations

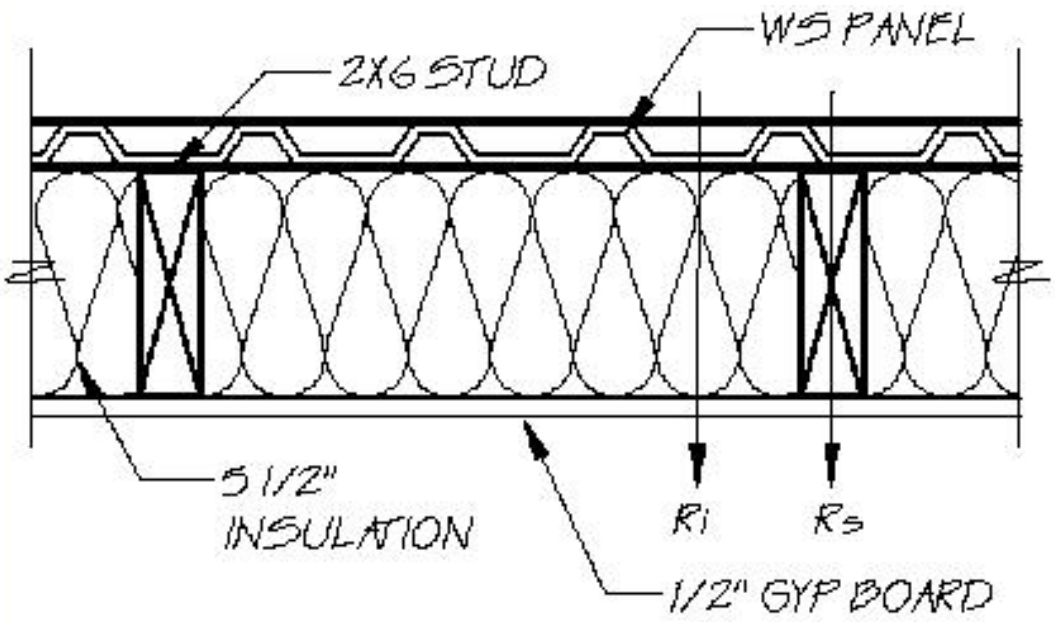

Rpanel := 1.645 kstud := 0.9 tstud := 5.5 Stud spacing = 16" o.c.

Cinsul := 0.048 Cgyp := 2.22 C = Conductance (inverse of R)

	R_s	R_i
WS Panel	Rpanel = 1.645	Rpanel = 1.645
Stud	$Rstud := \frac{tstud}{kstud} = 6.111$	----------
Insulation	----------	$Rinsul := \frac{1}{Cinsul} = 20.833$
Gyp Board	$Rgyp := \frac{1}{Cgyp} = 0.45$	Rgyp = 0.45

Rs_total := Rpanel + Rstud + Rgyp = 8.207

Ri_total := Rpanel + Rinsul + Rgyp = 22.929

1/Rtotal = $Utotal := \left(\frac{1.5}{16}\right)\cdot\left(\frac{1}{Rs\_total}\right) + \left(\frac{14.5}{16}\right)\cdot\left(\frac{1}{Ri\_total}\right) = 0.051$

$Rtotal := \frac{1}{Utotal} = 19.628$ ft^2-hr-°F/Btu